Focal Adhesion Kinase and ARHGAP26 in Cardiac and Skeletal Muscle Development

Jason Thomas Doherty

A dissertation submitted to the faculty of the University of North Carolina at Chapel Hill in partial fulfillment of the requirements for the degree of Doctor of Philosophy in the Department of Pathology and Laboratory Medicine.

Chapel Hill
2010

Approved by:

Joan M. Taylor, Ph.D.

Christopher P. Mack, Ph.D.

Frank L. Conlon, Ph.D.

Monte S. Willis, M.D., Ph.D.

Mark W. Majesky, Ph.D.

ABSTRACT

Jason Thomas Doherty: Focal Adhesion Kinase and ARHGAP26 in Cardiac and Skeletal Muscle Development

(Under the direction of Joan M. Taylor, Ph.D.)

Cardiac and skeletal muscle are highly specialized tissue types and the normal development of these striated muscles during embryogenesis requires very tightly regulated processes such as cell-type specific proliferation, expression of relevant marker genes, and formation of functional sarcomeres. Focal adhesion kinase (FAK) is a non-receptor tyrosine kinase which has been shown in various model systems to regulate processes required for both cardiac and skeletal muscle development. While FAK has been shown to regulate late-phase cardiogenic steps such as ventricular septation and cardiac compaction, it is currently unknown whether FAK regulates earlier steps of cardiogenesis. In order to address this possibility, we utilized an antisense morpholino strategy to deplete FAK during frog embryogenesis. The data described herein demonstrate that FAK morphant embryos exhibited markedly diminished cardiomyocyte proliferation in pre-looped heart tubes and that these heart tubes failed to fully undergo looping morphogenesis.

FAK interacts with a variety of binding partners including ARHGAP26, which is also referred to as, GTPase activating protein for Rho associated with FAK, (Graf). This Rho-specific GAP protein has been demonstrated to regulate actin cytoskeleton dynamics and is known to be expressed in terminally differentiated tissue types. However, very little is known about what role Graf might play during embryogenesis. Herein we demonstrate that Graf is

expressed during frog embryogenesis in a variety of tissue types including heart, brain, and somites. Utilizing an antisense morpholino approach, we establish for the first time that Graf is required during embryogenesis since all Graf-deficient embryos died during tadpole stages. Furthermore, Graf morphant embryos exhibited cardiac dysmorphogenesis and aberrant somite formation leading to a dystrophic phenotype resulting in swimming defects and paralysis. Our studies indicate that Graf depletion leads to markedly decreased muscle marker gene expression, aberrant sarcomere formation, and disruption of cellular attachments to the extracellular matrix. Taken together, the data provided in this dissertation greatly enhance our understanding of the roles of FAK and Graf in regulating the proper development of both the heart and skeletal muscle during embryogenesis.

ACKNOWLEDGEMENTS

I would first like to thank my advisor, Joan Taylor, for taking a chance on me and allowing me to make the transition from lab technician to graduate student in her lab. Not many PIs would take that chance and I am grateful for the opportunity she provided. In addition, Joan is a very skilled scientist and her guidance and scientific insight have been crucial to my development as a researcher. I owe a further debt of gratitude to Frank Conlon for teaching me the frog model and being so helpful in guiding the progression of my research project. I would also like to acknowledge the other members of my committee, Chris Mack, Monte Willis, and Mark Majesky for valuable advice on experimental design and approach. My project has benefitted greatly from all.

My scientific career has also been positively impacted by the people in the lab who helped maintain a fun atmosphere wherein even the tough days invariably included at least one good laugh. Dean, Matt, Jeremiah, Alicia, Laura, Rebecca, Lee, and a number of other past and present lab members have been good friends to me over the years. While it is unlikely that a sitcom will ever be set in a molecular biology lab, I'm sure the above people could have made one entertaining. They all deserve stickers. I would also like to acknowledge Kathleen Christine, Daniel Brown, and Chris Showell from the Conlon lab. They taught me a lot and were always very giving with their time and attention when I needed it.

I would also like to thank the people in the department who have helped me in a variety of ways. Dr. Charles Jennette is a great advocate for students, Dr. Bill Coleman has

always kept his office door open to students who need a chat or advice, Dr. Frank Church has also always been very helpful and open to conversations with me anytime I needed it, and Mrs. Dorothy Poteat has been a tremendous resource and someone who I looked forward to dropping in to visit with when time allowed. I also must give a great shout of thanks to Dr. Bob Bagnell and the staff of the microscopy core, Vicki Madden and Steve Ray. Not only did these people play a vital role in teaching me the microscopy skills I needed to make this project possible but they also are wonderful people and a joy to be around. Give me 100 Bob Bagnells and I guarantee I could move a mountain and have fun doing it.

I would especially like to say thanks to Dean for all the laughs he has brought me over the past year when I needed them the most. He has been an invaluable friend to me. I also must acknowledge Hunter Best, who could generally be relied on for a lunch-trip to Wendy's and proved that the importance of vegetables in the human diet could, potentially, just be a suggestion. Finally, many thanks to Kathleen Nevis for being both a wonderful friend and my go-to pool buddy. I have been very blessed to have a number of friends outside of the science world; people who have been a great source of joy and laughs for many years. You know who you are. And thanks..

I am also in debt to Dr. Jennifer Jahn (jj) who has shown nothing but patience, support, and love throughout this process. It doesn't hurt that she knows exactly what it is like to work toward a Ph.D. But there is no doubt that without her being beside me, I would have stumbled many more times than I did. I give loving thanks to her for all she provides.

I am ever thankful for my great family. They have supported me throughout my life and they have seen me through the good times and the bad. My brothers and sister -- Paul,

John, Stacie, and Brian -- are awesome and have always been there when I needed them. You can't ask for a better group of people. I know I can always count on them and I love them all.

Finally, I give thanks to my mother, Ellen. She is the best mom imaginable. She's the kind of mom that believes one can achieve anything they put their mind to. She might actually be right about that. She taught me many other things in life. I wish I had written them all down. Without her unwavering love and support, I would be nothing. I love you, mom.

TABLE OF CONTENTS

LIST OF TABLES

CHAPTER 2

CHAPTER 3

LIST OF FIGURES

CHAPTER 2.

CHAPTER 3

LIST OF ABBREVIATIONS

BAR	BIN-amphiphysin-RSV
bFGF	basic-fibroblast growth factor
BMP	bone morphogenetic protein
BrdU	bromo-deoxyuridine
CAS	cellular apoptosis susceptible
CHD	congenital heart disease
DGC	dystrophin-glycoprotein complex
DMD	Duchenne muscular dystrophy
DMEM	Dulbecco's modified eagle medium
DMSO	dimethyl sulfoxide
DNA	deoxyribonucleic acid
ECM	extracellular matrix
EDTA	ethylene-diamine-tetra-acetic acid
EGTA	ethylene glycol tetra acetic acid
ERK	extracellular signal responsive kinase
FAK	focal adhesion kinase
FGF	fibroblast growth factor
FGFR1	fibroblast growth factor receptor
FRNK	FAK-related non-kinase
GAP	GTPase activating protein
GDI	guanine diphosphate dissociation inhibitor
GDP	guanine diphosphate

GEF	guanine nucleotide exchange factor
GFP	green fluorescent protein
Graf	GTPase activating protein for Rho associated with FAK
GTP	guanine triphosphate
kDa	kilo-dalton
MAP	mitogen activated protein
MEF	myocyte enhancement factor
MHC	myosin heavy chain
Mo	morpholino-oligonucleotide
MOI	multiplicity of infection
MRF	myogenic regulatory factor
MTJ	myotendinous junction
NIH	National Institutes of Health
OCT	optimum cutting temperature
PBS	phosphate-buffered saline
PBSTD	PBS + tween + DMSO
PCR	polymerase chain reaction
PH	pleckstrin homology
pH3	phospho-histone H3
PYK2	protein tyrosine kinase 2
RIPA	radioimmunoprecipitation assay
RNA	ribonucleic acid
ROCK	Rho-associated kinase

RT-PCR	reverse transcription – polymerase chain reaction
SDS	sodium dodecyl sulfate
SH3	SRC homology3
SHF	secondary heart field
siRNA	short-interfering RNA
SRF	serum response factor
TBS	tris buffered saline
TBST	tris-buffered saline + tween
TBX	T-box
TEM	transmission electron microscopy
Tm	tropomyosin
TNT	transcription/translation assay
TnT	troponin-T
UTP	uridine triphosphate
UTR	untranslated region

INTRODUCTION

In this thesis, I describe my work highlighting the importance of focal adhesion kinase (FAK) and its binding partner, ARHGAP26, in cardiac and skeletal muscle development. ARHGAP26 is also referred to as GTPase Regulator Associated with FAK (Graf) and, for simplicity, will be referred to as Graf throughout this thesis. I begin with an introduction to cardiac and skeletal muscle development, integrin signaling, FAK, and Graf. I further describe the known roles for these proteins in cardiac and skeletal muscle development and disease and define important gaps in our current understanding. In Chapter II, I investigate a specific role for FAK in the early cardiac development of the African clawed frog, *Xenopus laevis*. Therein, I demonstrate that deletion of FAK protein leads to gross cardiac dysmorphogenesis and embryonic lethality. In Chapter III, I examine a role for Graf in cardiac and skeletal muscle differentiation and development. In this chapter, I demonstrate that Graf is required for normal morphological development of the heart and somites, which give rise to swimming muscle in tadpoles. Furthermore, I demonstrate that Graf-depletion during embryogenesis induces paralysis and a defect in somite structure and integrity that closely phenocopies the skeletal muscle defects found in models of muscular dystrophy.

CARDIAC AND SKELETAL MUSCLE DEVELOPMENTAL DEFECTS (OVERVIEW)

Congenital Heart Disease (CHD) affects at least 1 in every 100 live births and leads to more infant deaths than any other developmental defect (Hoffman, 1995; Hoffman and

Kaplan, 2002). Furthermore, more than one-fourth of all infants born with a congenital heart defect will require invasive treatment or will die in the first year of life (Rosamond et al., 2008). The most common congenital cardiac defect is the ventricular septal defect. Other defects include atrial septal defects, pulmonary and aortic stenosis, transposition of the great arteries, and patent ductus arteriosus.

Muscular dystrophy is a heterogenous group of skeletal muscle disorders caused by at least 30 known genetic disruptions in humans (Stenson et al., 2003). The highest incidence of these disorders is Duchenne muscular dystrophy (DMD), an X-linked disease caused by mutation in dystrophin, which represents the most common lethal pediatric disease in humans (Guglieri and Bushby). Muscular dystrophies are characterized by progressive loss of muscle strength, often beginning at birth, and typically lead to paralysis during childhood and death by the 2nd decade of life. While there are a variety of therapeutic approaches to disease treatment currently under investigation, the clinical approach to the disease at present consists of management of symptoms (Guglieri and Bushby). A better understanding of the mechanisms involved in the pathogenesis of these striated muscle disorders could lead to novel treatment options in the future.

CARDIAC DEVELOPMENT

The heart is the first organ to form in the embryo and, in mammals, a functioning heart is prerequisite for life during early embryogenesis. In fact, congenital heart defects are the most common birth defect and account for most of the heritable during the first year of life and their frequency in miscarried pregnancies is estimated to be tenfold higher (Hoffman, 1995; Hoffman and Kaplan, 2002). Although in the past decade, much has been discovered

regarding the molecular mechanisms underlying cardiac morphogenesis, there are many details that remain to be revealed. Discovering these critical mechanisms will provide new therapies to restore cardiac function in patients with congenital heart disease.

While the final form of the adult heart varies amongst vertebrate species, the mechanisms that regulate the early steps of heart formation are remarkably conserved (Harvey, 2002; Mohun *et al.*, 2003; Olson, 2006; Srivastava and Olson, 2000). Furthermore, the basic morphogenesis of the embryonic heart is surprisingly similar between species even though adult hearts can have two chambers, as in fish, three chambers in frogs, or four chambers in mammals. The initial step of heart formation occurs during gastrulation when two bilateral patches of cells originating in the anterior lateral mesoderm become specified and begin an anterior and ventral migration toward the embryonic ventral midline. During this midline migration, a variety of transcription factors begin to be expressed that regulate further steps of cardiac proliferation and differentiation. These include the evolutionarily conserved members of the NKX, GATA, T-box, myocyte enhancement factor (MEF2), and Hand families of transcription factors (Olson, 2006). The bilateral patches of specified cardiac precursor cells (cardioblasts) continue to migrate until they eventually fuse at the ventral midline to form a continuous epithelial sheet. Failure of midline migration and fusion often leads to cardia bifida, a condition in which two separate hearts develop. Cardia bifida can be caused by defects in cardiomyocyte differentiation, endoderm-derived signaling interactions, and/or cardioblast migration (Alexander *et al.*, 1999; Christine and Conlon, 2008; Dickmeis *et al.*, 2001; Kikuchi *et al.*, 2001; Kikuchi *et al.*, 2000; Reiter *et al.*, 1999; Schier *et al.*, 1997; Trinh and Stainier, 2004b; Yelon *et al.*, 2000). After fusion at the ventral midline, the heart field undergoes intricate morphogenetic processes that result in the rolling

up of the cardiac field into a linear heart tube. Subsequently, the heart undergoes cardiac looping which is required to bring the atria in alignment with the ventricles to form the four-chambered mammalian heart (or the three-chambered frog heart). Recent evidence suggests that proper cardiac looping requires both cardiomyocyte proliferation and directed cardiomyocyte migration; however, the precise mechanisms have not been fully elucidated and require additional investigation.

SKELETAL MUSCLE DEVELOPMENT

Skeletal muscle development is also a tightly regulated process involving the specification of mesodermal precursors into proliferating myoblasts which are induced to exit the cell cycle and undergo differentiation and fusion into multinucleated myotubes. Vertebrate skeletal muscle derives from tissues known as somites which eventually give rise to embryonic skeletal muscle, dermis, and bone. Notably, in *Xenopus leavis*, the somites appear to give rise almost exclusively to embryonic swimming muscles (Mohun T, 1994). For excellent reviews of various aspects of early vertebrate somitogenesis, see the works of Hamilton, Keller, and Pourquie (Hamilton, 1969; Keller, 2000; Pourquie, 2001). Skeletal muscle is initially specified in a tissue compartment of the gastrula embryo termed the presomitic mesoderm. During gastrulation, the somitic precursor tissue is localized in a ring-shape around the circumference of the embryo and somitogenesis proceeds by morphogenetic movements of this tissue to the dorsal aspect of the embryo along the anteroposterior axis adjacent to the notochord (Mohun T, 1994). *Xenopus laevis* somites are arranged as blocks of cells which undergo rotation in a coordinated anterior to posterior wave during the stages of neurulation (Hamilton, 1969). These blocks of cells then elongate along

the anteroposterior axis and undergo further terminal differentiation but do not undergo myotube fusion to become multinucleated skeletal muscle, as occurs in mammals and fish.

The early specification and differentiation of the somites is regulated by the MyoD family of muscle regulatory factors (MRFs) which includes MyoD, Myf5, Myogenin, and MRF4. These transcription factors bind to the E-box target sequence of many skeletal muscle genes. A variety of transgenic mouse models have helped to elucidate the specific roles of these transcription factors. Mice deficient in both MyoD and Myf5 contain no myoblasts and do not form skeletal muscle (Rudnicki *et al.*, 1993) suggesting that MyoD and Myf5 are required for initial specification of skeletal myoblasts. Disruption of myogenin in the developing mouse led to defects in muscle differentiation and embryonic or perinatal lethality (Hasty *et al.*, 1993; Nabeshima *et al.*, 1993). Mrf4 was also traditionally thought to regulate the differentiation of specified cells; however, recent evidence has determined that Mrf4 can regulate skeletal muscle specification as well (Kassar-Duchossoy *et al.*, 2004).

The MRFs interact with proteins such as myocyte enhancement factor-2 (MEF2) and serum response factor (SRF) to regulate skeletal muscle gene expression. The interaction with SRF is mediated by the myocardin family of cofactors which includes myocardin and the myocardin related transcription factors A and B (MRTF-A and MRTF-B). Additionally, a fourth member of the family, MASTR, has been identified in *Xenopus* which can cooperate with MyoD and Myf5 to induce skeletal muscle differentiation (Meadows *et al.*, 2008). The interactions of MRFs, MEFs, and SRF (along with the myocardin-family members) lead to upregulation of skeletal muscle-specific genes that contribute to formation of mature sarcomeres that provide skeletal muscle integrity and regulate stretch and force-transmission.

Cells interact with the extra-cellular matrix (ECM) via adhesive complexes, termed focal adhesions. At focal adhesions, the actin cytoskeleton links to the ECM through a variety of transmembrane proteins. One important class of cell surface receptors capable of connecting the ECM to the actin cytoskeleton is the group known as integrins. Experimental evidence from flies, worms, chicks, frogs, and mammals demonstrates that integrins are required for numerous developmental processes such as cellular adhesion, migration, proliferation, differentiation, and survival. Notably, integrins have been implicated in the pathogenesis of a variety of cardiac and skeletal muscle congenital and adult-onset disorders.

Integrins are heterodimeric transmembrane receptors composed of one α and one β subunit and generally contain a single membrane spanning segment and a short cytoplasmic tail (Giancotti and Ruoslahti, 1999; Guan, 1997). At least 18 α-subunits and 8 β-subunits are known to exist in mammals and can combine in at least 24 known configurations (van der Flier and Sonnenberg, 2001). The specific α/β configurations direct ligand specificities to such extracellular matrix components as fibronectin and laminin (Mayer, 2003).

Within this large family of integrins, a small number of α and β chains are specific to the heart. In cardiomyocytes, six distinct α subunits (α_1, α_3, α_5, α_6, α_7, and α_{10}) are expressed (van der Flier and Sonnenberg, 2001; Zhidkova *et al.*, 1995). Some integrins, including α_1 and α_5 (fibronectin-binding) are expressed embryonically but are downregulated in the adult, when α_7 (laminin-binding) becomes the predominant form (Mayer, 2003; Ross and Borg, 2001).

Similar to their role in cell:ECM interactions in cardiomyocytes, integrins are the major cell surface adhesion receptors in skeletal muscle and have been shown to coordinate many steps of skeletal muscle development including myoblast migration, differentiation,

and subsequent fusion into myotubes (Mayer, 2003). The α_5 and α_6 integrins are down-regulated after myotube formation and, thereafter, α_7 integrin predominates in adult skeletal muscle. The β_1 integrin is the most common form in skeletal muscle. This form is alternatively spliced into several variants found in skeletal muscle with the embryonic form, β_{1A}, eventually being replaced by the β_{1D} form in adult muscle.

Upon ligand binding, integrins cluster into focal contacts, areas enriched in specific cytoskeleton proteins such as talin, vinculin, α-actinin, and actin (Burridge *et al.*, 1988). While integrins play a vital structural role in connecting the cell to the ECM, they also regulate a variety of downstream biological pathways through signaling mechanisms via kinases such as FAK (Ilic *et al.*, 2004).

FAK Coordinates Integrin Signaling

FAK is recruited to sites of focal adhesions and becomes activated upon integrin clustering (Guan, 1997) and by activation of certain growth factors, G-protein coupled receptor agonists, and mechanical stimuli (Hildebrand *et al.*, 1993). FAK contains an N-terminal integrin-binding domain, a C-terminal focal adhesion targeting (FAT) domain, and a central kinase domain. Activation of FAK, predominantly at tyrosine 397 (Y397) can induce the tyrosine phosphorylation of FAK-binding partners such as p130Cas and paxillin (Hildebrand *et al.*, 1993). FAK regulates a variety of biological processes via interactions with these binding partners and through signaling mechanisms downstream of FAK, such as the MAP kinase pathway. Such biological processes include cellular adhesion, migration, proliferation, and survival. FAK is also thought to regulate the turnover of focal adhesions and actin cytoskeleton dynamics, in part through modulating signaling via the small GTPases

of the Rho-family. This process may involve the FAK binding partner Graf, as discussed later in this thesis (Hildebrand *et al.*, 1996).

In developing mouse embryos, FAK is ubiquitously expressed and this expression gradually increases from E8.0 onward (Furuta *et al.*, 1995). FAK is required for mammalian embryonic development and viability as the germline deletion of FAK in mice results in embryonic lethality between E8.5-10.5 (Furuta *et al.*, 1995). The FAK deficient embryos exhibited a general mesodermal deficiency similar to that induced by fibronectin deficiency (George *et al.*, 1997; George *et al.*, 1993; Georges-Labouesse *et al.*, 1996) and died as a result of generalized cardiovascular and mesodermal defects. *In vitro* analyses of cells derived from FAK-null mice displayed defects in cell proliferation, differentiation, and migration.

GRAF IS A FAK BINDING PARTNER

Graf was initially discovered using an expression cloning technique in an effort to identify binding partners for FAK and was determined to exhibit GAP activity toward the small-molecular weight GTPase, Rho (Hildebrand *et al.*, 1996; Taylor *et al.*, 1998; Taylor *et al.*, 1999). Graf (Graf1) has two related family members, Graf2 and Oligophrenin-1. Oligophrenin-1 has been implicated in cases of X-linked mental retardation (Ramakers, 2002); however, little is currently known about the function of Graf1 and Graf2.

RHO-FAMILY GTPASES AND THEIR REGULATION

The Rho-family GTPases comprise a group of small molecular weight intracellular signaling molecules that have well-demonstrated importance in regulating actin cytoskeleton

dynamics. The best characterized of these are RhoA, Rac, and CDC42. Rac and CDC42 are known to induce formation of lamellapodia and filopodia, respectively. RhoA regulates the formation of stress fibers and focal adhesions (Ridley and Hall, 1992). In addition to their effects on cytoskeletal dynamics, Rho family members have been shown to alter gene expression via p38/Jun NH2-terminal kinase and serum response factor (SRF) activity and G1-S cell cycle progression (Ridley, 1996). Finally, RhoA has been implicated in striated muscle differentiation and organogenesis, as described in greater detail in Chapters I and III.

The activity of Rho-family proteins is regulated by the binding of GTP (guanine triphosphate), in the active state, or GDP (guanine diphosphate), in the inactive state. The binding of GTP and GDP is tightly regulated by three classes of proteins, GEFs (Guanine Exchange Factors), GDIs (Guanine Dissociation Inhibitors), and GAPs (GTPase Activating Proteins) which each have specific affinities toward one or more Rho-family members. GEFs upregulate GTPase activity by promoting the release of GDP and the binding of GTP. GDIs serve to switch off GTPase activity in two ways: by promoting GDP binding and by sequestering the GTPase in the cytosol where it is less accessible to downstream effectors. Finally, GAPs typically serve to downregulate the activity of GTPases by promoting the hydrolysis of GTP to GDP. Notably, the intrinsic rate of GTP hydrolysis by small GTPases is much lower than that observed in heterotrimeric G-proteins; thus GAPs are critical for maintaining the fine balance between the active- and inactive- states of the small GTPases of the Rho-family.

The human genome is predicted to encode a large number of GAP-domain containing proteins. Further, the number of RhoGAP-containing proteins exceeds the number of Rho-GTPases by 2-3 fold (Tcherkezian and Lamarche-Vane, 2007). The abundance of RhoGAPs

is partially explained by the specificity of many GAPs for only certain Rho GTPases. Additionally, many GAPs are expressed in a time- or tissue-dependent manner. Furthermore, GAP activity is regulated by a variety of mechanisms including lipid binding, protein-protein interactions, and phosphorylation via upstream signaling mechanisms such as MAP kinases. Graf, like many GAP proteins, contains numerous functional domains which may be important to its biological function. These include an N-terminal BAR and PH domain, both of which may serve to bind phospholipid membranes, a proline/serine rich domain which may regulate Graf's activity, and a C-terminal SH3 domain through which Graf interacts with FAK (Hildebrand *et al.*, 1996; Longenecker *et al.*, 2000; Taylor *et al.*, 1998; Taylor *et al.*, 1999). Cell culture experiments have demonstrated that Graf overexpression leads to clearance of Rho-mediated stress fibers and that the GAP domain of Graf is both necessary and sufficient for this effect. Further evidence suggests that Graf may be regulated by phosphorylation by mitogen activating protein (MAP) Kinase at serine 510, which is localized within the serine/proline rich domain. Such activation could lead to an "open" conformation, as suggested by band-shifting evident by Western blot analysis, which could increase Graf's ability to bind FAK through its SH3 domain.

Graf has been shown in adult mammals to be highly expressed in terminally differentiated tissues such as heart and brain. In addition, evidence has emerged recently that Graf may have possible tumor-suppressor activity. Notably, several reports suggest that some cases of acute myeloid leukaemia and myelosdysplastic syndrome are caused by downregulation of Graf through genetic mutation, deletions, translocations, and aberrant methylation of the Graf promoter region (Bojesen *et al.*, 2006; Borkhardt *et al.*, 2000;

Panagopoulos *et al.*, 2004). Despite these advances, little is known about how Graf is regulated during development or what role it plays *in vivo*.

INTEGRINS AND THE DYSTROPHIN-GLYCOPROTEIN COMPLEX ARE DEFECTIVE IN VARIOUS MUSCULAR DYSTROPHIES

Strong interactions between the actin cytoskeleton and the ECM are necessary in order to generate force-transmission and stretch responsiveness. In the absence of these interactions, severe muscular degeneration occurs as seen in muscular dystrophies. Indeed, mutations in genes encoding members of the integrin family (e.g. integrin $\alpha_7\beta_1$) and/or the dystrophin-glycoprotein complex (DGC) (e.g. β–dystroglycan) leads to dystrophic phenotypes in humans and mice.

Mature skeletal muscle is surrounded by a basement membrane containing extracellular matricies including laminin, collagen IV, perlecan, and nidogen-1 (Timpl and Brown, 1996). Laminin-binding is primarily mediated through interactions with the laminin-specific receptors $\alpha_7\beta_1$-integrin and the α-sarcoglycan component of the DGC. Mutation of dystrophin leads to Duchenne's and Becker muscular dystrophy and mutations of other DGC components have also been implicated in human muscular dystrophy (Mayer, 2003). The α_7-integrin subunit is also mutated in certain forms of human muscular dystrophy and this finding was corroborated in an α_7-integrin mouse model (Hayashi *et al.*, 1998; Mayer *et al.*, 1997). Notably, the combined disruption of both dystrophin and α_7-integrin in mice led to a more severe dystrophic phenotype than either mutation alone and resulted in death by four weeks of age (Rooney *et al.*, 2006). Furthermore, overexpression of α_7-integrin reduced the dystrophic phenotype of mice lacking both dystrophin and the dystrophin homolog, utrophin (Burkin *et al.*, 2001). Finally, mutations in the ECM components, collagen IV and laminin,

have been implicated in various forms of congenital muscular dystrophies (Lisi and Cohn, 2007). Taken together, these findings firmly demonstrate the requirement for strong interactions between the actin cytoskeleton and the extracellular matrix (especially laminin) via the laminin-receptors integrin $\alpha_7\beta_1$ and the DGC.

FAK IN CARDIAC AND SKELETAL MUSCLE DEVELOPMENT

As noted above, the germline deletion of FAK in mice induces embryonic lethality between E8.5 and E10. This phenotype was characterized by defects in mesoderm formation and generalized cardiovascular defects; however, a more specific investigation of later stages of cardiac development was precluded due to the early timing of lethality. A more specific role for FAK in cardiac development has been aided greatly by the use of conditional knockouts, which allow for tightly controlled temporal activation and deletion of FAK in a tissue-specific manner. Specifically, our lab recently reported that FAK deletion in NKX2.5-expressing cells, which contribute to the primary and secondary heart fields, leads to defects in ventricular septation, outflow tract alignment, and persistent truncus arteriosus (Hakim *et al.*, 2007). Utilizing a different strategy, our lab showed that overexpression of FAK-related non-kinase (FRNK), which can serve as a dominant negative inhibitor of FAK, in cardiac progenitor cells beginning at E10.5 leads to a severe ventricular noncompaction defect associated with reduced cardiomyocyte proliferation (DiMichele *et al.*, 2009).

In addition to its role in heart development, FAK has been shown to play a vital role in the development of skeletal muscle. In *Xenopus*, FAK mRNA expression increases between stages 20-26, concomitant with increased skeletal muscle differentiation (Zhang *et al.*, 1995) and FAK protein was found to localize at the myotendinous junction (MTJ) of

Xenopus somites (Baker *et al.*, 1994). Inactivation of FAK in the developing *Xenopus* somites by injection of FRNK into the presumptive somites (at the 4-cell stage) led to defects in somite rotation and disruption of somite boundaries and fibronectin deposition (Kragtorp and Miller, 2006). Furthermore, *in vitro* differentiation experiments utilizing the C2C12 myoblast cell line demonstrated that dynamic regulation of FAK activity (FAK inactivation followed by increased FAK activation) promoted myoblast differentiation into multinucleated myotubes (Clemente *et al.*, 2005). FAK signaling has also been shown to specifically promote myotube fusion, potentially through upregulation of pro-fusion genes such as caveolin-3 and the β_{1D} integrin subunit (Quach *et al.*, 2009). Notably, while FAK appears to regulate cell proliferation (via cyclinD-mediated processes) and myotube fusion, no evidence was found in these studies to suggest that FAK altered the myogenic differentiation of C2C12 or primary myocytes as assessed by skeletal marker gene expression analyses. Thus, FAK may serve a biphasic role in muscle maturation but not through direct regulation of muscle marker gene expression.

FAK interacts with a variety of proteins localized at cellular focal adhesions and many of these also play a vital role in the development of mesodermally-derived tissues such as heart and skeletal muscle. Fibronectin is a major component of the extracellular matrix and is the strongest upstream activator of FAK. Disruption of fibronectin during development leads to embryonic lethality in both frogs and mouse. In the frog, injection of fibronectin-interfering antibodies into single-cell embryos caused defects in gastrulation and blastopore closure, eye formation, anterior-posterior axis elongation, and pericardial edema (Marsden and DeSimone, 2001). In the fibronectin-deficient mouse, early development through gastrulation was relatively unperturbed; however, at later stages of development,

severe defects were observed in tissues of mesodermal origin. Most notably, fibronectin-null mouse embryos displayed a dysmorphic heart and defects in somite formation, despite normal specification of precursor cells (George *et al.*, 1997; George *et al.*, 1993; Georges-Labouesse *et al.*, 1996). The similarities between the fibronectin- and FAK-null phenotypes suggests that cell:ECM interactions via FAK and fibronectin are crucial for proper cardiac and skeletal muscle development.

Other FAK binding partners exhibiting critical functions during embryonic development include p130CAS, paxillin, and vinculin. p130cas is an adaptor molecule that is activated by FAK and serves roles in cell migration and proliferation. CAS null embryos die by embryonic day 12.5, exhibit marked growth retardation, and develop abnormal hearts with myofibrillar disorganization and disruption of the Z-disks (Honda *et al.*, 1998). Paxillin is phosphorylated after integrin activation and mediates signals downstream of integrins. Paxillin-null mice displayed a similar phenotype to fibronectin-null mice, as described above. Paxillin-null cells cultured from these embryos exhibited defects in focal adhesion formation, FAK localization to focal adhesions, and cell migration (Hagel *et al.*, 2002). Finally, vinculin-null mice demonstrated embryonic lethality between E8-10 (Xu *et al.*, 1998). Vinculin knockout caused severe defects in neural structures such as the neural tube and resulted in small and dysfunctional cardiac tissue. Fibroblasts derived from homozygous null mice were deficient for adhesion to a number of ECM proteins and exhibited diminished migratory capacity.

RHO IN CARDIAC AND SKELETAL MUSCLE DEVELOPMENT – IMPLICATIONS FOR GRAF

As described previously, Rho plays a variety of biological roles including regulation of actin cytoskeleton dynamics, cell proliferation, migration, and differentiation. Perhaps the earliest known functions of Rho during embryogenesis relate to its role in coordinating cellular adhesion during gastrulation (Wunnenberg-Stapleton *et al.*, 1999) and these processes are thought to operate downstream of Wnt-derived signals (Habas *et al.*, 2001). Indeed, Rho has been shown to act downstream of Wnt-signals emanating from the organizer region of the gastrula embryo to coordinate migratory movements of cardiac precursor cells, perturbation of which results in cardia bifida (Yue *et al.*, 2008). Other roles for Rho during cardiogenesis have also been demonstrated in a variety of experimental systems. For example, inhibition of Rho by cardiomyocyte-specific overexpression of the Rho-GDIα, led to decreased cardiomyocyte proliferation and disrupted cardiac morphogenesis (Wei *et al.*, 2002) and similar results were obtained by treatment of embryonic hearts with an inhibitor of the Rho-effector, Rho-associated coiled-coil kinase (ROCK) (Zhao and Rivkees, 2003). Studies in isolated chick cardiomyocytes suggest that Rho also plays a specific role in myofibrillogenesis, as treatment with the Rho-inhibiting toxin, C3, led to disaggregation of both focal adhesions and myofibrils (Wang *et al.*, 1997). While these studies are intriguing, much remains unknown about the various roles of Rho during the intricate process of cardiac development.

In addition to its role in cardiogenesis, Rho has been extensively studied with respect to its role in skeletal muscle differentiation. Rho has been found to both promote and block differentiation of skeletal muscle in a variety of experimental contexts. It is unclear to what extent these differences can be attributed to differences in model organism and experimental design (e.g. methods and timing of genetic perturbation); however, recent evidence suggests

that Rho activity must be very tightly regulated during skeletal muscle differentiation. For example, while Rho activity appears to be necessary for maintenance of myogenic potential (Castellani *et al.*, 2006) and can coordinate myogenic marker gene expression through SRF (Carnac *et al.*, 1998; Hill *et al.*, 1995; Wei *et al.*, 1998), it also must be later downregulated for optimal differentiation and myotube fusion (Charrasse *et al.*, 2006; Meriane *et al.*, 2000; Nishiyama *et al.*, 2004). The specific effectors which regulate this dynamic modulation of Rho activity during these critical processes remain mostly undefined. Chapter III of this thesis describes intriguing evidence that Graf is a key Rho-effector during embryogenesis and plays specific roles in the differentiation and morphogenesis of cardiac and skeletal muscle.

MODELS UTILIZED HEREIN

In order to study the roles of FAK in cardiac development and of Graf in cardiac and skeletal muscle development, I have employed translational inhibition of FAK and Graf protein through the use of antisense morpholinos in the developing frog (*Xenopus laevis*). In this section I will briefly describe these model systems, the rationale for their use in my studies, and some important information to provide further insight into the experiments described in the remainder of this thesis.

Xenopus laevis is a well-characterized model system of early embryonic development and has been extensively utilized in the study of embryonic heart and skeletal muscle development. Some of the attractive features of using this species are: high fecundity (females can lay up to 1000 eggs/day), large egg size which allows for ease of micro-injection experiments, embryos develop externally for ease of observation, and embryonic

development occurs rapidly (embryos develop a fully functioning heart within 72 hours post-fertilization). In addition, as opposed to mammalian development which requires a fully-functioning cardiovascular system early during embryogenesis, frogs do not have a similar requirement until at least the late tadpole stages because they are capable of nutrient exchange via simple diffusion.

In order to determine an *in vivo* role for FAK and Graf during embryonic development, I have utilized an antisense morpholino-based approach to deplete developing frog embryos of these proteins. This approach is a well-established experimental methodology for examining protein function during embryonic development. Morpholinos are anti-sense oligonucleotides which recognize their cognate sequence (the transcript encoding the protein of interest) and bind with high specificity and affinity. The morpholin-ring attached to these oligos sterically hinders ribosomal attachment and, thus, generation of functional protein. Morpholinos are diluted in an appropriate buffer and micro-injected into single-cell fertilized embryos. As cellular divisions proceed during development, the morpholino is evenly distributed to all cells of the embryo, which allows for depletion of the protein of interest in all tissue types. In addition, individual blastomeres may be targeted for micro-injection. For example, unilateral micro-injection of morpholinos into only one blastomere at the two-cell stage leads to distribution of the morpholino into only one half of the embryo.

Frog development is temperature-dependent and, therefore, developmental progression is tracked according to stages of development (as assessed by consistent morphological cues) rather than in hours or days post-fertilization. Germane to this body of work are the stages of gastrulation (stages 9-12), neurulation (stages 12-24), tailbud (stages

24-32), and tadpole (stage 32 onward). Both the FAK- and Graf- deficient phenotypes are embryonic lethal during tadpole stages (by stage 42) and subsequent staging will not be described. Specific information concerning the relevant timing of important development processes in cardiac and skeletal muscle development will be described within chapters II and III, as necessary.

GOAL OF THESIS

While FAK has been demonstrated to play a role in both cardiac and skeletal muscle development, much remains unknown about its exact function in these processes. As noted above, germ-line and tissue-specific deletion of FAK leads to various cardiovascular defects in the mouse, yet confers no obvious phenotype in the fly. We were interested in determining whether FAK plays an important role in cardiac development in the frog model, *Xenopus laevis*, since frogs have a more complex, three-chambered heart than the linear heart tube of the fly. In Chapter II of this thesis, I utilized an antisense morpholino approach to block translation of FAK in developing frog embryos in order to test the hypothesis that FAK is required for normal heart development in the frog. I demonstrate that FAK morphant embryos undergo normal early development, express several markers of cardiac specification and differentiation in a specified spatiotemporal pattern, and develop a normal cardiac heart tube. However, by later stages, FAK-depletion leads to disruption of normal cardiac morphology, pericardial edema, and early embryonic lethality. Our mechanistic data suggests that the abnormal looping morphogenesis induced by FAK-depletion is likely due, in part, to impaired cardiomyocyte proliferation via an FGF-dependent pathway.

In Chapter III of this thesis, I examine a novel role for Graf in the development of cardiac and skeletal muscle. Previous studies have demonstrated that Graf serves to downregulate Rho activity (via its Rho-GAP domain) and that this downregulation leads to cytoskeletal rearrangements in cultured cells. However, to date, no research has been conducted on a specific *in vivo* role for Graf. Due to the tissue-specific expression of Graf and its role in modulating Rho activity, a protein known to be important for skeletal and cardiac muscle differentiation, we hypothesized that Graf may play a vital role in early cardiac and skeletal muscle development. We used antisense morpholinos to block Graf translation in frog embryos and our studies revealed that Graf is required for normal somite formation. Graf-depleted embryos are partially paralyzed and exhibit diminished cardiac and skeletal muscle marker gene expression, aberrant sarcomeric structure, and dysregulated intersomitic junction formation and/or maintenance. These skeletal muscle defects, coupled with the disruption of laminin and β-dystroglycan deposition in the intersomitic space strongly demonstrates that Graf-depletion phenocopies many of the skeletal muscle abnormalities seen in models of muscular dystrophy. Furthermore, Graf-depleted embryos exhibit marked pericardial edema, aberrant cardiac morphology, and die during tadpole stages of development, suggesting that Graf plays an essential role for both cardiac and skeletal muscle development.

FOCAL ADHESION KINASE IS ESSENTIAL FOR CARDIAC LOOPING AND MULTI-CHAMBER HEART FORMATION

ABSTRACT

Focal adhesion kinase (FAK) is a critical mediator of matrix- and growth factor-induced signaling during development. Myocyte-restricted FAK deletion in mid-gestation mice results in impaired ventricular septation and cardiac compaction. However, whether FAK regulates early cardiogenic steps remains unknown. To explore a role for FAK in multi-chambered heart formation, we utilized anti-sense morpholinos to deplete FAK in *Xenopus laevis*. *Xenopus* FAK morphants exhibited impaired cardiogenesis, pronounced pericardial edema, and lethality by tadpole stages. Spatial-temporal assessment of cardiac marker gene expression revealed that FAK was not necessary for midline migration, differentiation, fusion of cardiac precursors, or linear heart tube formation. However, myocyte proliferation was significantly reduced in FAK morphant heart tubes and these tubes failed to undergo proper looping morphogenesis. Collectively our data imply that FAK plays an essential role in chamber outgrowth and looping morphogenesis likely stimulated by fibroblast growth factors (and possibly other) cardiotrophic factors.

INTRODUCTION

Heart formation involves an intricate and complex series of events that must occur in a coordinated spatial and temporal manner. The heart develops from bilaterally symmetric cardiogenic primordia that migrate and fuse at the embryonic midline, proliferate, and form a primitive heart tube (Dehaan, 1963; Goetz and Conlon, 2007; Kolker *et al.*, 2000; Mohun *et al.*, 2003; Mohun *et al.*, 2000; Trinh and Stainier, 2004a). In species with multi-chambered hearts the primitive heart tube rapidly undergoes looping morphogenesis and maturation to form a fully functioning heart with outflow tracts aligned with the vasculature.

Appropriate cardiac morphogenesis requires regional coordinated recruitment, differentiation, and proliferation of cardiomyocytes. A large body of evidence indicates that signals secreted from the endoderm including soluble factors (e.g. fibroblast growth factors (FGFs), bone morphogenic proteins (BMPs) and extracellular matrix (ECM) proteins (e.g. fibronectin) are prominent inducers of the cardiogenic field (Ahuja *et al.*, 2007; Chen *et al.*, 2004; Choi *et al.*, 2007; Lavine and Ornitz, 2008; Lavine *et al.*, 2005). Via incompletely understood mechanisms, these signals induce the expression of critical myocardial transcription factors in discrete (often chamber-specific) locales. Notably, genetic studies in chick, zebrafish, frogs, and mice have revealed that spatiotemporal induction of myocyte enhancement factor 2 (MEF2) and GATA factors are necessary for regulated myocyte differentiation, while Nkx2.5, Tbx2, and Tbx3 are required for coordinating myocyte proliferation (Moorman and Christoffels, 2003; Srivastava and Olson, 2000; Zaffran and Frasch, 2002).

The non-receptor tyrosine kinase, focal adhesion kinase (FAK) is strongly activated by fibronectin-binding integrins ($\alpha5\beta1$) and growth factors (Parsons, 2003) and is a likely candidate to integrate downstream signals from these diverse pathways during myocardial

development. Indeed, studies by our group and others have indicated that myocyte-specific depletion of FAK (or inactivation of FAK) leads to early embryonic lethality associated with left ventricular non-compaction (DiMichele *et al.*, 2009; Peng *et al.*, 2008). Although these studies highlight an essential role for FAK during mid-gestational cardiac growth, a limitation of these studies is that FAK signaling is not significantly depleted in these hearts until embryonic day 13.5 (E13.5) or later, precluding determination of whether FAK activity is necessary for earlier stages of cardiac morphogenesis. Importantly, FAK is expressed in the mouse mesoderm prior to cardiogenesis (E7.5) and germ-line deletion of FAK in the mouse induces a variety of mesodermal defects and early embryonic death within a time frame either prior to or during looping morphogenesis (between E8.5-10.5 in mice) (Furuta *et al.*, 1995). In stark contrast, depletion of the FAK ortholog FAK56 in *Drosophila* does not affect viability of this organism and no defects in heart formation were reported (Grabbe *et al.*, 2004). Since the *Drosophila* heart consists of a linear tube that does not undergo the marked morphological changes that occur during multi-chambered heart formation, we speculated that looping morphogenesis may be a key developmental process regulated by FAK in higher organisms.

To study the possible requirement for FAK in this intricate morphogenetic event, we depleted FAK in *Xenopus laevis* by microinjection of inhibitory antisense morpholino oligonucleotides. This model system is particularly suited to studying cardiac development because of the ease of temporal analysis of morphogenetic events and because *Xenopus* do not require heart function to survive (at least until the late tadpole stage of development) since nutrient exchange readily occurs by diffusion. Herein, we show that FAK-depleted tadpoles exhibit abnormal myocardial morphogenesis accompanied by pericardial edema and

early embryonic lethality. Our mechanistic studies reveal that FAK activation, likely by FGFs, facilitates myocyte proliferation in the pre-looped heart tube, thus contributing to the complex process of looping morphogenesis.

RESULTS

Inhibition of FAK by morpholino-injection

FAK plays a critical function in murine development and is necessary for myocardial compaction. However, no studies to date have addressed a specific role for FAK in early cardiac development, specifically in regulating cardiac morphogenesis ((DiMichele *et al.*, 2009; Furuta *et al.*, 1995; Peng *et al.*, 2008). To study the time-dependent requirements for FAK during this intricate process, we depleted FAK protein in *Xenopus*, which develop a fully functioning three-chambered heart by 72 hr post-fertilization. To this end, we designed two FAK-specific antisense morpholinos to target sequences either upstream of, or flanking, the start codon of *Xenopus fak* (denoted FAK Mo and xFAKst, respectively). Both morpholinos significantly reduced flag-tagged FAK protein production in an *in vitro* transcription/translation assay, with FAK Mo being slightly more potent (data not shown).

To establish that FAK Mo effectively blocks FAK translation *in vivo*, we injected standard quantities (20 and 40ng) into single-cell fertilized *Xenopus* embryos. Western blot analysis of stage 22, 26, and 39 embryos confirmed that FAK protein levels were reduced in a dose-dependent manner (Fig. 2.1A). We next performed further temporal analysis of FAK levels during development in embryos injected with 40 ng of either control morpholino (Con Mo) or FAK Mo. As previously reported we found that a low level of maternal FAK was apparent in fertilized eggs which persisted throughout the onset of gastrulation (stage 10.5) at

which time embryonic FAK protein was markedly induced (Hens and DeSimone, 1995). As expected, maternal FAK was not depleted by FAK Mo, which was designed to block translation of nascent transcripts. However, injection of FAK Mo at the one-cell stage did reduce embryonic FAK levels by stage 10.5 and FAK protein was nearly undetectable by Western analysis in the morphants during cardiogenesis (stage 28-39) (Fig. 2.1A, B). Densitometric analysis of Western blot band intensities demonstrated that FAK protein expression in FAK morphant embryos was reduced by greater than 80% as compared to controls by stage 28 (Fig. 2.1C). FAK activity was also ablated in FAK-depleted embryos at these stages as assessed by Western blotting for phospho-FAK with Y-397 antibody (data not shown). Importantly, no changes in FAK expression were evident after injection of a control five-base mismatch morpholino (data not shown). Moreover, Western blot analysis for the protein tyrosine kinase, PYK2, demonstrated that FAK Mo did not disrupt the translation of this closely related FAK family member (Fig. 2.1D).

FAK-depletion results in abnormal cardiac morphogenesis

FAK morphant embryos exhibited a slight developmental delay beginning around stage 10 but underwent normal gastrulation and neurulation as assessed by gross morphology (data not shown). Furthermore, *in situ* hybridization analysis demonstrated that the mesodermal markers, chordin, brachyury, and Myo-D were expressed in the appropriate spatiotemporal pattern in both Con Mo- and FAK Mo-injected embryos at stages 10, 16, and 22 (Fig. 2.2) suggesting that early mesodermal development was also unperturbed in the FAK morphants. The lack of effect on these early developmental processes is not surprising given that heterozygous FAK null mice are viable (Ilic *et al.*, 1995) and that FAK protein

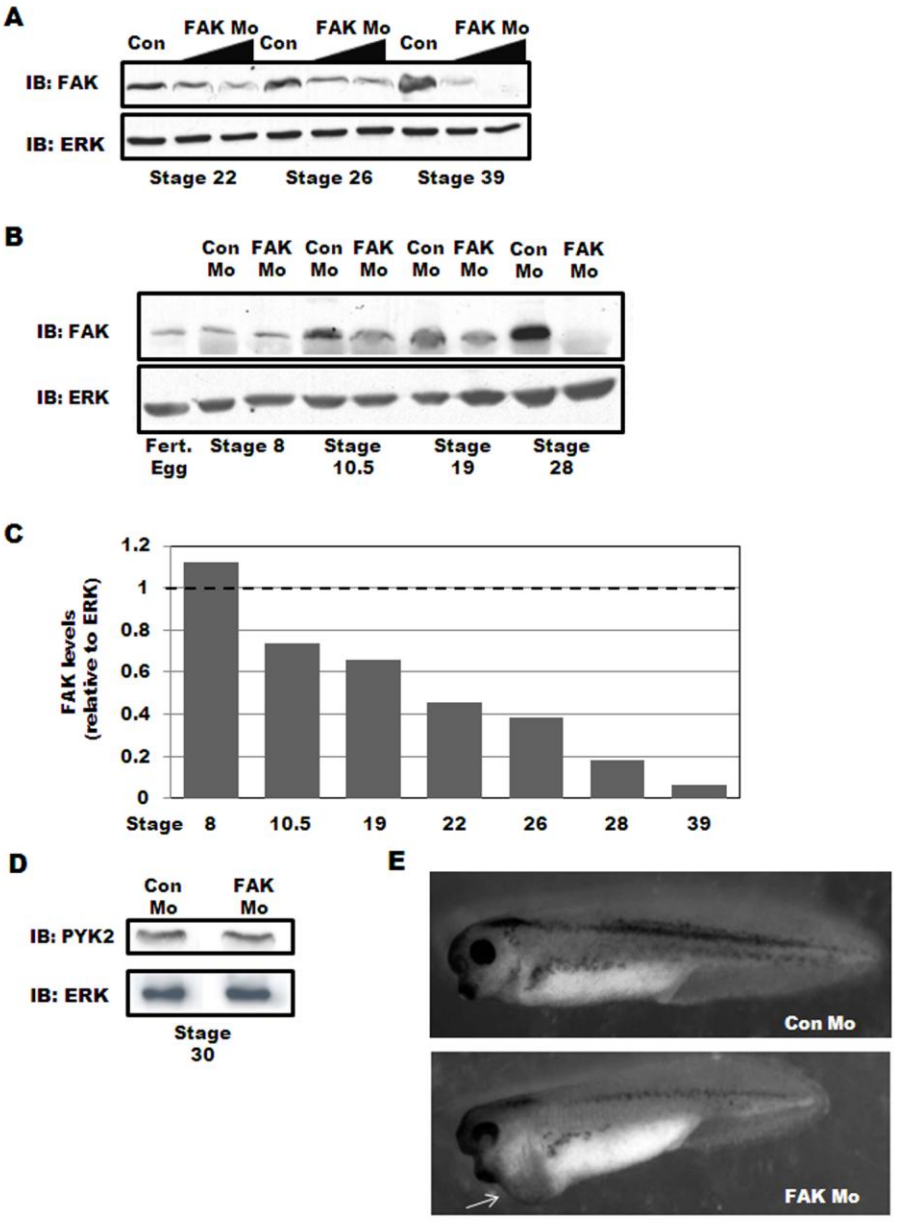
A
Con
FAK Mo
Con
FAK Mo
Con
FAK Mo
IB: FAK
IB: ERK
Stage 22
Stage 26
Stage 39
B
Con Mo
FAK Mo
Con Mo
FAK Mo
Con Mo
FAK Mo
Con Mo
FAK Mo
IB: FAK
IB: ERK
Fert. Egg
Stage 8
Stage 10.5
Stage 19
Stage 28
C
FAK levels (relative to ERK)
1.2
1
0.8
0.6
0.4
0.2
0
Stage 8
10.5
19
22
26
28
39
D
Con Mo
FAK Mo
IB: PYK2
IB: ERK
Stage 30
E
Con Mo
FAK Mo

Figure 2.1. Depletion of FAK in Xenopus laevis leads to pericardial edema. A) FAK or Control morpholinos (20 and 40 ng) were injected into fertilized oocytes and embryonic FAK protein levels were assessed at the indicated stages by Western blotting. Levels of ERK are shown as a control for loading. B) Western blot analysis for FAK in Con Mo- and FAK Mo-injected embryos (40 ng/embryo) at the indicated stages of development. Levels of ERK are shown as a control for loading. C) Densitometric analysis of Western blots comparing FAK band intensity relative to ERK. Data are presented as FAK levels in FAK Mo-embryos relative to Con Mo-embryos (set to 1) at each developmental stage analyzed. D) Western blot analysis for PYK2 (and ERK) in stage 30 Con Mo- and FAK Mo-injected embryos. E) Gross morphology of Control and FAK morphant tadpoles at stage 37. FAK morphants exhibit a slightly shortened anteroposterior axis and pericardial edema (arrow).

Incidence of Edema

	Con Mo	FAK Mo
Trial 1	0% (n=51)	85.2% (n=27)
Trial 2	2.5% (n=79)	92.3% (n=78)
Trial 3	4% (n=26)	61.4% (n=44)

Table 2.1. FAK depletion leads to marked pericardial edema. Embryos were scored for pericardial edema between stages 34-39 in three separate trials.

Phenotypic Analysis of FAK Morphants

	Total # Embryos	A/P axis defects (% of total)	Anterior Defects (% of total)
Con Mo	174	5 (3%)	3 (2%)
FAK Mo	191	22 (12%)	16 (8%)

Table 2.2. Phenotypic analysis of gross morphological abnormalities in FAK morphant embryos. Embryos exhibiting truncated or bent anteroposterior body axis (A/P axis defects) or anterior defects (such as small head) were scored between stages 27-30 in at least three separate experiments and aggregate totals for each phenotype are reported. As noted in the text, these embryos (and embryos exhibiting developmental arrest prior to stage 30) were not utilized for later analysis of heart development.

levels in our model system were not reduced by greater than 50% until after commencement of these critical developmental stages (Fig. 2.1C).

Interestingly, by stage 34, a large percentage of FAK-depleted embryos (79.6%) showed pronounced pericardial edema (Fig. 2.1E and Table 1), indicating a morphogenetic cardiac abnormality. Indeed, whole mount immunohistochemical staining of stage 39 hearts with cardiac myosin heavy chain (MHC) or tropomyosin antibodies revealed marked dys-morphogenesis in the majority of FAK morphant embryos. Although all hearts in Con Mo-injected embryos were fully looped with three distinct chambers, FAK Mo-injected embryonic hearts exhibited bent or twisted heart tubes that failed to fully undergo looping (Fig. 2.3). Other less penetrant phenotypes included anterior defects (such as decreased head size), a shortened antero-posterior axis, and developmental arrest prior to stage 30 (Supplemental Table 1). Embryos that exhibited signs of these less frequent abnormalities were excluded from subsequent analysis of cardiac morphology. Notably, all FAK-depleted tadpoles died by stage 42 indicating an essential role for FAK in *Xenopus* development.

To further confirm that looping morphogenesis was dependent on FAK, we utilized a phenotypic rescue approach. After aligning the sequences of *Xenopus* and chicken *fak*, we reasoned that FAK Mo would not interfere with chicken FAK translation, and subsequent *in vitro* transcription/translation assays confirmed this assertion (data not shown). Thus, we injected embryos at the one cell stage with either FAK Mo or a combination of FAK Mo and 2ng chicken FAK capped-RNA (cFAK; denoted 'rescue') and assessed cardiac morphology at stage 37-39. Importantly, Western blot analysis confirmed that rescued embryos expressed FAK protein at near endogenous levels (Fig. 2.3B). We next assessed cardiac morphology using whole-mount MHC antibody staining and quantified properly looped hearts. As shown

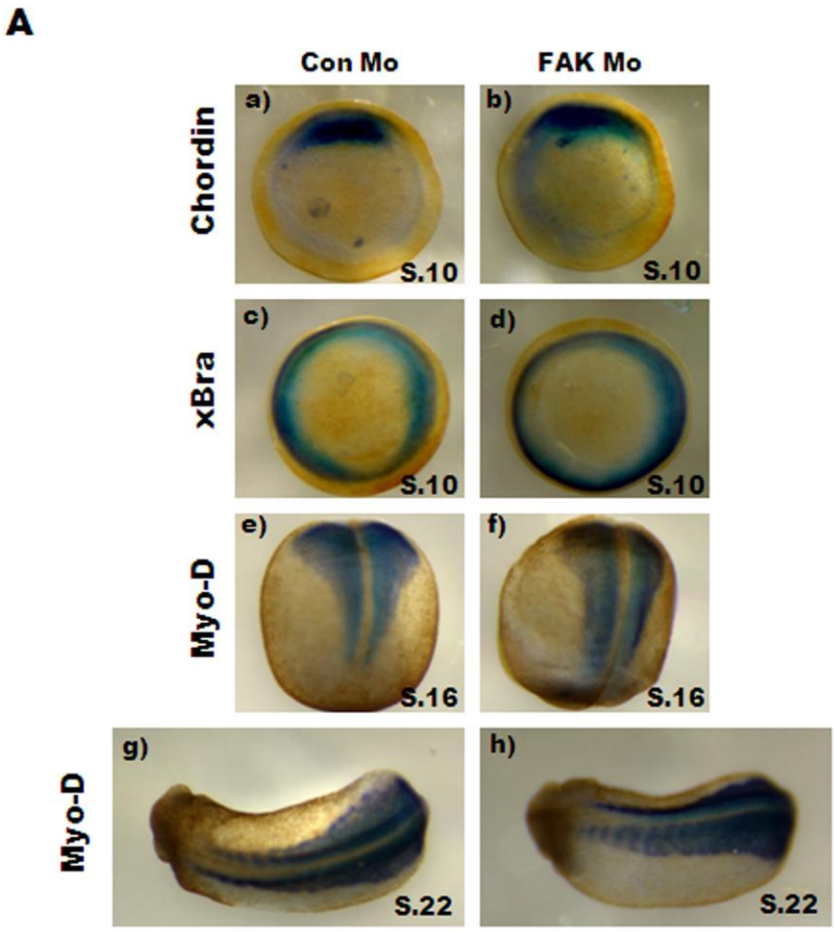
A
Con Mo
FAK Mo
Chordin
a)
S.10
b)
S.10
xBra
c)
S.10
d)
S.10
Myo-D
e)
S.16
f)
S.16
Myo-D
g)
S.22
h)
S.22

Figure 2.2. Gastrulation and neurulation proceed normally in FAK morphant embryos. *In situ* hybridization analysis for chordin (a, b) and brachyury (xBra) (c, d) were performed at stage 10. Views for a-d are vegetal with dorsal to the top. Myo-D *in situ* hybridization was performed at stage 16 (e, f – dorsal view) and stage 22 (g, h – dorsal view with anterior to the left).

in figure 2.3C and D, expression of 2ng cFAK induced a demonstrable rescue of the morphant phenotype, as 67% of dually-injected embryos exhibited normal three-chambered hearts, compared to only 30% observed following injection of FAK Mo alone. Collectively, these results demonstrate that FAK is required for appropriate morphogenesis of the multi-chambered heart.

FAK morphants exhibit appropriate specification, midline migration and differentiation of cardiac precursors

To define the FAK-dependent mechanisms involved in chamber morphogenesis, we analyzed control and FAK-depleted hearts at various stages of development. As noted above, the initial step of heart formation involves the bilateral movement of cardiac progenitors (cardioblasts) to the ventral midline of the embryo where they fuse prior to formation of the linear heart tube, a process that occurs between stages 28 and 32 in *Xenopus* embryos. We performed *in situ* hybridization to examine the spatiotemporal expression pattern of several cardioblast marker genes to determine whether the cardiac precursors were specified and properly redistributed in the FAK morphants. The nkx2.5, tbx5, and tbx20 expression domains of Con Mo- and FAK Mo-injected embryos were comparable between stage 26-32 and semi-quantitative PCR analysis confirmed similar transcript levels of these cardioblast markers in Con Mo- and FAK Mo-injected embryos at stages 30 and 32 (Fig. 2.4A, B and data not shown). Moreover, the myocyte differentiation markers tropomyosin and troponin I were expressed at similar levels in FAK Mo- and Con Mo- injected embryos as assessed by semi-quantitative RT-PCR and immunohistochemistry (Figure 2.4C and data not shown). Indeed, 3-D rendering of MHC-stained stage 30 FAK morphant embryos revealed a continuous sheet of myocytes, confirming appropriate differentiation and fusion at the ventral

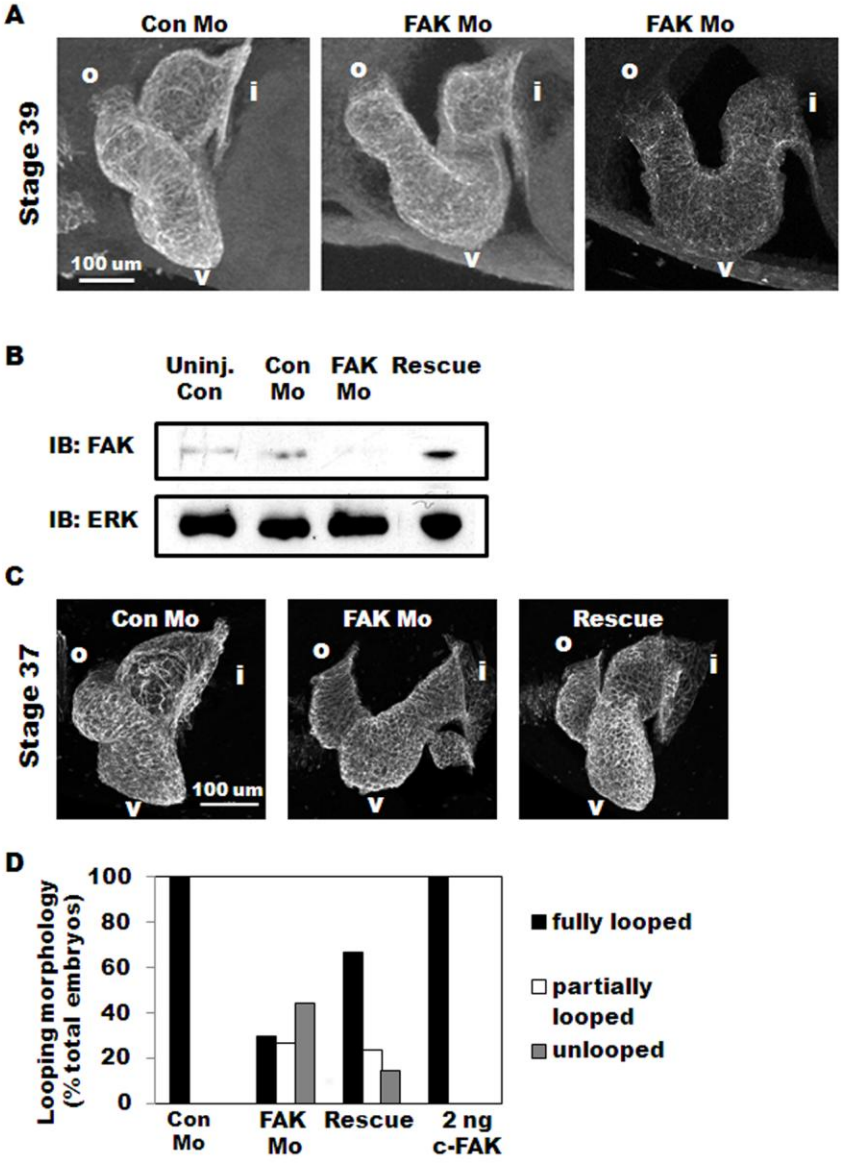
A
Con Mo
FAK Mo
FAK Mo
Stage 39
o
i
v
100 um
B
Uninj. Con
Con Mo
FAK Mo
Rescue
IB: FAK
IB: ERK
C
Con Mo
FAK Mo
Rescue
Stage 37
100 um
D
Looping morphology (% total embryos)
100
80
60
40
20
0
Con Mo
FAK Mo
Rescue
2 ng c-FAK
fully looped
partially looped
unlooped

Figure 2.3. FAK morphant embryos exhibit marked cardiac dysmorphogenesis. A) Lateral view of whole-mount immunohistochemistry for tropomyosin reveals a fully looped three-chambered heart in Con Mo- injected embryos while those injected with FAK Mo appear distended and partially looped (middle panel) or unlooped (right panel). Anterior is to the left and dorsal toward the top in all panels. Regions of interest are labeled as follows: i= inflow tract, v=ventricle, o=outflow tract. B) Western blot analysis for FAK in uninjected, Con Mo-injected, FAK Mo-injected, and rescue embryos at stage 37. Levels of ERK are shown as a control for loading. C) Lateral view of whole-mount immunohistochemistry for MHC reveals rescue of the FAK morphant phenotype is achieved by co-expression of 2ng chicken FAK. D) Heart morphology analysis of Con Mo-injected, FAK Mo-injected, rescue (FAK Mo and 2 ng chicken FAK co-injection), and 2ng chicken FAK alone demonstrates that while FAK morphant embryos exhibit full looping in only 30% of embryos examined, rescue embryos exhibit full looping morphology in 67%. Total number of embryos analyzed were n=27 (Con Mo), n=34 (FAK Mo), n=42 (Rescue), n=20 (2ng c-FAK), collected from two separate experiments.

midline (Fig. 2.4D). Moreover, despite subsequent aberrant morphogenesis, FAK-depleted cardiac tissue exhibited normal rhythmic contractions (data not shown). Collectively, these results indicate that specified cardiac precursors migrated to the ventral midline and expressed markers of terminal differentiation in a FAK-independent manner.

FAK morphants form linear heart tubes but fail to undergo appropriate looping morphogenesis

Considering that the initial stages of cardiogenesis were not affected by FAK depletion, we hypothesized that FAK may play an integral role in looping morphogenesis. To test this possibility, we performed additional whole-mount tropomyosin antibody staining and analyzed cardiac morphology using laser scanning confocal microscopy and 3D isosurfacing. By stage 32, when the heart tube is undergoing closure at the dorsal surface, Con Mo- and FAK Mo- injected embryos appeared similar (Fig. 2.5A); however analysis of the dorsal aspect of the heart revealed that complete closure of the heart tube had not occurred in FAK morphant embryos at this time (Fig. 2.6). Despite this delay, all FAK morphant embryos analyzed at later stages exhibited fully closed heart tubes (Fig. 2.6). However, analysis of FAK morphants at stage 34 onward demonstrated a marked deficiency in heart tube looping. Indeed, the majority of stage 34 FAK morphant hearts exhibited a straight or only slightly bent appearance (Fig. 2.5B and Fig. 2.6). Notably, injection with either Con Mo or five-base mismatch morpholinos did not affect cardiac morphogenesis when compared to uninjected embryos, indicating that the phenotypes observed were due to FAK depletion.

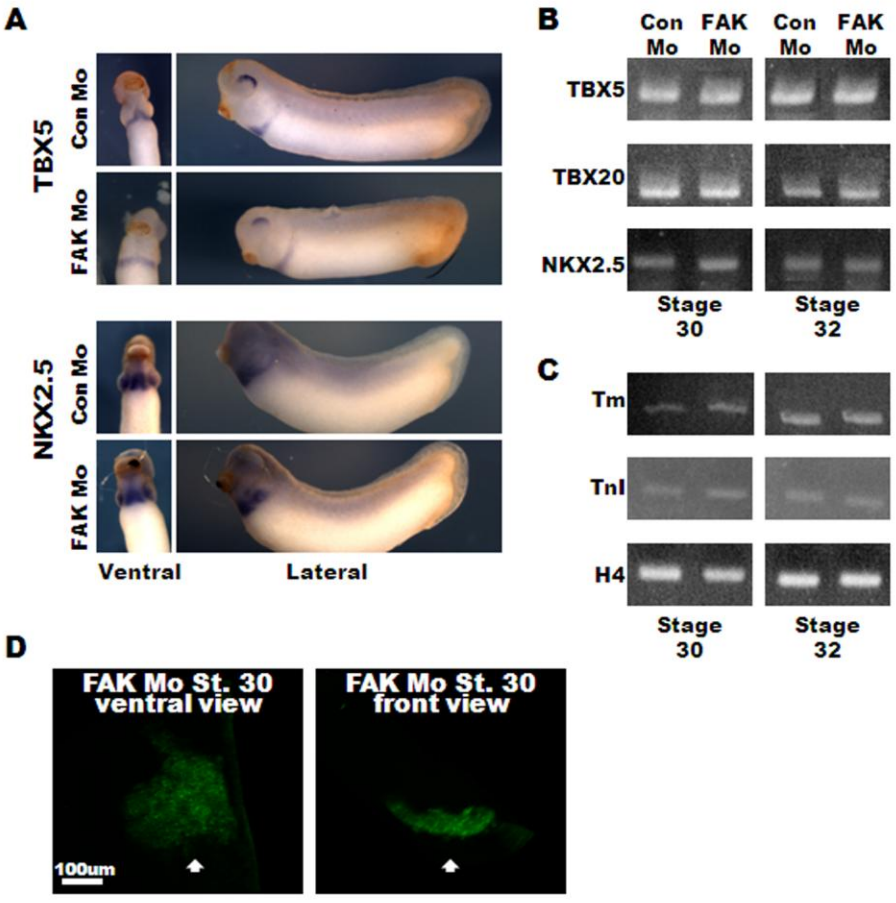
A
TBX5
Con Mo
FAK Mo
NKX2.5
Con Mo
FAK Mo
Ventral
Lateral
B
Con Mo
FAK Mo
Con Mo
FAK Mo
TBX5
TBX20
NKX2.5
Stage 30
Stage 32
C
Tm
TnI
H4
Stage 30
Stage 32
D
FAK Mo St. 30 ventral view
FAK Mo St. 30 front view
100um

Figure 2.4 FAK depletion does not impact cardiac specification or differentiation. A) *In situ* hybridization of stage 30 embryos for TBX5 and NKX2.5. Ventral views (left panels) are oriented with anterior toward the top, lateral views (right panels) are oriented with anterior to the left and dorsal to the top. B and C) RT-PCR analysis at stages 30 (left panels) and 32 (right panels) for TBX5, TBX20, NKX2.5 (B), and tropomyosin (tm), and Troponin T (TnT) (C). Histone H4 (H4) serves as a control. Data represent results from 10 embryos per condition and experiments were repeated at least twice. D) Ventral and front views of whole-mount immunohistochemistry for MHC reveals a continuous and fused sheet of differentiated myocytes at the ventral midline (indicated by white arrow) in FAK Mo-injected embryos. Images represent 3D reconstructions of confocal z-stack sections..

Since differential rates and/or locales of cell proliferation within the heart tube have been correlated with appropriate looping morphogenesis (Ribeiro *et al.*, 2007), we determined whether cardiomyocyte proliferation was impaired in FAK-depleted embryos. To test this possibility, we immunostained Con Mo- and FAK Mo- injected embryonic heart tubes for tropomyosin and phospho-specific histone H3 (pH3) and imaged the hearts using laser scanning confocal microscopy. As shown in figure 2.7, we observed a significant decrease in the total number of pH3-positive cardiomyocytes in pre-looped (stage 32) FAK Mo hearts relative to controls. Notably, pH3 staining in the surrounding non-cardiac tissue was comparable between Con Mo- and FAK Mo- injected embryos, indicating that FAK depletion did not induce a global reduction in cellular proliferation (Fig. 2.7B). Double-immunolabeling with tropomyosin and cleaved caspase 3 antibodies revealed no significant difference in cardiomyocyte apoptosis between Con Mo- and FAK Mo-injected embryos (Fig. 2.8), consistent with our previous findings that FAK depletion does not induce apoptosis in developing mouse hearts (Hakim *et al.*, 2007). Collectively, these data indicate that the looping defect found in FAK morphant embryos may be due, at least in part, to impaired cardiomyocyte proliferation.

FAK regulates FGF-dependent myocyte proliferation

Proper development of the myocardium is dependent on the close interaction with (and signaling from) the endo- and epi-cardium. FGFs are potent regulators of embryonic myocyte proliferation (Lavine and Ornitz, 2008; Lavine *et al.*, 2008), and given evidence from our lab that FAK activity is required for FGF-induced Map kinase signaling (DiMichele *et al.*, 2009) and that inactivation of FAK phenocopies the non-compaction defects observed

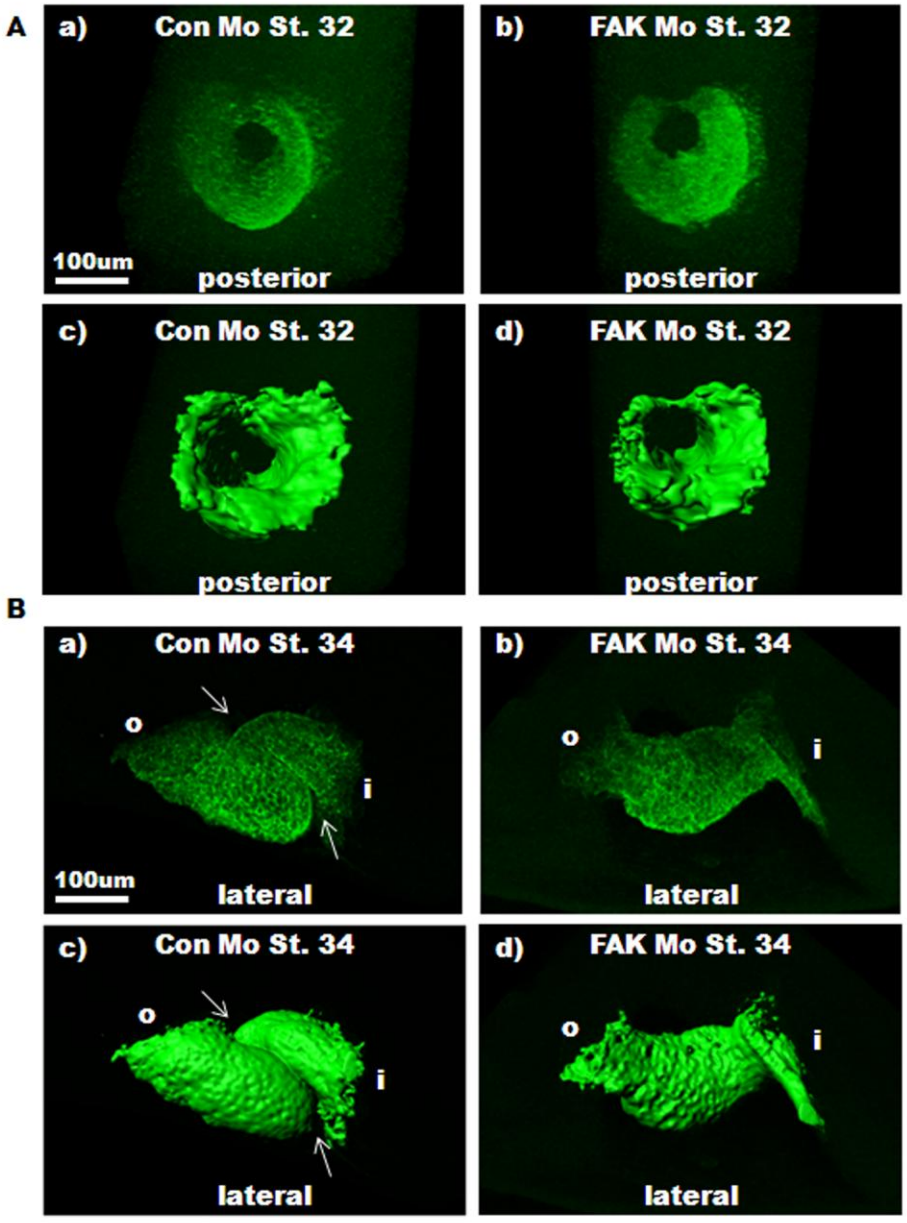
A
a) Con Mo St. 32
b) FAK Mo St. 32
100um
posterior
posterior
c) Con Mo St. 32
d) FAK Mo St. 32
posterior
posterior
B
a) Con Mo St. 34
b) FAK Mo St. 34
o
i
o
i
100um
lateral
lateral
c) Con Mo St. 34
d) FAK Mo St. 34
o
i
o
i
lateral
lateral

Figure 2.5 FAK depletion impairs looping morphogenesis. Whole mount immunohistochemical staining for tropomyosin was performed on stage 32 (A), and 34 (B) embryos that were injected with either Con Mo (left) or FAK Mo (right) at the one-cell stage. Images represent 3D reconstructions of confocal z-stack sections (top) and Imaris isosurfacing (bottom). Stage 32 view is from the posterior looking through the heart tube toward the anterior end; dorsal is to the top. Stage 34 view is lateral with anterior to the left, dorsal to the top. Note that looping is perturbed in stage 34 FAK morphants. Arrows point to region of interest where the heart takes on a spiral shape indicative of looping morphogenesis.

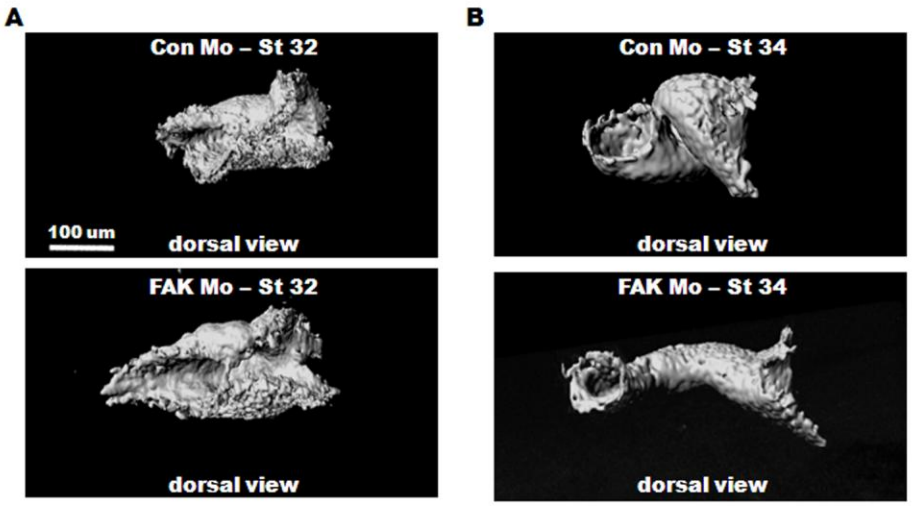
A
Con Mo – St 32
100 um
dorsal view
FAK Mo – St 32
dorsal view
B
Con Mo – St 34
dorsal view
FAK Mo – St 34
dorsal view

Figure 2.6 Isosurfacing of Con Mo and FAK Mo hearts revealed a delay in closure of the heart tube at the dorsal surface at stage 32 but not 34. A) Dorsal view of isosurfaced and 3-D rendered images from stage 32 hearts (anterior is to the top). Note that FAK morphant hearts have only begun to close at the dorsal aspect of the heart tube, while controls have undergone complete closure. B) By stage 34, closure of the heart tube is complete (dorsal view).

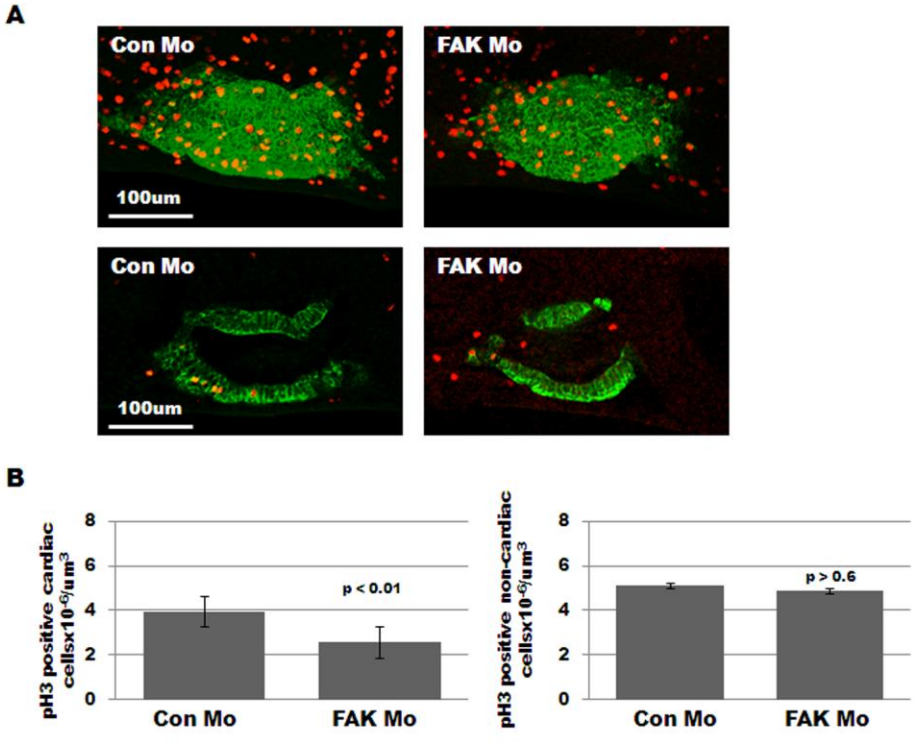
A
Con Mo
FAK Mo
100um
Con Mo
FAK Mo
100um
B
pH3 positive cardiac cellsx10-6/um3
8
6
4
2
0
p < 0.01
Con Mo
FAK Mo
pH3 positive non-cardiac cellsx10-6/um3
8
6
4
2
0
p > 0.6
Con Mo
FAK Mo

Figure 2.7 Myocyte mitosis is attenuated in FAK morphant heart tubes. A. Whole mount immunohistochemical staining for tropomyosin (green) and phospho-Histone H3 (red) was performed on pre-looped (stage 32) embryos that were injected with either Con Mo (left) or FAK Mo (right) at the one-cell stage. Images represent 3D reconstructions of confocal z-stack sections (top panels) or a single optical section (bottom panels). B. Total number of pH3 positive myocytes and non-cardiac cells were counted in each optical section of Con Mo- and FAK Mo-injected embryos (19 embryos were analyzed per condition, collected from at least 3 separate experiments).

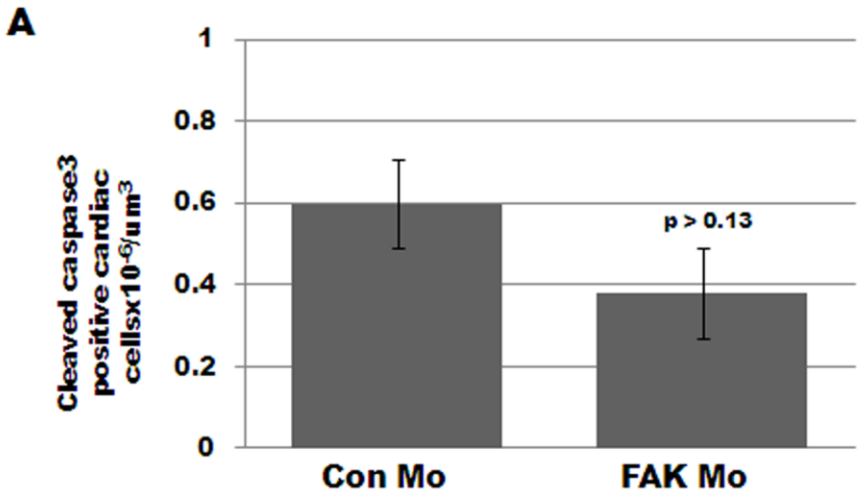
A
Cleaved caspase3 positive cardiac cellsx10-6/um3
1
0.8
0.6
0.4
0.2
0
p > 0.13
Con Mo
FAK Mo

Figure 2.8 FAK deficiency does not alter myocyte survival. Whole mount immunohistochemical staining for tropomyosin and cleaved caspase 3 was performed on pre-looped (stage 32) embryos that were injected with either Con Mo (left) or FAK Mo (right) at the one-cell stage. Total number of cleaved caspase 3- positive myocytes per unit area of myocardium were counted as described in figure 5 (3 embryos for each condition were analyzed in three separate experiments).

in FGF Receptor 1 (FGFR1) knock-out mice, we reasoned that FAK may play a major role in regulating cardiac morphogenesis mediated by epicardial-derived FGFs.

To test whether FGF signaling was required for *Xenopus* heart looping, we treated embryos with a selective FGFR1 tyrosine kinase inhibitor, SU5402 (Langdon *et al.*, 2007; Mohammadi *et al.*, 1997). As shown in figure 2.9, continuous exposure of embryos to SU5402 (50 μM) during cardiogenesis (stage 25-37) resulted in small and dysmorphic hearts, although the embryos appeared relatively normal in size and shape (Fig. 2.9A, B). Importantly, the hearts of the SU5402-treated embryos resemble the FAK morphant hearts in that they fail to undergo looping (Fig. 2.9B and Table 2.3). This phenotype was highly penetrant (observed in 94% of treated embryos) while no looping defects were observed in embryos treated with DMSO (vehicle). These data indicate that both FGF- and FAK-dependent signals play an important role in coordinating chamber growth and morphogenesis.

To determine whether FAK might coordinate mitogenic cues initiated by FGF, we first determined whether FGF stimulates FAK activity in rat primary cardiomyocytes in culture. Importantly, Western blot analysis showed that basic fibroblast growth factor (bFGF) induced a marked increase in FAK activity in cardiomyocytes and that SU5402, dramatically reduced this response (Fig. 2.10A). It is well established that the FAK splice variant, FAK-related non-kinase (FRNK), can serve as a dominant interfering mutant that downregulates FAK-mediated signaling pathways (Richardson and Parsons, 1996). We previously generated FRNK adenoviruses that are well-suited for studying FAK-dependent processes in cultured cardiomyocytes. Therefore, to determine whether FAK was essential for FGF-stimulated myocyte proliferation, we infected embryonic rat cardiomyocytes with 10 multiplicity-of-

infection (m.o.i) green fluorescent protein (GFP) or GFP-FRNK adenovirus (Figure 2.10B) and examined the rate of proliferation of these cells in serum-free (SF) medium in the absence or presence of bFGF. GFP and GFP-FRNK were efficiently expressed in 100% of the cardiomyocyte population as determined by immunofluorescence (data not shown). Under these conditions, bFGF induced the rate of 5-bromo-2-deoxyuridine (BrdU) incorporation in GFP-infected cells by approximately 20%, whereas only 4% of FRNK-infected cells were BrdU-positive (Fig. 2.10C). Collectively, these data indicate that FAK activity is necessary for mediating FGFR-dependent cardiomyocyte proliferation, an event that may control both looping morphogenesis and growth of the embryonic heart.

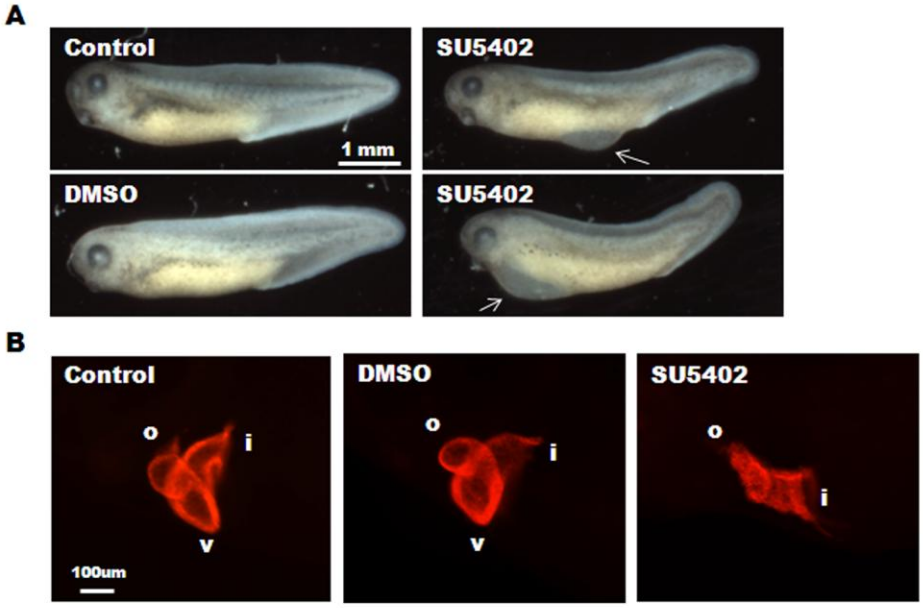
A
Control
1 mm
SU5402
DMSO
SU5402
B
Control
o
i
v
100um
DMSO
o
i
v
SU5402
o
i

Figure 2.9 Treatment with the FGFR1-inhibitor, SU5402, impairs cardiac looping. Widefield microscopic analysis (A) of gross morphology of untreated control, DMSO-treated (2.5 µM), or SU5402-treated (50 µM) embryos at stage 37 reveals that SU5402 treatment induces edema in the middle-ventral region of the embryo (top right panel) or pericardial edema (bottom right panel) in some embryos. Arrows point to regions of edema. B) Lateral view of whole-mount immunohistochemistry for MHC reveals a fully looped three-chambered heart in untreated and DMSO-treated embryos while those treated with SU5402 appear unlooped. Anterior is to the left and dorsal is to the top in all panels. Total number of embryos analyzed for heart morphology were: n=22 (untreated), n=34 (DMSO), and n=35 (SU5402) and were collected from 3 separate experiments.

Phenotypic analysis after treatment with SU5402

Treatment (# embryos)	untreated (n=22)	DMSO (n=34)	SU5402 (n=35)
Anterior defect	0 (0%)	1 (3%)	1 (3%)
Middle-ventral region edema	0 (0%)	0 (0%)	4 (11%)
Pericardial edema	0 (0%)	0 (0%)	12 (34%)
Unlooped heart	0 (0%)	0 (0%)	33 (94%)

Table 2.3. Treatment with SU5402 causes defects in cardiac looping morphology. Embryos were scored for gross morphology in three separate experiments. As shown, SU5402 induced edema and cardiac looping defects. Several embryos exhibited both edema and an unlooped heart, therefore the totals do not add up to 100%.

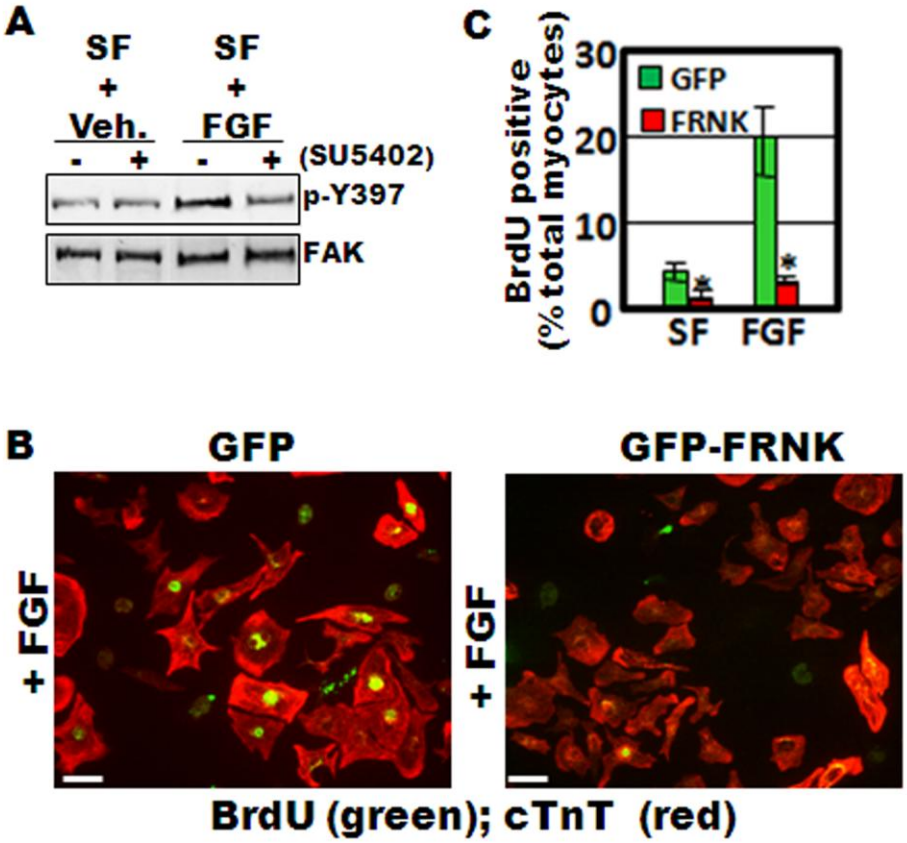
A
SF
+
Veh.
SF
+
FGF
- + - +
(SU5402)
p-Y397
FAK
C
BrdU positive
(% total myocytes)
30
20
10
0
GFP
FRNK
SF
FGF
B
GFP
GFP-FRNK
+ FGF
+ FGF
BrdU (green); cTnT (red)

Figure 2.10 FAK is activated by FGF and is necessary for FGF-dependent myocyte proliferation. A) Western blot analysis of cell lysates isolated from primary embryonic rat cardiomyocytes. Cells were maintained in serum free (SF) media and treated with bFGF (100ng/ml) or vehicle (veh.) for 30 min with or without 10 min pre-treatment with the specific FGFR-inhibitor, SU5402 (10 μM). Lysates were immunoblotted with antibodies directed towards phospho-specific Y397-FAK or total FAK B) BrdU incorporation in isolated embryonic cardiomyocytes infected with GFP- or GFP-FRNK adenovirus (10 m.o.i). Cells were maintained in serum-free medium and treated with vehicle (not shown) or bFGF (100 ng/ml) for 24 hr. Costaining with anti–cardiac troponin T (cTnT) was performed to identify cardiomyocytes. C, Quantification of BrdU- positive cardiomyocytes (means±SEM; N=3; minimum of 300 cells/condition). Scale bar is 20 μm.

DISCUSSION

Previous studies have demonstrated an essential role for FAK during embryonic development in mice but not flies (Grabbe *et al.*, 2004; Ilic *et al.*, 1995). FAK null mice exhibit general cardiovascular defects that were not reported in FAK-depleted *Drosophila*. A major notable difference between the cardiovascular systems of these two species is that *Drosophila* contains a simple linear heart tube that does not undergo looping morphogenesis. Although recent studies in myocyte-restricted FAK-depleted mouse hearts revealed that FAK is necessary for growth of the four chambered heart (DiMichele *et al.*, 2009; Peng *et al.*, 2008), no studies to date have addressed a role for FAK in regulating cardiac looping. Our current findings show that FAK-depleted *Xenopus* embryos exhibit pronounced pericardial edema, cardiac dysmorphogenesis, and embryonic death. Temporal assessment of cardiac morphogenesis revealed that FAK depletion did not affect the midline migration or differentiation of cardiac precursors. However, depletion of FAK markedly reduced proliferation in pre-looped hearts in comparison to stage-matched controls and induced a profound defect in looping morphogenesis.

We found that FAK-depleted *Xenopus* embryos died by stage 42, which is relatively late in development in comparison to FAK-depleted mice (E8-10.5). Prolonged survival in FAK-depleted *Xenopus* may be due, in part, to the enhanced nutrient exchange that is known to permit uncoupling of heart and embryonic development in this species until late tadpole stages. However, it is also possible that the presence of maternal FAK (which is refractory to the FAK morpholino) may have been sufficient to drive early FAK-dependent morphogenetic processes in the studies presented herein. Indeed, we found a low level of maternal FAK protein in both Con Mo- and FAK Mo- injected embryos until at least stage

10.5 (the onset of gastrulation), consistent with previous studies of FAK expression during *Xenopus* development (Hens and DeSimone, 1995). Therefore, while FAK-depleted *Xenopus* embryos gastrulate and neurulate normally, the role of FAK in gastrulation has not been addressed in this study. Nonetheless, the translation of embryonically expressed FAK protein was dramatically reduced in the FAK morphants from stage 10.5 onwards, and FAK protein was nearly undetectable in these embryos during cardiogenesis. Thus, our findings that the migration of specified cardioblasts from the bilateral heart fields to the ventral midline and their differentiation into mature cardiomyocytes was not altered in the FAK morphants, indicates that these processes are both FAK-independent.

The finding that cardioblast migration was FAK-independent was somewhat surprising given that several published studies from our laboratory and others have indicated that FAK is essential for cell motility (Parsons, 2003). Notably, we previously showed that directional motility of cardiomyocytes requires FAK (Hakim *et al.*, 2007). Moreover, previous studies in zebrafish have revealed that the coordinated motility of cardioblasts to the midline is regulated by fibronectin (Trinh and Stainier, 2004b) and studies in *Drosophila* revealed a strong genetic interaction between the *Drosophila* β1 integrin and the guidance cue, Slit, in regulating cardioblast movement (Engel *et al.*, 2005; MacMullin and Jacobs, 2006). However, consistent with our finding that midline fusion of cardioblasts occurs normally in FAK-depleted *Xenopus* embryos, MacMullin et. al. found no phenotypic interaction between FAK and Slit (MacMullin and Jacobs, 2006), leading us to reason that distinct integrin-induced signals regulate cardioblast and cardiomyocyte motility. Indeed, cardioblast motility involves a sheet-like movement that is known to be dependent on cell-cell interactions, whereas we have shown that myocytes exhibit directional motility that

requires FAK-dependent lamellipodial protrusions (Hakim *et al.*, 2007). While previous studies have indicated a role for FAK in scratch wound closure of a confluent monolayer of fibroblasts (Hsia *et al.*, 2003; Sieg *et al.*, 1999) we have found that FAK is not necessary for wound closure in smooth muscle cells, indicating that the mechanisms that regulate sheet-like movements may be cell type specific (unpublished observations, JMT).

Our mechanistic studies herein indicate that FAK is essential for regulating myocyte proliferation within the developing heart tube. We found that FAK morphant hearts exhibited a decrease in mitotically active myocytes relative to controls prior to looping. This finding is significant because recent studies in zebrafish have demonstrated that looping morphogenesis is associated with a shift from homogeneous proliferation to increased proliferation within the presumptive atrial and ventricular chambers (Ribeiro *et al.*, 2007).

Several studies suggest that members of the FGF family (Itoh and Ornitz, 2004), including FGF-1 (Engelmann *et al.*, 1991, , 1993), bFGF (David *et al.*, 2003; Pasumarthi *et al.*, 1996), and FGF9 (Lavine *et al.*, 2005) are critical endoderm-derived mediators of myoycte proliferation during myocardial development. Interestingly, our previous studies indicated that myocyte-restricted inactivation of FAK in mice phenocopies the non-compaction defects observed in mice with myocyte-restricted deletion of FGFR-1 and FGFR-2 (DiMichele *et al.*, 2009). We now show that inhibition of either FAK or FGFR signaling in *Xenopus* leads to a failure of heart looping, that FGF stimulates FAK activity, and that FAK activation is necessary for FGFR-dependent myocyte proliferation *in vitro*. Since SU-5402 is an effective inhibitor of FGFR1, we hypothesize that FGFR1-dependent FAK activation is necessary for heart looping. However, it is formally possible that this compound may also inhibit other FGF receptor subtypes including FGFR4 and FGFR2 which

have been reported to be expressed at higher levels than FGFR1 in the developing *Xenopus* heart (Lea *et al.*, 2009). In terms of signaling, FGF receptors are linked to the MAPK signaling pathways which terminate in activation of ERK, c-Jun N-terminal kinase, and p38. Interestingly, several recent studies have indicated that p38 may function at the G_2/M checkpoint to block cardiomyocyte cell cycle progression (Engel *et al.*, 2006; Engel *et al.*, 2005) and we recently showed that expression of FRNK (or inactivation of FAK) promotes p38 activity and regulates expression of the p38-dependent cell cycle modifier, $p27^{kip}$ (DiMichele *et al.*, 2009). Thus, we hypothesize that FGFR-stimulated FAK activation leads to p38 repression and induction of the proliferative signals that may be necessary to drive looping morphogenesis.

Although FGFs provide mitogenic signals to embryonic cardiomyocytes, recent evidence in zebrafish indicates that FGFs are also necessary for recruitment and differentiation of the secondary heart field (SHF) (de Pater *et al.*, 2009). This population of cells contributes to right ventricle and outflow tract formation in zebrafish, chick, and mouse hearts, and was also recently identified in *Xenopus* (Brade *et al.*, 2007; de Pater *et al.*, 2009; Martinsen *et al.*, 2004; Sadaghiani and Thiébaud, 1987). Although the precise timing and extent of SHF contribution during frog heart development remains unclear, studies performed in chick and mouse indicate that SHF is not typically recruited until after looping morphogenesis (de Pater *et al.*, 2009; Martinsen *et al.*, 2004; Sadaghiani and Thiébaud, 1987). Thus, while it is formally possible that the abnormal morphogenesis observed in FAK morphant hearts may, in part, arise from a defect in this FGF-dependent process, this is unlikely the primary cause of dysmorphogenesis, since FAK morphants exhibit defects in pre-looped heart tubes.

In summary, our studies are the first to indicate that FAK is necessary for viability and cardiogenesis in *Xenopus*. FAK-depleted cardiac precursor cells migrated to the ventral midline, fused, and formed a linear heart tube. However, FAK morphant heart tubes exhibited a marked reduction in proliferating myocytes and a concomitant failure to undergo looping. Our studies in cultured cardiomyocytes confirmed that FAK regulates myocyte proliferation in a cell autonomous fashion and that FAK acts downstream of FGFRs to regulate this critical function.

MATERIALS AND METHODS

Embryo culture and microinjection

Preparation and injection of *X. laevis* embryos was carried out as previously described (Wilson and Hemmati-Brivanlou, 1995). Staging was performed according to Nieuwkoop and Faber (Nieuwkoop and Faber, 1994). Anti-sense morpholino oligonucleotides were designed against either the start site (xFAKst Mo) or the 5'-untranslated region (xFAKup Mo) of *Fak*. Sequences used were: xFAKup, 5' CTG ATG CTA GGT GTC TGT CAT ATT C 3' and xFAKst, 5' TCC AGG TAA GCC GCA GCC ATA GCC T 3'. We utilized two control morpholinos, a five-base mismatched morpholino, in which five nucleotides of the xFAKup Mo sequence were changed such that the morpholino no longer reacted with *Xenopus fak*, and a standard control morpholino (Con Mo) (Gene Tools, Philomath, OR, USA). Morpholinos were injected at a concentration of 40ng/embryo at the one-cell stage, except where indicated. All *in vivo* data shown herein represent experiments performed with xFAKup (hereafter referred to as FAK Mo). Similar results were obtained with xFAKst Mo (data not shown).

Capped chicken FAK RNA used for rescue experiments was first generated using the mMessage/mMachine capped RNA kit (Ambion), according to the manufacturer's instructions. RNA was quantified by spectrophotometry and diluted in RNase-free water. For overexpression, RNA was microinjected at a concentration of 2ng/embryo in a 10nL injection volume. For rescue experiments, FAK capped-RNA was mixed with FAK Mo in order to achieve 40ng FAK Mo and 2ng FAK capped-RNA per embryo (10nL injection volume).

Inhibitor treatments

Embryos for inhibitor experiments were cultured in normal culture media until stage 25, at which time the culture media was supplemented with 2.5mM dimethyl sulfoxide (DMSO) or 50μm SU5402 (Pfizer) (Langdon *et al.*, 2007). Embryos were cultured under these conditions until stage 37 and processed for immunohistochemical analysis to analyze heart morphology.

In vitro transcription/translation assays

In vitro transcription/translation assays were performed using the TnT Quick-Coupled Transcription/Translation System according to the manufacturer's instructions (Promega, Madison, WI, USA).

Whole mount- immunohistochemistry and -in situ *hybridization*

Embryos were prepared for whole-mount immunohistochemistry by fixation in Dent's fixative (80% methanol/20% dimethyl sulfoxide) or 4% paraformaldehyde and were then processed as previously described (Kolker *et al.*, 2000), except that the rehydration steps

were omitted for embryos fixed in paraformaldehyde. Fixed embryos were incubated overnight at 4°C with a primary antibody against α-myosin heavy chain (α–MHC) (Abcam, Cambridge, MA, USA) (1:500), tropomyosin (DSHB, Iowa City, Iowa, USA) (1:200), phospho-Histone H3 (pH3) (1:250) (Millipore, Billerica, MA, USA), or cleaved caspase 3 (1:250) (Cell Signaling, Danvers, MA, USA). Embryos were then washed and incubated overnight at 4°C with the appropriate Cy-3 or Alexa-488 conjugated secondary antibodies (1:200) and Topro-3 (1:1000) (Molecular Probes, Carlsbad, CA, USA) to stain the nuclei.

Whole-mount *in situ* hybridization was performed as previously described (Harland, 1991). Plasmids for MyoD, chordin, xBra, NKX2.5, TBX5, and Tbx20 were linearized and used to generate digoxigenin-UTP-labeled (Roche, Mannheim, Germany) antisense RNA probes using the appropriate restriction endonuclease and polymerase. Color detection was determined by BM Purple substrate (Roche) after incubation with alkaline-phosphatase conjugated anti-digoxigenin antibody.

Western Blot Analysis

Embryos (n=5-10) were snap-frozen in liquid nitrogen and protein lysates were generated as previously described (Kragtorp and Miller, 2006). Briefly, 5-10 embryos were lysed by brief (1-2 second) sonication in a modified RIPA buffer (10mM Tris pH 7.5, 100mM NaCl, 1mM EDTA, 1mM EGTA, 20mM $Na_4P_2O_7$, 1% Triton X-100). Cardiomyocytes were lysed in modified radioimmune precipitation assay buffer (50 mM Hepes, 0.15 M NaCl, 2 mM EDTA, 0.1% Nonidet P-40, 0.05% sodium deoxycholate, pH 7.2). Each lysis buffer contained a cocktail of protease and phosphatase inhibitors including 1 mM Na_3VO_4, 40 mM NaF, 10 mM Na_2 pyrophosphate, 100 μM leupeptin, 1 mM 4-(2-aminoethyl)benzenesulfonyl fluoride hydrochloride, 0.02 mg/ml soybean trypsin inhibitor,

and 0.05 trypsin inhibitory units/ml aprotinin. Samples were clarified by centrifugation twice at 14,000 x *g* at 4^{o}C and the supernatant was retained. Fifty micrograms of total protein was boiled in sample buffer and loaded onto a 10% SDS-acrylamide gel. Separated proteins were transferred onto nitrocellulose, blocked in 5% dry milk in Tris-Buffered Saline (TBS) + 0.1%Tween (TBST), and incubated overnight with primary antibody diluted in blocking solution. The following antibodies were utilized at a dilution of 1:1000 : FAK Clone 4.47 (Millipore), phospho-FAK Y397 (Invitrogen, Carlsbad, CA, USA), PYK2 (Cell Signaling), and ERK-CT (Millipore). Blots were incubated with the appropriate horseradish peroxidase-conjugated secondary antibodies (1:2000 dilution) (GE Healthcare, Piscataway, NJ, USA) and proteins were visualized by chemiluminescence (Thermo Scientific, Rockford, IL, USA). Densitometry of Western blot band intensities was performed using ImageJ 1.37v software (NIH).

RT-PCR Analysis

RNA was isolated from 10 embryos following lysis in Trizol according to the manufacturer's specifications (Invitrogen). Reverse transcription reactions were performed using the iScript cDNA kit (Bio-Rad, Hercules, CA, USA) and PCR reactions were performed using ExTaq polymerase (Takara Bio, Japan) following previously published primer sets and cycling parameters (Meadows *et al.*, 2008; Small *et al.*, 2005). Histone H4 primers were as follows: Forward 5' GGG ATA ACA TTC AGG GTA TC 3' and Reverse 5' CAT GGC GGT AAC TGT CTT C 3'.

Myocyte cell isolation, culture, infection, and treatment

Cardiomyocytes were isolated from embryonic day 13.5 (E13.5) rats with trypsin and collagenase digestion and were purified as described previously (Taylor *et al.*, 2000). The cells were re-suspended in medium containing a 4:1 mixture of Dulbecco's Modified Eagle Medium (DMEM):Media 199 containing 10% fetal calf serum and 1% penicillin-streptomycin and plated on tissue culture plastic for two consecutive 1-hr periods to remove non-cardiomyocyte cells, resulting in cultures with >95% myocytes. The cardiomyocytes were then plated on tissue culture dishes pre-coated with fibronectin (10 μg/ml). For adenoviral infection, cells were infected with replication-defective Ad5- GFP or GFP-FRNK at a concentration of 10 multiplicity of infection (m.o.i) for the indicated times in serum-containing media. Cells were then serum starved overnight and treated for the indicated times with FGF-2 (100ng/ml) or vehicle. 5-bromo-2-deoxyuridine (BrdU) labeling was performed as previously described (DiMichele *et al.*, 2009). The FGF-receptor 1 (FGFR1) inhibitor, SU-5402, was a generous gift from Pfizer (Kalamazoo, MI).

Widefield and laser scanning confocal microscopy, image deconvolution, and 3D rendering

Embryos were cleared for microscopic analysis in 2:1 benzyl benzoate:benzyl alcohol and placed on a glass coverslip. Embryos were analyzed by widefield microscopy using a Leica MZFLIII fluorescence dissecting scope or Olympus IX81 microscope or by confocal microscopy using an Olympus FV500 laser scanning confocal microscope (Olympus, USA) and Fluoview v5.1 software. Confocal z-stacks were obtained using a 1.24μm step-size. Z-series stacks were deconvolved using Autodeblur Gold v. X.1.4.1 software (Autoquant, Media Cybernetics, Bethesda, MD, USA). Deconvolved images were then imported to Imaris x64 6.1.5 software (Bitplane AG, St. Paul, MN, USA) for 3D rendering and isosurfacing.

To assess proliferation and apoptosis in *Xenopus* hearts, we immunostained embryos for tropomyosin (to label cardiomyocytes) and either pH3, to label proliferating cells, or cleaved caspase-3, to label cells undergoing apoptosis. Z-stack images of each heart were obtained by laser scanning confocal microscopy and each optical slice was examined individually throughout the thickness of the heart. Each cell that was immunoreactive for both tropomyosin and pH3 or cleaved caspase 3 was scored as a positive cardiomyocyte. In order to ensure that cells were not counted twice, we confirmed our results by counting all double-immunoreactive cells from optical sections that were 12 steps (14.88μm) apart (the approximate size of the embryonic myocyte). The surface area of the heart (μm^2) was calculated by isosurfacing the tropomyosin positive area using Imaris software. This calculated value was then multiplied by 28μm (the approximate thickness of the heart wall at this stage of development), resulting in a calculation of total heart volume (μm^3). Total non-cardiomyocytes were scored and compared to the volume of the tissue section analyzed. Statistical analyses were performed using a two-tailed t-test (two-sample, equal variance-homoscedastic).

GRAF IS REQUIRED FOR EMBRYONIC CARDIAC AND SKELETAL MUSCLE DEVELOPMENT

INTRODUCTION

Cells interact with the extra-cellular matrix (ECM) via adhesive complexes, termed focal adhesions, predominantly through interactions with integrins. Integrins serve both a structural role and are required for transduction of signaling pathways that regulate cellular adhesion, migration, proliferation, and differentiation. Notably, integrins have been implicated in a variety of model organisms to regulate embryonic cardiac and skeletal muscle development.

A key transducer of integrin signaling is the non-receptor tyrosine kinase, focal adhesion kinase (FAK). Integrin clustering induces FAK localization to focal adhesions and leads to its activation. Activated FAK binds a variety of focal adhesion proteins and can activate downstream signaling mechanisms such as those of the MAP kinase pathway. Through these and other mechanisms, FAK has been shown to be important for a variety of cellular processes such as cellular adhesion, migration, and regulation of cytoskeleton dynamics. In addition, FAK plays a vital role in organogenesis including cardiac and skeletal muscle development. Specifically, inactivation of FAK in *Xenopus* impairs somite rotation (Kragtorp and Miller, 2006) and we have recently shown that FAK is required for proper cardiac morphogenesis (see Chapter II of this thesis).

Striated (cardiac and skeletal) muscle development requires fine spatiotemporal coordination of multiple cellular processes including myoblast specification, exit from the

cell cycle, expression of muscle-specific transcripts, cellular attachment to the extracellular matrix (ECM), and elongation of myofibers (via maturation of the contractile apparatus). Skeletal and cardiac muscle cell-fate is controlled by the combinatorial activities of a variety of transcription factors which regulate specification and differentiation. For example, in skeletal muscle, myogenic basic helix-loop-helix transcription factors including MyoD induce specification and myogenin and MEF factors (MEF2a, MEF2c) induce differentiation by upregulation of muscle marker gene expression. Proper myogenic differentiation is a vital step in the development of the skeletal muscle and the heart as demonstrated in a variety of experimental systems.

RhoA has been demonstrated in cultured myoblasts to play critical roles during skeletal muscle differentiation. While early studies appeared controversial in that RhoA was found to both promote (Carnac *et al.*, 1998; Charrasse *et al.*, 2002; Kontaridis *et al.*, 2004; Sordella *et al.*, 2003; Takano *et al.*, 1998; Wei *et al.*, 1998) and interfere with (Beqaj *et al.*, 2002; Castellani *et al.*, 2006; Charrasse *et al.*, 2006; Meriane *et al.*, 2000; Travaglione *et al.*, 2005) the skeletal muscle differentiation program, more recent studies indicate that RhoA activity must be tightly regulated in a finely coordinated time-dependent manner during the intricate process of skeletal muscle development (Castellani *et al.*, 2006; Iwasaki *et al.*, 2008). Specifically, it appears that RhoA activity is necessary for the specification of myoblasts but RhoA activity must be down-regulated for the subsequent differentiation and fusion of myotubes.

RhoA is a member of a large family of small molecular weight GTPases which serve diverse roles in cytoskeletal dynamics, cell-cycle progression, cellular adhesion and migration, gene transcription, and differentiation (Etienne-Manneville and Hall, 2002). Rho-

family members switch between an active GTP-bound state and an inactive GDP-bound state. The intrinsic rate of hydrolysis of GTP- to GDP-binding can be accelerated by GTPase Activating Proteins (GAPs) and this typically leads to downregulation of Rho activity and downstream signaling events.

We previously cloned and characterized a GTPase activating protein for RhoA termed Graf that is poised to regulate and fine tune integrin- and Rho-dependent signals since it interacts directly with the C-terminus of focal adhesion kinase (Hildebrand *et al.*, 1996; Taylor *et al.*, 1998). Graf (GTPase regulator associated with FAK) is a 116-kDa protein that is comprised of an N-terminal BAR domain, a PH domain, a central Rho-GAP domain, a serine/proline rich domain, and a C-terminal SH3 domain. We previously reported that Graf is a specific GAP for RhoA (i.e. induces inactivation of GTP-RhoA) and that Graf is particularly abundant in terminally differentiated cells such as cardiomyocytes and neurons (Taylor *et al.*, 1999). We show for the first time that Graf is also specifically expressed in embryonic skeletal muscle concomitant with differentiation of this tissue type, suggesting that Graf may play a vital role in modulating Rho activity during this crucial time. We utilized antisense morpholinos to block Graf translation during *Xenopus* embryonic development and determined that Graf-depletion leads to decreased skeletal muscle marker expression, defective somite formation, and partial paralysis. In addition, Graf morphant embryos exhibited pericardial edema, cardiac dysmorphogenesis, and embryonic lethality by tadpole stages. Taken together, our data strongly suggest that Graf plays an essential role in myogenic differentiation *in vivo* and implicate Graf as a crucial regulator of Rho during embryonic cardiac and skeletal muscle development.

RESULTS

Expression of Graf in Xenopus embryos

Given our previous findings that Graf was most abundantly expressed in terminally differentiated cells of mammalian adult tissues (heart and brain), and that Graf acts as a GAP for RhoA in cultured cells, we predicted that Graf might play an important role in facilitating cell cycle withdraw and promoting cellular differentiation during development. To test this hypothesis, we sought to deplete Graf protein using an antisense-morphilino based approach in developing Xenopus embryos, a well-characterized model of early embryonic development. Notably, xGraf contains each of the functional domains previously defined in chicken and mammalian Graf including, in tandem, an N-terminal BAR domain, PH domain, GAP domain and C-terminal SH3 domain. Moreover, the overall identity/similarity of xGraf protein to its orthologues in human and mouse is 83.8% and 77.4%, respectively, indicating that the function of this protein is likely evolutionarily conserved between these species.

As the expression profile of xGraf had not been previously reported, we first performed semi-quantitative RT-PCR analysis of wild-type *Xenopus* embryos during development to identify the time-course of Graf expression. As shown in figure 3.1A, xGraf transcript is present at low levels throughout early development and expression increases from stage 25 through tadpole stages. In order to specifically assess the tissue distribution of Graf in Xenopus, we next performed a whole-mount in situ hybridization analysis of stage 29 embryos using a probe directed towards the 3'UTR of Graf. In accordance with our previous findings in rodents, we observed xGraf expression in the heart and brain (Figure 3.1B). Graf expression was also apparent in the neural tube, dorsal root ganglia, and somites (Figure 3.1B and C)

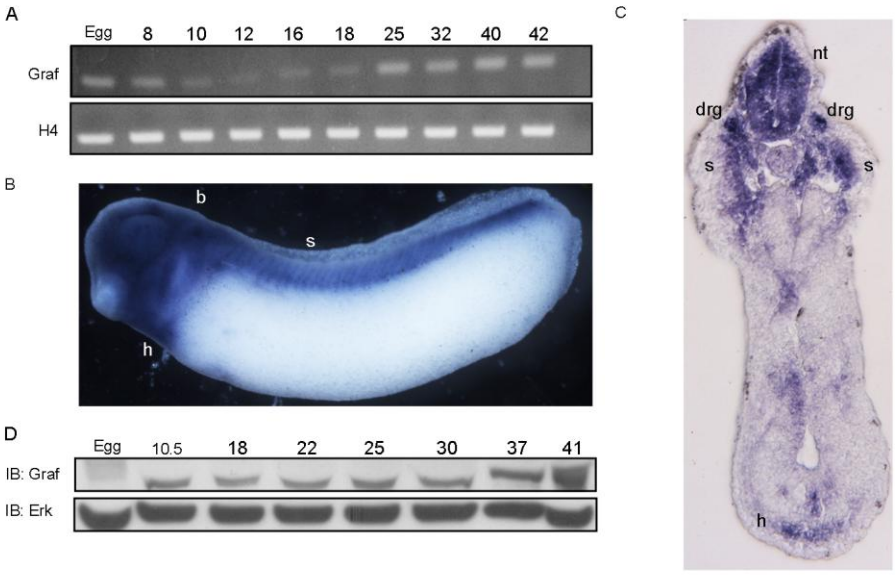
A
Egg 8 10 12 16 18 25 32 40 42
Graf
H4
B
b
s
h
C
nt
drg
drg
s
s
h
D
Egg 10.5 18 22 25 30 37 41
IB: Graf
IB: Erk

Figure 3.1. Graf is expressed during embryonic frog development. A) RT-PCR analysis was performed using RNA isolated from embryos at the indicated stages. Histone H4 (H4) serves as a control. B) Whole-mount *in situ* hybridization of *Xenopus* embryo at stage 29 using an antisense probe specific for xGraf. Dorsal is to the top, anterior to the left. Tissues expressing Graf are labeled: h, heart; b, brain; s, somites. C) Transverse section from whole-mount Graf *in situ* hybridization. Tissues expressing Graf are labeled: nt, neural tube; drg, dorsal root ganglia; s, somite; h, heart . D) Western blot analysis of Graf expression at the indicated stages. Erk serves as a loading control.

Inhibition of Graf by antisense morpholinos

We developed an antisense morpholino-based approach to specifically block translation of Graf *in vivo* during *Xenopus* development. To this end, we designed two Graf-specific antisense morpholinos to target sequences either upstream of, or flanking, the start codon of *Xenopus* graf (denoted xGrafup and xGrafst, respectively). Both xGrafup and xGrafst significantly reduced flag-tagged *Xenopus* Graf protein production in an *in vitro* transcription/translation assay but had no effect on translation of a control plasmid encoding human graf (Figure 3.2A). Furthermore, the mixture of the two morpholinos (hereafter termed Graf Mo) induced the strongest response in these assays.

We developed polyclonal antibodies directed towards a 22-mer peptide in the C-terminal tail of Graf that is completely conserved between *Xenopus*, mouse, rat, and human Graf. This antibody recognizes a specific band of the appropriate molecular weight (116 kDa) in adult *Xenopus* heart lysates and cellular extracts derived from COS cells transfected with a plasmid encoding xGraf (Figure 3.2B). In order to determine the developmental timecourse of xGraf protein expression, we performed Western analysis of lysates derived from wild-type *Xenopus* embryos at a variety of developmental stages and determined that Graf protein was expressed during gastrulation and appeared to increase during late tailbud and tadpole stages (Figure 3.1D; see also Figure 3.6 A).

In order to establish that Graf Mo blocked Graf translation *in vivo*, we next injected control morpholino (Con Mo) or Graf Mo into single-cell *Xenopus* embryos and performed Western blot analysis at various stages during development. Importantly, injection of Graf Mo at the one-cell stage resulted in a reduction of embryonic Graf levels at all stages tested between stage 18 and 37 (Figure 3.2C, also see Figure 3.6A, B). Injection of five-base

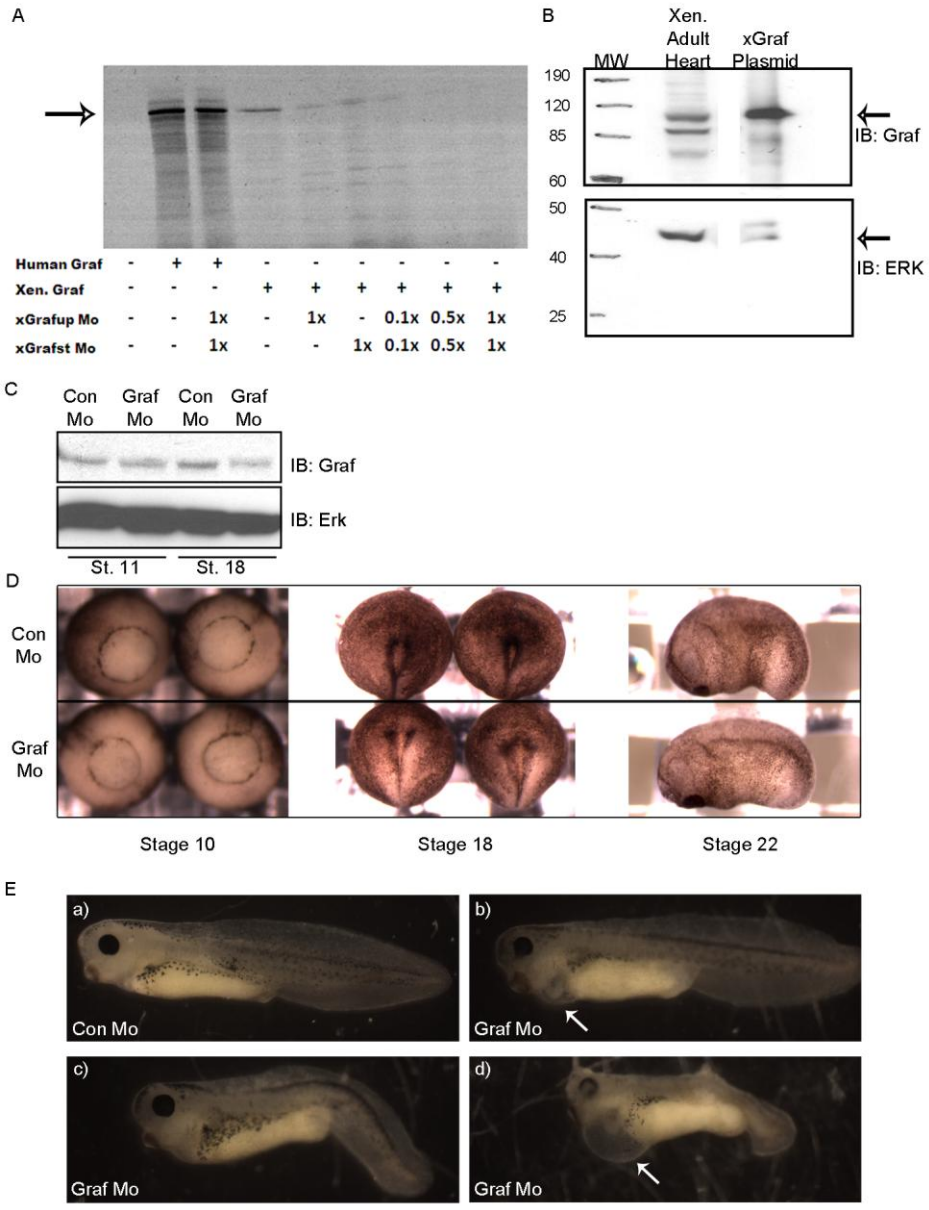
A
Human Graf - + + - - - - - -
Xen. Graf - - - + + + + + +
xGrafup Mo - - 1x - 1x - 0.1x 0.5x 1x
xGrafst Mo - - 1x - - 1x 0.1x 0.5x 1x
B
MW
Xen. Adult Heart
xGraf Plasmid
190
120
85
60
50
40
25
IB: Graf
IB: ERK
C
Con Mo
Graf Mo
Con Mo
Graf Mo
IB: Graf
IB: Erk
St. 11
St. 18
D
Con Mo
Graf Mo
Stage 10
Stage 18
Stage 22
E
a)
Con Mo
b)
Graf Mo
c)
Graf Mo
d)
Graf Mo

Figure 3.2. Graf Mo blocks Graf translation *in vivo* and results in cardiac edema and anteroposterior axis defects. A) In vitro transcription/translation assays (with S35-labeling) were performed utilizing plasmids for human Graf or *Xenopus* Graf, as indicated, and with varying amounts of each Graf morpholino (xGrafup or xGrafst) as shown. B) Western blot analysis utilizing antibodies generated to recognize *Xenopus* Graf in lysates derived from adult Xenopus heart or from COS cells transfected with a plasmid encoding *Xenopus* Graf (xGraf) demonstrate the specificity of the antibody. C) Western blot analysis for Graf in Con Mo- and Graf Mo-injected embryos at the indicated stages of development demonstrates that Graf Mo injection leads to a decrease in Graf protein expression. Levels of ERK are shown as a control for loading. D) Gross morphological assessment of Con Mo- and Graf Mo- injected embryos at the indicated stages. Stage 10 embryos are visualized with vegetal layer to the top. Stage 22 embryos are oriented with dorsal to the top, anterior to the left. No apparent defects in gross morphology were observed at these stages. E) Gross morphological assessment of stage 39 Con Mo- and Graf Mo-injected embryos demonstrates pericardial edema (b), anteroposterior axis defects (c), and apparent developmental arrest (d). Dorsal is the top, anterior to the left in all panels.

Table 3.1. Graf morpholino injection leads to gross morphological defects.

	Eye Defect	Anteroposterior Defect	Pericardial Edema	No Swim Response	Partial Paralysis
Con Mo	0/106 (0%)	1/106 (1%)	0/106 (0%)	0/106 (0%)	0/106 (0%)
Graf Mo	19/88 (22%)	13/88 (15%)	72/88 (82%)	43/88 (49%)	45/88 (51%)

Table 3.1. Graf morpholino injection leads to gross morphological defects.

Con Mo- and Graf Mo-injected embryos were analyzed for gross morphological defects between stages 37-39. Data are presented as a ratio of each phenotype to the total number of embryos examined (percentages are shown in parentheses). Data are taken from two separate representative batches of embryos and similar data were observed in at least five additional separate batches of embryos (data not shown). Note that many embryos exhibited more than one type of defect; therefore the percentages do not add to 100%.

mismatch morpholinos had no effect on Graf protein levels as assessed by Western blot analysis. The specificity of the Graf antibody and the *in vivo* specificity of Graf Mo was further demonstrated by reduced Graf expression in the somites as assessed by whole-mount Graf antibody staining (see Figure 3.9B).

Graf depletion leads to gross morphological defects including pericardial edema and disrupted cardiac morphogenesis

Gross morphological assessment of developing Con Mo- and Graf Mo-injected embryos indicated that gastrulation and neurulation were unperturbed by Graf Mo injection (Figure 3.2D). However, at tadpole stages, some Graf morphant embryos exhibited defects in anteroposterior axis elongation (Figure 3.2E, panel c, and Table 3.1). Some Graf Mo-injected embryos appeared to have arrested during development as assessed by marked anteroposterior axis shortening and diminished eye pigmentation (Figure 3.2E, panel d). These embryos were not utilized for later analyses of cardiac and skeletal muscle formation. Furthermore, we noted that Graf morphant embryos exhibited marked pericardial edema and died by the time Con Mo-injected sibling embryos reached stage 42 (Figure 3.2C, panel b and d (arrows), and Table 3.1).

These findings, coupled with our *in situ* hybridization analysis demonstrating Graf expression in the heart, suggested the possibility that Graf is required during embryonic heart development. In order to assess this possibility, we performed whole mount immunohistochemical staining for myosin heavy chain (MHC) on Con Mo- and Graf Mo-injected embryos and examined heart morphology using widefield microscopy at stage 37, after completion of looping morphogenesis in control embryos. Notably, we determined that 50% (8 of 16 embryos examined) of Graf morphant embryos exhibited defects in cardiac

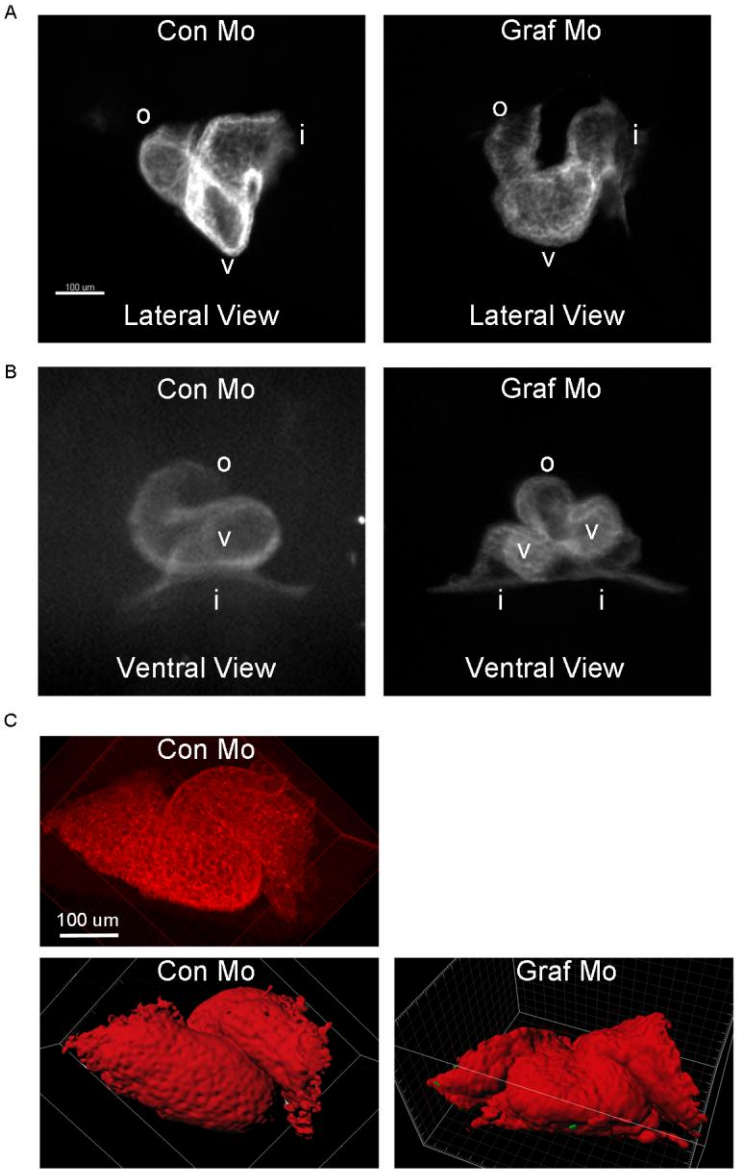
A
Con Mo
o
i
v
100 um
Lateral View
Graf Mo
o
i
v
Lateral View
B
Con Mo
o
v
i
Ventral View
Graf Mo
o
v
v
i
i
Ventral View
C
Con Mo
100 um
Con Mo
Graf Mo

Figure 3.3. Graf depletion leads to marked defects in cardiac looping morphogenesis and partial cardia bifida. A) Whole-mount MHC antibody staining and widefield microscopic analysis of stage 37 Con Mo- and Graf Mo- injected embryonic hearts indicates abnormal looping morphogenesis in Graf morphant embryos (6 of 16 embryos examined) whereas all Con Mo-injected embryos exhibited normally looped hearts (20 of 20 embryos examined). Lateral view with dorsal to the top, anterior to the left. B) Whole-mount MHC antibody staining and widefield microscopic analysis of stage 37 Con Mo- and Graf Mo-injected embryonic hearts reveals partial cardia bifida in 2 of 16 Graf morphant embryos examined. Ventral view with anterior to the top. The data represent one experiment examining 20 Con Mo- and 16 Graf Mo-injected embryos. Similar cardiac morphological defects have been observed in Graf Mo-injected embryos in at least 5 separate experiments. Scale bar in left panel of A corresponds to all panels in A and B. C) Whole-mount tropomyosin antibody staining of stage 34 Con Mo- and Graf Mo-injected embryos were analyzed by laser scanning confocal microscopy and 3D rendering. Tropomyosin fluorescence is shown in top panel. Bottom panels represent isosurfacing of fluorescent images from Con Mo- and Graf Mo-injected embryos. Ventral view with anterior to the left. Scale bar corresponds to all panels in C.

morphology, whereas all control hearts appeared normal. The most prevalent cardiac abnormality induced by Graf depletion (6 embryos) was aberrant cardiac looping which caused Graf morphant hearts to appear U-shaped (Figure 3.3A). A less penetrant cardiac abnormality (2 embryos, 12.5%) was partial cardia bifida in which Graf-depleted embryos displayed hearts containing two pairs of inflow tracts and ventricles, with a single common outflow tract (Figure 3.3B). In order to more precisely determine the onset of the cardiac defect, we analyzed stage 34 Con Mo- and Graf Mo-injected embryos by whole-mount tropomyosin antibody staining and subsequent laser scanning confocal microscopic analysis (Figure 3.3C). These analyses demonstrated that Graf Mo-injected embryos exhibited abnormal morphology at the earliest onset of cardiac looping. Taken together, these date demonstrate that Graf is required for normal cardiac morphogenesis.

Graf depletion leads to paralysis and marked somite defects

Our analysis of swimming tadpole staged embryos (stages 35-39) demonstrated that Graf Mo-injected embryos exhibited a striking paralysis defect (Table 3.1). Specifically, whereas Con Mo-injected embryos swam normally in response to touch, Graf morphant embryos were either completely unable to swim or exhibited very limited movement of the tail. In addition, spontaneous swimming behavior as seen in control tadpoles was completely absent in Graf morphant embryos suggesting that the defect was likely not simply a defect in touch response alone. Importantly, injection of 5-basepair mismatch morpholinos (in two separate experiments) did not result in these observed phenotypic defects, suggesting that these phenotypes are specifically a result of Graf depletion. Furthermore, as shown in figure 3.4A, unilateral injection of Graf Mo into one cell at the two-cell stage led to lateral bending of the embryo toward the Graf Mo-injected side (100%, n=22), a phenotype often caused by

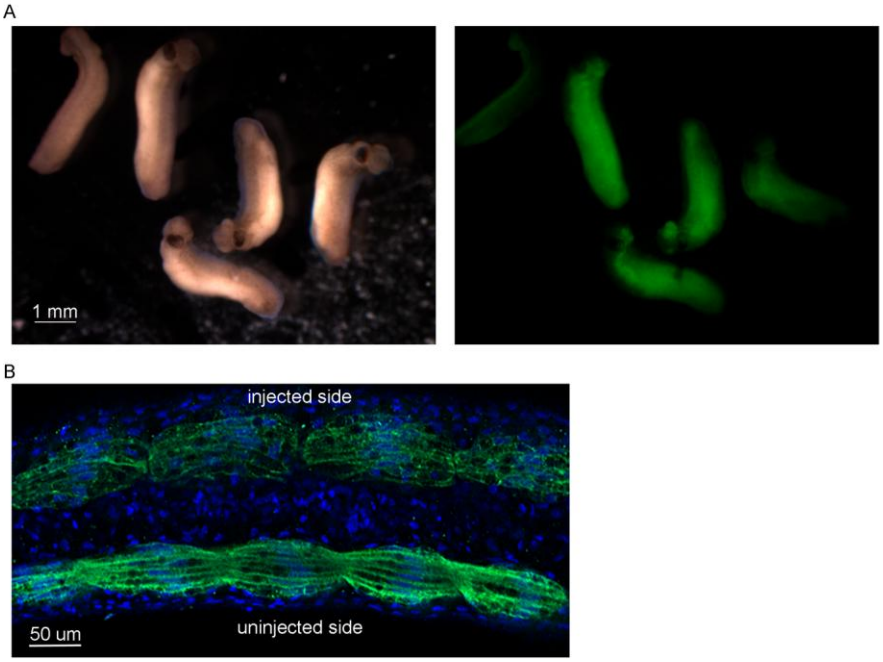
A
1 mm
B
injected side
50 um
uninjected side

Figure 3.4. Graf depletion leads to lateral bending and somite defects. A) Gross morphological assessment of embryos unilaterally injected with Graf Mo into one cell at the two-cell stage and allowed to develop to stage 30. Brightfield (left panel) and green fluorescence (right panel) to visualize the Graf Mo-injected (Graf Mo is conjugated with fluorescein isothyocyanate (FITC)) side reveals that all embryos exhibit lateral bending toward the Graf Mo-injected side. Graf Mo is conjugated to exhibit green fluorescence. B) Whole-mount tropomyosin staining and confocal microscopic analysis of these embryos demonstrate reduced tropomyosin staining and somite structural defects in Graf Mo-injected side of embryo. Dorsal view.

defective somite formation. To assess this possibility, we performed whole mount immunohistochemical staining for tropomyosin on these embryos. As shown in figure 3.4B, a marked reduction in the level of tropomyosin staining (and cellular organization) was observed in the somites on the Graf Mo- injected side in comparison to the Con Mo-injected side of the embryos. These results suggest that Graf depletion induces defects in somite formation, possibly through disruption of myogenic differentiation.

Graf depletion does not disrupt somite specification, rotation, or elongation

Given the remarkable evidence that Graf-depletion led to defective somite formation and reduced expression of the skeletal differentiation marker, tropomyosin, we strove to determine whether Graf was necessary for myocyte specification and/or differentiation. Somite development in the frog requires tight regulation of steps involving myocyte specification, rotation, elongation, and maturation. In an effort to define the precise Graf dependent step(s) during *Xenopus* somitogenesis, we first assessed whether Graf depletion altered the early specification of the somites by whole-mount *in situ* hybridization analysis of Myo-D. At stages 25 and 34, we found no differences in the spatial distribution of Myo-D expression in Con Mo- or Graf Mo- injected embryos, suggesting that somites were properly specified in the absence of Graf (Figure 3.5A). Furthermore, the number and spacing of the somites in Graf morphants appeared similar to controls suggesting that Graf-depletion did not affect the rotation or elongation of the somites. We further confirmed that somite rotation and elongation were unaffected by Graf-depletion by whole-mount immunostaining of the muscle marker, 12-101, and the nuclear stain, Topro3, of stage 25 embryos utilizing laser scanning confocal microscopic analysis (Figure 3.5B). While Graf morphant myofibers appeared grossly normal at this stage, 12-101 staining was much less intense in these embryos as

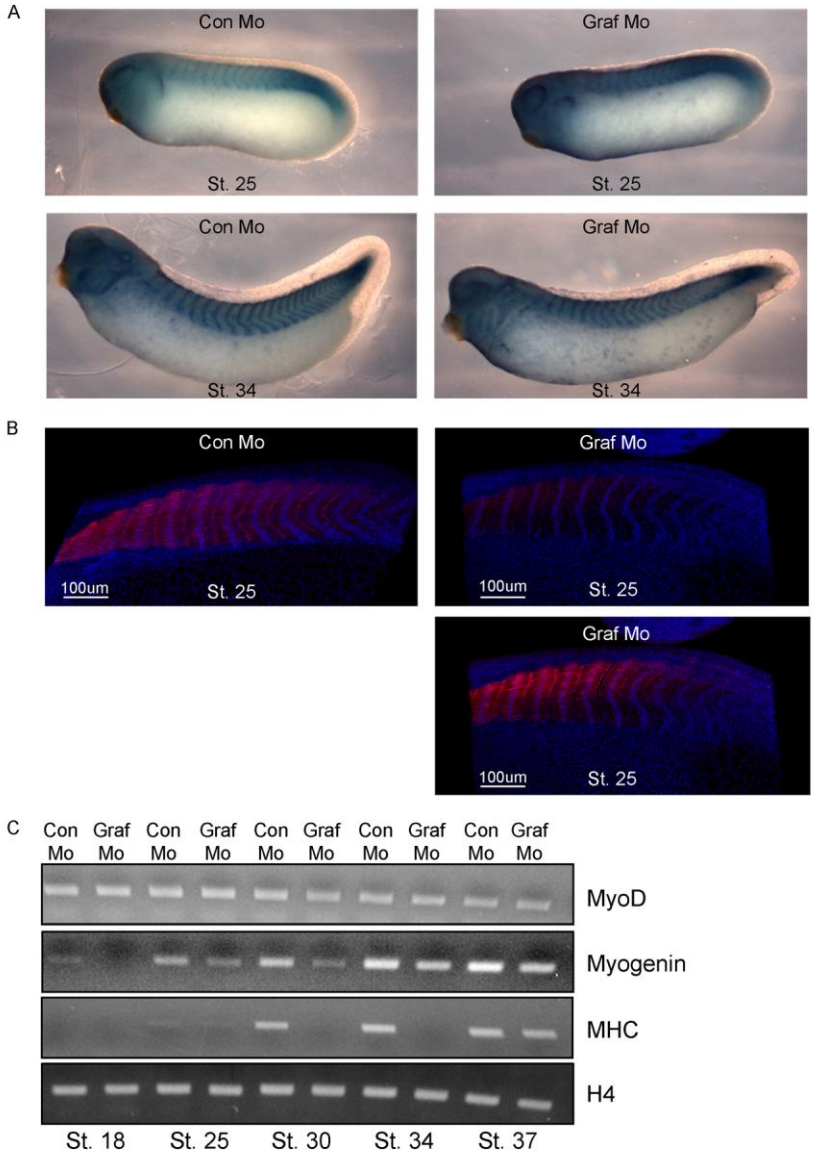
A
Con Mo
St. 25
Graf Mo
St. 25
Con Mo
St. 34
Graf Mo
St. 34
B
Con Mo
100um
St. 25
Graf Mo
100um
St. 25
Graf Mo
100um
St. 25
C
Con Mo
Graf Mo
Con Mo
Graf Mo
Con Mo
Graf Mo
Con Mo
Graf Mo
Con Mo
Graf Mo
MyoD
Myogenin
MHC
H4
St. 18
St. 25
St. 30
St. 34
St. 37

Figure 3.5. Graf depletion does not affect somite specification, rotation, or elongation but results in a marked decrease in transcription of skeletal muscle marker genes. A) In situ hybridization analysis of Myo-D at stage 25 (top two panels) and 34 (bottom two panels) in Con Mo- and Graf Mo-injected embryos. Dorsal is to the top, anterior is to the left. B) Whole-mount 12-101 (red) and Topro3 (blue) antibody staining and laser scanning confocal microscopic analysis of Con Mo- and Graf Mo-injected embryos at stage 25 reveals reduced 12-101 expression in the somites (compare top right Graf Mo panel to Con Mo panel). Bottom Graf Mo panel light levels were increased using Adobe Photoshop CS4 to show detail. C) RNA from Con Mo- and Graf Mo-injected embryos (n=10) was isolated and utilized for RT-PCR analysis of Myo-D and MHC expression analysis. Histone H4 (H4) serves as a control.

compared to controls (reminiscent of our findings reported above for tropomyosin), and was nearly absent in the posterior-most somites indicating that Graf-depletion led to decreased skeletal muscle differentiation by stage 25. Taken together, these data indicate that early somite specification, rotation, and elongation are Graf-independent but that skeletal muscle differentiation/maturation may require Graf.

Graf is essential for myocyte differentiation

To further explore a role for Graf in skeletal muscle differentiation, we analyzed Con Mo- and Graf Mo-injected embryos by semi-quantitative RT-PCR analysis for Myo-D and the skeletal muscle differentiation markers, myogenin and MHC. In accordance with our *in situ* hybridization analysis of MyoD, we observed no obvious differences in the levels of expression of Myo-D between Con Mo- and Graf Mo- injected embryos (Figure 3.5C), confirming that early skeletal muscle specification was unaffected by Graf depletion. However, Graf-depleted embryos exhibited marked reductions in the transcription of both myogenin and MHC between stage 22 and 34, demonstrating that Graf depletion caused a disruption to skeletal muscle differentiation.

In order to confirm that Graf-depletion caused a disruption in skeletal muscle differentiation, we performed Western blot analysis on lysates isolated from Con Mo- and Graf Mo- injected embryos at various stages during skeletal muscle development. As shown in figure 3.6A, Graf depletion led to decreased expression of all myocyte marker genes evaluated between stages 22-37 including skeletal α-actin, tropomyosin, and MHC. Furthermore, at stage 37 the skeletal muscle markers α-actinin and troponin T were similarly reduced between Con Mo- and Graf Mo-injected embryos (Figure 3.6B). Interestingly, RhoA activity was significantly increased in whole embryo lysates from Graf Mo- injected embryos

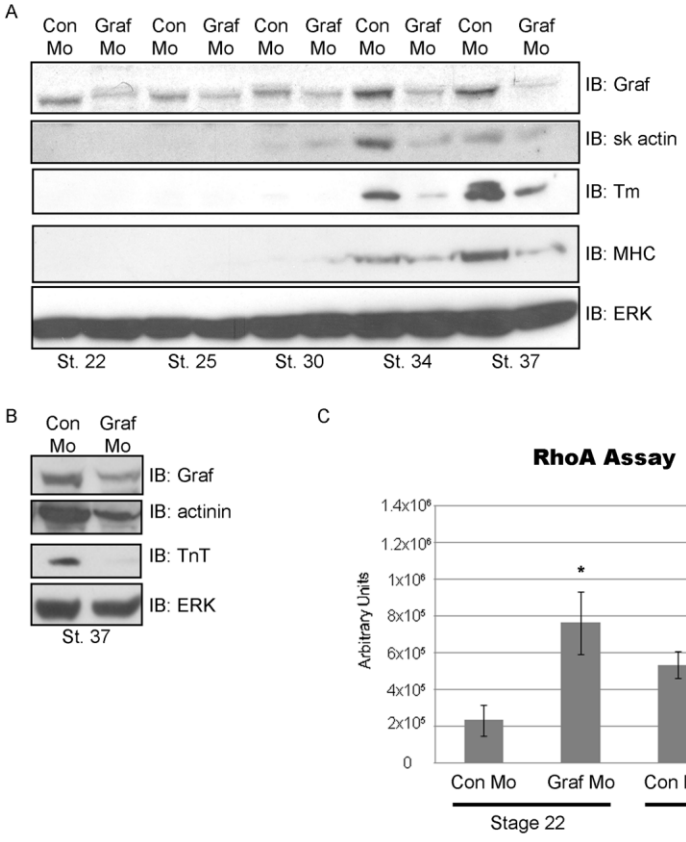
A
Con Mo
Graf Mo
Con Mo
Graf Mo
Con Mo
Graf Mo
Con Mo
Graf Mo
Con Mo
Graf Mo
IB: Graf
IB: sk actin
IB: Tm
IB: MHC
IB: ERK
St. 22
St. 25
St. 30
St. 34
St. 37
B
Con Mo
Graf Mo
IB: Graf
IB: actinin
IB: TnT
IB: ERK
St. 37
C
RhoA Assay
Arbitrary Units
1.4x10⁶
1.2x10⁶
1x10⁶
8x10⁵
6x10⁵
4x10⁵
2x10⁵
0
*
*
Con Mo
Graf Mo
Con Mo
Graf Mo
Stage 22
Stage 25

Figure 3.6. Graf depletion leads to a marked decrease in skeletal muscle marker gene expression and upregulation of Rho-activity. A, B) Western blot analysis at the indicated stages for Graf, skeletal α-actin (sk actin), α-actinin (actinin), tropomyosin (tm), and MHC from lysates of Con Mo- and Graf Mo-injected embryos. Erk serves as a loading control. C) ELISA-based Rho activity assays of lysates isolated from stage 22 and 25 Con Mo- and Graf Mo-injected embryos. Rho activity was measured by a standard ELISA-based GST-Rhotekin assay and data are shown in relative arbitrary units. Lysates were isolated from 10 embryos, in batch, for each stage and treatment. Experiment was performed three times in triplicate. Asterisk denotes $p < 0.05$.

compared to the same stage Con Mo- injected embryos at the onset of skeletal muscle differentiation (stage 22 and 25), suggesting that Graf serves to downregulate Rho activity during these critical stages of embryonic development (Figure 3.6C). Collectively, these data strongly support our contention that the marked somite defect and partial paralysis caused by Graf-depletion is, at least in part, due to failure to complete the myogenic differentiation program, an event that may be due to persistent RhoA activation in Graf-depleted embryos.

Xenopus Graf is necessary for skeletal muscle integrity

A detailed analysis of somite organization in the Graf morphants at stage 37 (when a swimming defect was readily apparent) further confirmed defective muscle formation (Figure 3.7A and B). As analyzed by whole-mount tropomyosin antibody staining and visualized by laser scanning confocal microscopy, somitic myofibers of Graf morphant embryos were often thin and disorganized as compared to controls. A striking defect was also noted in somite boundary formation. In some morphant embryos, myofibers were discontinuous across the length of the somite, suggesting that either the myofibers had not extended the full length of the somite or had torn away from the myoseptum due to lack of structural integrity. In many cases the typical horizontal intersomitic junctions were markedly disrupted; some myofibers appeared to stretch across a two-somite length, while others were terminated mid-somite.

Ultrastructural analysis by electron microscopy confirmed myofiber disorganization in Graf morphant somites. As shown in figure 3.8, the relative myofibril content was reduced in Graf morphant myocytes, as exemplified by more sarcoplasm and less myofibers per myocyte in comparison to controls. Notably, intact skeletal muscle tissue was remarkably absent from Graf morphant somites (as assessed by observable intact sarcomeres) and the TEM views of Graf Mo-injected somites demonstrated in Figure 3.8 represent the

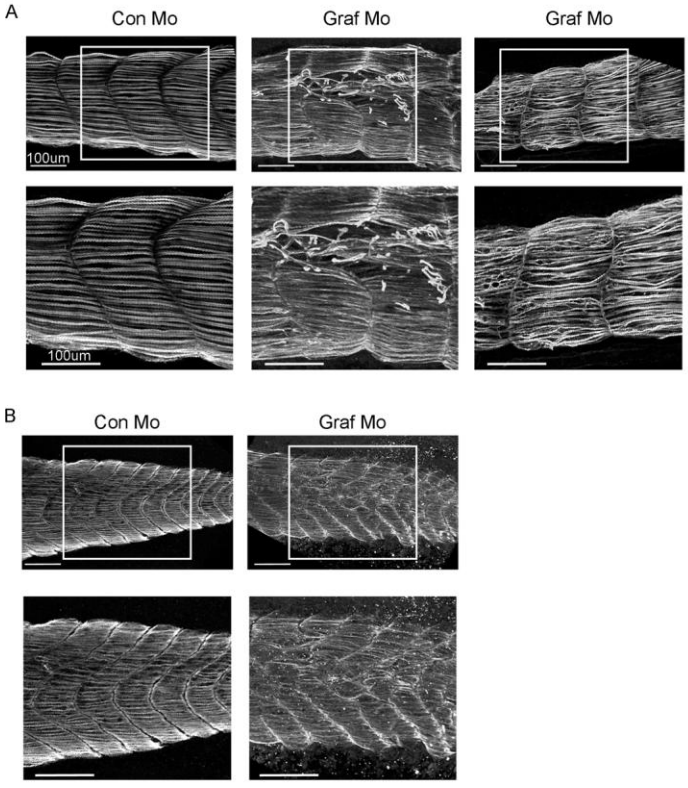
A
Con Mo
Graf Mo
Graf Mo
100um
100um
B
Con Mo
Graf Mo

Figure 3.7. Graf morphant embryos demonstrate striking defects in somite morphology and sarcomeric integrity. Whole-mount tropomyosin antibody staining and laser scanning confocal microscopic analysis of stage 39 Con Mo- and Graf Mo-injected anterior (A) and posterior (B) somites. Dorsal is to the top, anterior to the left. Lower panels in A and B represent enlarged views of regions boxed in top panels.

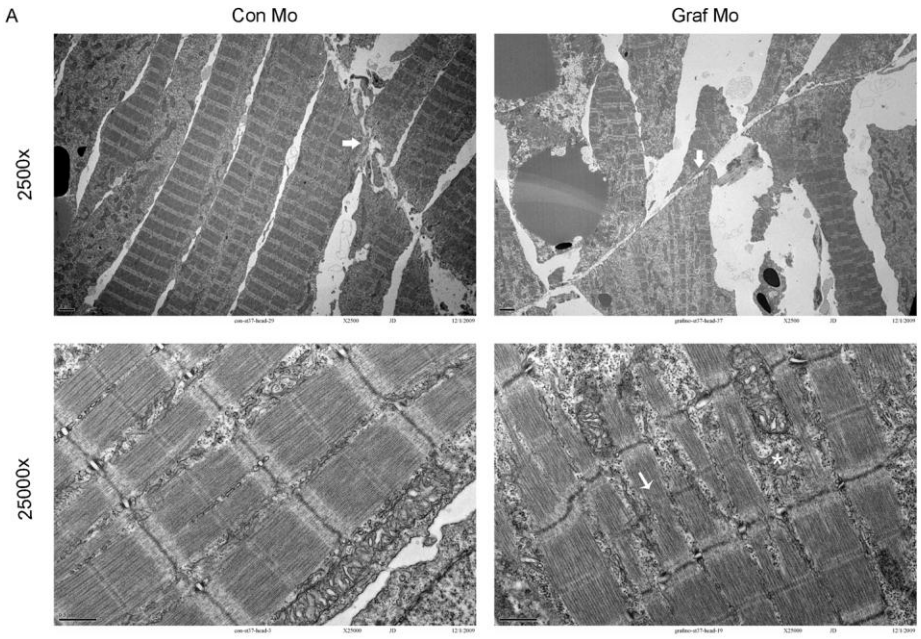
A
Con Mo
Graf Mo
2500x
25000x

Figure 3.8. Transmission electron microscopic analysis reveals ultrastructural defects in sarcomere formation in Graf Mo-injected embryos. Parasagittal sections of Con Mo- and Graf Mo-injected embryos were examined by transmission electron microscopic analysis at stage 37. Myoseptum is denoted by thick arrows in top panels. Thin arrow points to region of Graf morphant somite exhibiting abnormal M-band. Asterisk labels region of Graf morphant somite lacking normal sarcomeric structure.

most clearly recognizable sarcomeric structure within the somites. In addition, defects in lateral myofibril alignment were observed in Graf Mo-injected somites wherein the Z bands were not aligned in register with adjacent myofibers, and the accompanying sarcoplasmic reticulum and mitochondria appeared disorganized. While many individual sarcomeres appear to have assembled properly in Graf Mo-injected somites, some M-band irregularities were also observed.

Interestingly, as assessed by whole-mount Graf antibody staining and visualized by laser scanning confocal microscopic analysis, immunolocalization of Graf at this time point in development revealed that Graf was predominantly concentrated at the tips of the myofibers directly adjacent to the myoseptum, although low levels of Graf were also apparent along the lateral edges of the myofibrils (Figure 3.9A). Importantly Graf immunoreactivity was markedly reduced in stage 37 Graf morphants, in further support of the specificity of this antibody staining (Figure 3.9B). Collectively, these data indicate that Graf is necessary for skeletal muscle formation and may play a role in facilitating the organization and anchorage of myofibrils to the myoseptum.

Graf depletion leads to marked disruption of intersomitic laminin deposition

Our striking finding that Graf morphant somites often exhibit abnormal intersomitic junctions suggested that Graf might regulate normal cell:ECM adhesions. In order to analyze this possibility, we determined whether laminin, a critical component of the intersomitic ECM, was properly deposited in Con Mo- and Graf Mo- injected embryos. To this end, we analyzed stage 25 and 37 Con Mo- and Graf Mo- injected embryos by triple whole-mount immunostaining of tropomyosin, laminin, and Topro3 followed by laser scanning confocal microscopic analysis and obtained z-stack images that we rendered into a 3D image of the

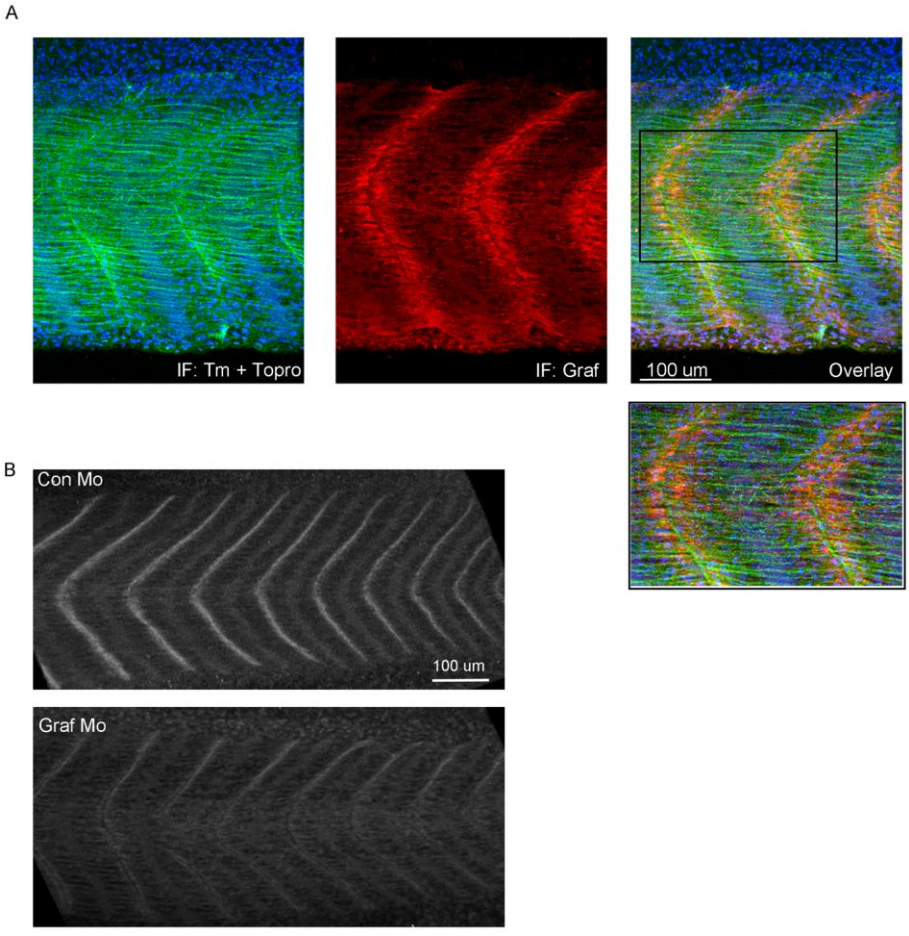
A
IF: Tm + Topro
IF: Graf
100 um
Overlay
B
Con Mo
100 um
Graf Mo

Figure 3.9. Graf localizes to the tips of somites near the myoseptum. A) Whole-mount Graf (red), tropomyosin (green), and Topro3 (blue) antibody staining and laser scanning confocal microscopic analysis of wild-type embryo somites at stage 37. Dorsal is to the top, anterior to the left. Bottom panel represents an enlarged view of the boxed region in the upper right panel demonstrating the precise localization of Graf to the region of the myotome adjacent to the myoseptum. B) Whole-mount Graf antibody staining and laser scanning confocal microscopic analysis of Con Mo- and Graf Mo-injected embryos at stage 37 reveals that Graf expression is reduced in Graf morphant embryos. Dorsal is to the top, anterior to the left.

somites. As shown in figure 3.10, some areas of the intersomitic space in Graf morphant somites were completely devoid of laminin staining and the proper delineation of the intersomitic space was dysregulated.

Graf appears to interact with β-dystroglycan at the myoseptum and Graf-depletion causes disruption to β-dystroglycan localization

Laminin interacts with the somitic cytoskeleton through both α7β1-integrin and the dystrophin-glycoprotein complex (DGC). The predominant laminin receptor in the DGC is α-dystroglycan which then binds to β-dystroglycan, for further structural linkage to the cytoskeleton. Since laminin deposition was disrupted in the mysepta of Graf Mo-injected embryos, we next determined whether deposition of β-dystroglycan was also disrupted by Graf-depletion. To this end, we performed whole-mount immunofluorescent staining of Graf, β-dystroglycan, and Topro3 and visualized the somites of stage 37 Con Mo- and Graf Mo-injected embryos by laser scanning confocal microscopic analysis and 3D-rendering. Indeed, similar to our results with laminin deposition, we found that Graf morphant embryos exhibited large regions of the intersomitic space that were devoid of β-dystroglycan (Figure 3.11, compare e, f). Notably, the regions of the myoseptum that lacked β-dystroglycan overlapped with regions where Graf staining appeared weakest (compare Figure 3.11 c, d and the overlay in g, h). Taken together, these remarkable findings strongly suggest that Graf-depletion leads to dysregulation of both laminin and β-dystroglycan localization and because of the strong correlation between Graf and β-dystroglycan immunolocalization, we surmised that these proteins may functionally interact, *in vivo*. Indeed, our recent evidence utilizing co-immunoprecipitation analysis corroborates the notion that Graf and β-dystroglycan do, indeed, form a complex in differentiating C2C12 myoblasts (unpublished data).

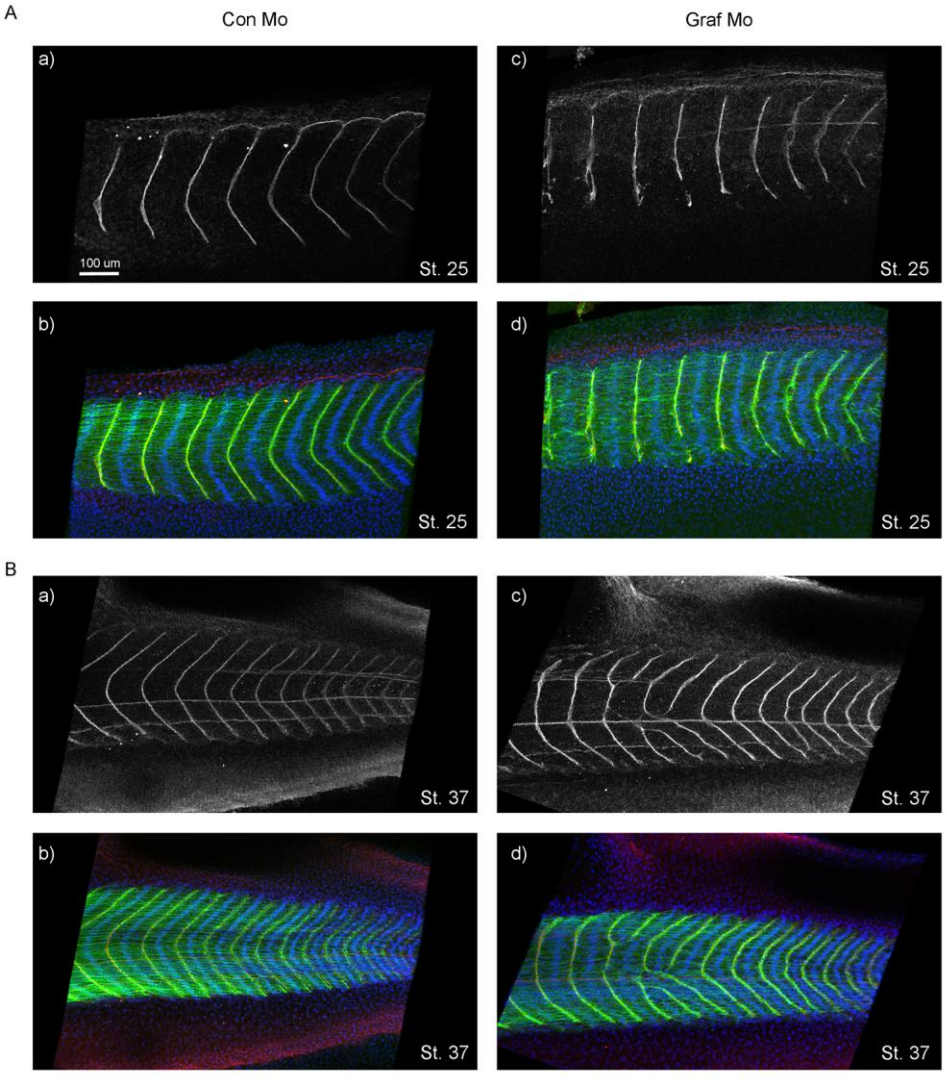
A
Con Mo
Graf Mo
a)
100 um
St. 25
c)
St. 25
b)
St. 25
d)
St. 25
B
a)
St. 37
c)
St. 37
b)
St. 37
d)
St. 37

Figure 3.10. Graf depletion leads to defects in intersomitic laminin deposition. A) Whole-mount tropomyosin (green), laminin (red), and Topro3 (blue) antibody staining and laser scanning confocal microscopic analysis of stage 25 (A) and 37 (B) Con Mo- (a, b) and Graf Mo-injected (c, d) embryos reveals disrupted intersomitic junctions and areas of the intersomitic junctions lacking laminin staining in Graf morphant embryos as compared to controls. Laminin immunoflourescence alone is shown in grayscale in panels a, c and full-color overlay is depicted in b,d. Note that the red fluorescence is not apparent in the overlay images due to colocalization with the more intense green fluorescent signal. Dorsal is to the top, anterior to the left. Scale bar in A corresponds to all panels.

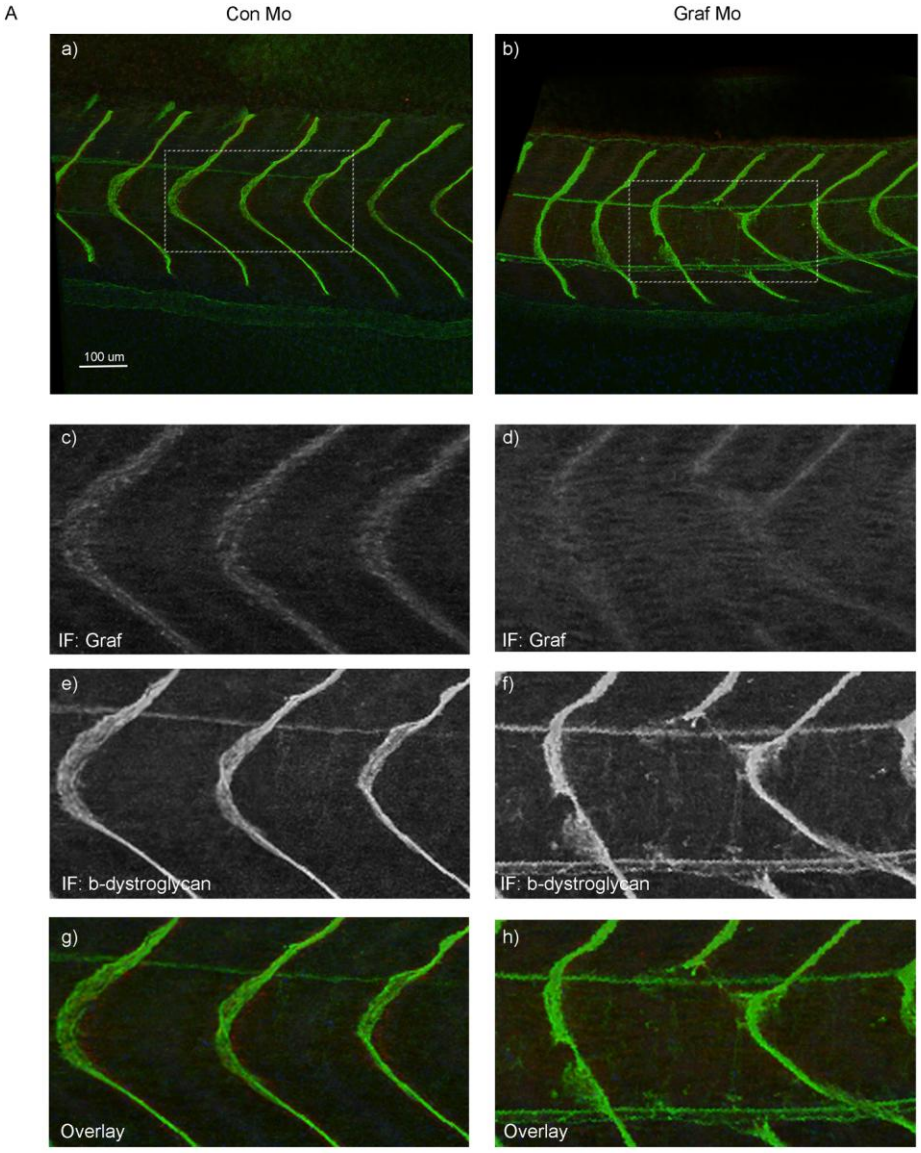
A
Con Mo
Graf Mo
a)
b)
100 um
c)
d)
IF: Graf
IF: Graf
e)
f)
IF: b-dystroglycan
IF: b-dystroglycan
g)
h)
Overlay
Overlay

Figure 3.11. β-dystroglycan immunolocalizes with Graf, *in vivo*, at the intersomitic junctions and β-dystroglycan deposition is disrupted by Graf-depletion. Whole-mount Graf (red) and β-dystroglycan (green) antibody staining of stage 37 Con Mo- (a, c, g, e) and Graf Mo-injected (b, d, f, h) embryos and laser scanning microscopic analysis demonstrates that Graf and β-dystroglycan appear to interact closely at the intersomitic junctions. Full-color overlay (a, b) is shown at the top. Note that the red fluorescence is not apparent in the overlay images due to colocalization with the more intense green fluorescent signal. Region of interest (box, panel a, b) is enlarged in c - h to show detail. Graf (c, d), β-dystroglycan (e, f), are depicted in grayscale. Full-color merge (g, h) is shown at the bottom. Note that regions absent of intense Graf staining (red) are also absent of β-dystroglycan (green) in Graf morphant embryos.

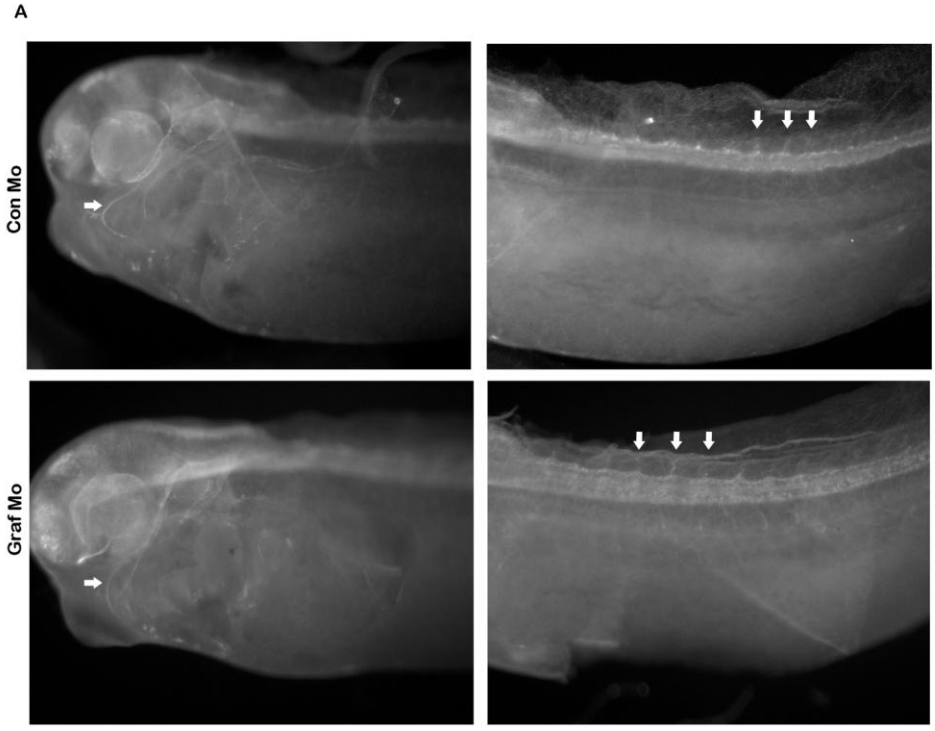
A
Con Mo
Graf Mo

Figure 3.12. Graf depletion does not appear to disrupt neuronal outgrowth. Whole-mount HNK antibody staining and laser scanning microscopic analysis of stage 37 Con Mo- and Graf Mo- injected embryos reveal apparently normal outgrowth of anterior (left panels) and intersomitic (right panels) neurons. Arrows point to representative HNK-expressing neurons

DISCUSSION

We have previously demonstrated that Graf induces cytoskeletal arrangements mediated via its GAP activity for Rho and is a binding partner for the non-receptor tyrosine kinase, FAK, thus positioning Graf as a potentially key nodal point for integrin signaling events. In addition, we previously showed that Graf is expressed in a tissue-specific manner, predominantly in terminally differentiated cells in heart and brain, suggesting that Graf may serve to mediate Rho-dependent differentiation in specific tissue compartments. Herein, we confirmed by *in situ* hybridization that Graf was expressed in developing *Xenopus laevis* embryos in a similar tissue-specific context and utilized antisense morpholino-based translational inhibition of Graf to demonstrate an *in vivo* role for Graf during frog development. We found that Graf Mo-injection led to a variety of developmental defects including pericardial edema, anteroposterior defects, and embryonic lethality. Furthermore, our data demonstrate that Graf depletion leads to defects in both somitogenesis and cardiogenesis.

Our finding that Graf-depletion (and the concomitant upregulation of RhoA) led to abnormal looping morphogenesis and cardia bifida was somewhat surprising in light of previous studies in chick that demonstrated that inhibition of RhoA (via injection of RhoA-specific siRNA) led to similar gross abnormalities in heart morphogenesis (Kaarbo *et al.*, 2003). There are two likely explanations for this apparent discrepancy. First, it is likely that the activity of RhoA must be tightly regulated during the crucial phases of cardiac morphogenesis and that either upregulation (as seen in our model of Graf depletion) or disruption of RhoA translation (via siRNA-mediated inhibition) can induce cardiac dysmorphogenesis. Another possibility is that although GAPs downregulate GTPase activity

by conversion to the inactive GDP-bound state, some GAPs simultaneously send a signal that is required for downstream signaling from its GTPase (Kozma *et al.*, 1996; McCormick, 1989; Paulssen *et al.*, 1996). Thus, while Graf depletion in our model system led to upregulation of Rho activity, it is possible that Graf is also required for signal transduction downstream of Rho during cardiogenesis. Additionally, we are unable from the studies conducted thus far to determine whether Graf's GAP activity is required during cardiogenesis and future studies will be required to demonstrate whether overexpression of human Graf and/or a GAP-dead mutant of human Graf are sufficient to rescue the heart phenotype in Graf morphant embryos.

Previous studies have demonstrated that cardiac-specific inactivation of Rho GTPases, by overexpression of RhoGDI, led to decreased cardiomyocyte proliferation and small, dysmorphic hearts. The specific contribution of RhoA to this phenotype, however, is difficult to discern since RhoGDI has been shown to downregulate the activity of RhoA, CDC42, and Rac. Nonetheless, these findings suggest that future analyses of Graf morphant hearts should investigate to what extent Graf may regulate Rho-dependent cardiomyocyte proliferation.

Clearly, further studies will be required to fully understand the mechanism by which Graf regulates cardiogenesis. Nonetheless, our finding that myogenic differentiation was reduced in Graf Mo-injected embryos is consistent with the possibility that Graf is required for cardiac differentiation as well as skeletal muscle differentiation. Indeed, several studies have implicated aberrant cardiomyocyte differentiation in both cardiac dysmorphogenesis and cardia bifida (Brown *et al.*, 2005; Christine and Conlon, 2008; Reiter *et al.*, 1999; Szeto *et al.*, 2002; Yelon *et al.*, 2000). It will be instructive in the future to isolate lysates from

isolated somites and hearts of both Con Mo- and Graf Mo-injected embryos and analyze myogenic marker gene expression in these tissues individually in order to demonstrate that both cardiogenesis and skeletal myogenesis are perturbed by Graf deficiency via diminished expression of marker genes.

Our analyses have demonstrated that Graf Mo-injection led to a striking paralysis phenotype characterized by lack of spontaneous- and touch sensitive- swimming response. We further demonstrated that Graf morphant embryos display marked defects in somitogenesis including aberrant sarcomeric organization and integrity. This range of defects strongly suggests that the paralysis phenotype can be attributed to a developmental requirement for Graf-mediated skeletal muscle differentiation and somite organization. However, these data do not rule out the possibility that Graf may also regulate the formation or function of intersomitic neurons, an effect that could also contribute to the paralysis phenotype. Our *in situ* hybridization analysis did, indeed, confirm Graf expression in neuronal tissues such as neural tube and dorsal root ganglia and we have previously shown that Graf is expressed in the neuronal precursor cell line, PC12. Furthermore, the characterization of a Trio-deficient mouse line demonstrated that mice lacking this RhoGEF died during embryogenesis and exhibited skeletal muscle defects and dysregulated neuronal development (O'Brien *et al.*, 2000) suggesting that the development of skeletal and neuronal tissues require tight regulation of Rho activity.

In order to partially address the possibility that Graf depletion also induced defects in neuronal development, we performed whole-mount HNK immunostaining (an antibody which reacts with embryonic neurons) in Con Mo- and Graf Mo-injected embryos and showed no clear difference in neuronal outgrowth (including intersomitic neurons) in either

group (Figure 3.12). Future work will be required to determine whether these neurons are functionally capable of innervating the somites. Nonetheless, our analyses of somite structure and the demonstration that skeletal muscle marker gene expression was markedly reduced in Graf morphant embryos strongly suggests that the primary defect in swimming behavior is due to diminished skeletal muscle differentiation and sarcomeric integrity. Finally, our recent unpublished data analyzing the differentiation of C2C12 and L6 myoblasts in culture have further confirmed that Graf plays a crucial and cell autonomous role in skeletal muscle differentiation. In these studies, we have demonstrated that Graf overexpression leads to precocious expression of α-actinin, skeletal α-actin, tropomyosin, MHC, and troponin T. In addition, we have shown that siRNA-mediated knockdown of Graf in these cell types (during differentiation) leads to decreased expression of MHC, further confirming our *in vivo* data.

While our data strongly implicate Graf as a crucial mediator of skeletal muscle differentiation, our immunoflourescence analyses of Graf Mo-injected somites suggests that Graf may play a further role in somite maintenance and integrity. First, Graf morphant somites often exhibited sarcomeres which were thin, misaligned, and appeared unattached to the myoseptum. In addition, laminin deposition was absent from some regions of the intersomitic space in many Graf Mo-injected embryos. Notably, this range of defects is seen in a variety of muscular dystrophies. Furthermore, Graf appeared to colocalize with β-dystroglycan and our unpublished data confirms that Graf immunoprecipitates with β-dystroglycan *in vitro*. Taken together, our findings lead us to the intriguing conclusion that Graf-deficiency leads to a dystrophic phenotype and suggest that Graf may be an important mediator of normal skeletal muscle integrity. Indeed, mutations in dystroglycan, laminin,

and α7β1-integrin are known to cause muscular dystrophies in humans and this has been confirmed in various animal models. Since Graf is a binding partner of FAK, which is known to mediate signaling downstream of integrins, and we have now shown Graf may interact with β-dystroglycan to strengthen cellular adhesion through laminin, our data are the first to suggest that Graf could mediate normal skeletal muscle formation and integrity through both integrin- and DGC-dependent mechanisms.

MATERIALS AND METHODS

Embryo culture and microinjection

Preparation and injection of *X. laevis* embryos was carried out as previously described (Wilson and Hemmati-Brivanlou, 1995). Staging was performed according to Nieuwkoop and Faber (Nieuwkoop and Faber, 1994). Anti-sense morpholino oligonucleotides were designed against either the start site (xGrafst Mo) or the 5'-untranslated region (xGrafup Mo) of *Graf*. Sequences used were: xGrafup, 5' ACGAGATCAGGAAGGCATTGACA 3' and xGrafst, 5' GGTAATCCCATCCTGGCGTATAGCA 3'. Equal concentrations of xGrafup and xGrafst morpholinos were mixed (hereafter referred to as Graf Mo) and injected at a concentration of 40ng/embryo at the one-cell stage, except where indicated. Similar results were obtained with each morpholino individually (data not shown). Five-base mismatched morpholinos were designed for both xGrafup and xGrafst, and the mixture of the two morpholinos was used as a control to assess the specificity of the morphant phenotype. The above morpholinos and a standard control morpholino (Con Mo) were obtained from GeneTools.

In vitro transcription/translation assays

In vitro transcription/translation assays were performed on plasmids encoding *Xenopus* Graf (xGraf) and human Graf using the TnT Quick-Coupled Transcription/Translation System according to the manufacturer's instructions (Promega).

Generation of xGraf polyclonal antibody

Amino acid sequences of human, mouse, and *Xenopus laevis* Graf were aligned and the conserved sequence CGTLNGKTGLIPENYVEFL corresponding to the extreme carboxy-terminus of Graf was selected for antibody production. Purified peptides were obtained commercially (Invitrogen) and rabbit polyclonal antibodies were generated commercially by standard procedures (Cocalico Biologicals). Sera were screened for immunoreactivity by Western analysis of lysates generated from COS cells transfected with plasmids encoding human or frog Graf and endogenous Graf isolated from mouse heart and brain. A consistent band of the predicted 116kDa size was also confirmed by Western analysis using *in vitro* translation assays utilizing recombinant human and frog Graf. Antisera were mixed with an equal volume of glycerol for long-term storage at -20^{o}C.

Whole mount- immunohistochemistry and -in situ *hybridization*

Embryos were prepared for whole-mount immunohistochemistry by fixation in Dent's fixative (80% *methanol*/20% dimethyl sulfoxide) or 4% paraformaldehyde for 2hr at room temperature. PFA-fixed embryos were washed in PBS and photobleached in 5% H_2O_2 in PBS for at least 4hr under bright light. Dent's-fixed embryos were bleached in 5% H_2O_2 in Dent's fixative for at least 4hr under bright light, rinsed in Dent's, and rehydrated in a series of methanol:PBS (75%, 50%, 25%, 5 minutes each). All embryos were then rinsed with PBS

and treated with 1μg/ml bovine testicular hyaluronidase in 50mM sodium acetate buffer for 45 minutes at RT. Embryos were rinsed twice in PBS, 1% Triton X-100, 1%DMSO (PBS-TD). Embryos were blocked for 4 hours at RT in PBS-TD containing 0.1M glycine, 2% powdered milk, and 5% goat serum. Embryos were incubated overnight at 4°C with the appropriate primary antibodies diluted in block buffer. Antibodies used were myosin heavy chain (MHC) (Abcam) (1:500), tropomyosin (DSHB) (1:200), 12-101 (DSHB) (1:250), laminin (Sigma) 1:200, β-dystroglycan (DSHB) (1:200), and HNK (a neuronal marker, ZN12 (DSHB)) (1:200). Embryos were then washed 6 times (1 hour each) in PBS-TD at RT and incubated overnight at 4°C with the appropriate Cy-3 or Alexa-488 conjugated secondary antibodies (1:250) and Topro3 (1:1000) to stain nuclei (Molecular Probes). Embryos were again washed 6 times (1 hour each) in PBS-TD, fixed in Dent's fixative, and stored in 100% methanol at 20°C.

Whole-mount *in situ* hybridization was performed as previously described (Harland, 1991). Plasmids for MyoD and xGraf were linearized and used to generate digoxigenin-UTP-labeled (Roche) antisense RNA probes using the appropriate restriction endonuclease and polymerase. Color detection was determined by BM Purple substrate (Roche) after incubation with alkaline-phosphatase conjugated anti-digoxigenin antibody. Embryos were examined by wide-field microscopic analysis using an Olympus Wild microscope. For cryosectioning, embryos were incubated overnight at 4°C in a 30% sucrose solution in PBS and, the next morning, were embedded in Tissue Tek OCT cryosectioning compound (Sakura Finetek). Cryosections (14 μm) were cut on a Leica cryostat (Leica Microsystems) and fixed to charged glass slides. Sections were imaged on a Leica microscope.

Western Blot Analysis

Embryos (n=5-10) were snap-frozen in liquid nitrogen and protein lysates were generated by brief (1-2 second) sonication in a modified RIPA buffer (10mM Tris pH 7.5, 100mM NaCl, 1mM EDTA, 1mM EGTA, 20mM $Na_4P_2O_7$, 1% Triton X-100) containing a cocktail of protease and phosphatase inhibitors including 1 mM Na_3VO_4, 40 mM NaF, 10 mM Na_2 pyrophosphate, 100 μM leupeptin, 1 mM 4-(2-aminoethyl)benzenesulfonyl fluoride hydrochloride, 0.02 mg/ml soybean trypsin inhibitor, and 0.05 trypsin inhibitory units/ml aprotinin. Samples were clarified by centrifugation twice at 14,000 x *g* at 4°C and the supernatant was retained. Fifty micrograms of total protein was boiled in sample buffer and loaded onto a 10% SDS-acrylamide gel. Separated proteins were transferred onto nitrocellulose, blocked in 5% dry milk in Tris-Buffered Saline (TBS) + 0.1% Tween (TBST), and incubated overnight with primary antibody diluted (1:1000) in blocking solution. Antibodies used were ERK-CT (Upstate), MHC (Abcam), skeletal α-actin (), α-actinin (), troponin T (CT3, DSHB), tropomyosin (CH1, DSHB). Blots were incubated with the appropriate horseradish peroxidase-conjugated secondary antibodies (1:2000 dilution) (GE Healthcare) and proteins were visualized by chemiluminescence (Thermo Scientific).

RT-PCR Analysis

RNA was isolated from 10 embryos following lysis in Trizol according to the manufacturer's specifications (Invitrogen). Reverse transcription reactions were performed using the iScript cDNA kit (Bio-Rad) and PCR reactions were performed using ExTaq polymerase (Takara Bio) following previously published primer sets and cycling parameters for xMHC and xMyogenin (Meadows *et al.*, 2008; Small *et al.*, 2005). Primers for Histone H4 and xGraf were as follows: Forward 5' GGG ATA ACA TTC AGG GTA TC 3' and

Reverse 5’ CAT GGC GGT AAC TGT CTT C 3’. xGraf-forward 5’-GCC AGG AGT CAA GAA TCA AGG-3’, xGraf-reverse 5’-CAA CTC CAA GGT TGG CTA CAG TC-3’

Widefield and laser scanning confocal microscopy, image deconvolution, and 3D rendering

Embryos were cleared for microscopic analysis in 2:1 benzyl benzoate:benzyl alcohol and placed on a glass coverslip. Embryos were analyzed by widefield microscopy using a Leica MZFLIII fluorescence dissecting scope or Olympus IX81 microscope or by confocal microscopy using an Olympus FV500 laser scanning confocal microscope and Fluoview v5.1 software. Confocal z-stacks were obtained using a 1.24µm step-size. Z-series stacks were deconvolved using Autodeblur Gold v. X.1.4.1 software (Autoquant, Media Cybernetics). Deconvolved images were then imported to Imaris x64 6.1.5 software (Bitplane AG) for 3D rendering.

Rho-activity assays

Ten embryos for each treatment (Con Mo- and Graf Mo-injected) were collected at stage 22 and stage 25 and snap frozen in liquid nitrogen for use in the G-LISA luminescence-based RhoA specific activation assay (Cytoskeleton). All buffers were supplied by the manufacturer and the assay performed according to the manufacturer’s instructions. Rho activity was measured in triplicate and statistical analyses were performed by paired two-tail t-test. Data were considered statistically significant at $p< 0.05$.

Transmission electron microscopy (TEM)

Stage 37 embryos were fixed in 2% PFA and 2.5% glyceraldehyde overnight at 4^{o}C. Embryos were then processed and visualized by TEM as previously described (Goetz *et al.*,

2006). Briefly, embryos were post-fixed in ferrocyanide-reduced osmium and embedded in Spurr's epoxy resin. Parasagittal ultra-thin (70nm) sections were mounted on copper grids and post-stained with 4% aqueous uranyl acetate followed by Reynold's lead citrate. Sections were imaged with a LEO EM-910 transmission electron microscope.

Discussion and Future Directions

FAK has an established role in mammalian cardiac development as demonstrated by germ-line and tissue-specific conditional expression model systems (DiMichele *et al.*, 2009; Hakim *et al.*, 2007; Ilic *et al.*, 1995). However, the evolutionary importance of FAK in cardiac development came into question with the finding that genetic ablation of the FAK gene, FAK56, in *Drosophila* resulted in no discernable phenotypic defect (Grabbe *et al.*, 2004). In order to address this disparity and to demonstrate whether FAK is required in the development of the 3-chambered frog heart, we used an antisense morpholino strategy to deplete *Xenopus laevis* embryos of FAK protein. We demonstrated that FAK was required for proper cardiac morphogenesis but not for the early specification and differentiation of cardiomyocytes or for the formation of the linear heart tube. We further established that FAK-depletion led to a reduction in cardiomyocyte proliferation in the heart tube during the initial steps of cardiac looping. Our analysis of cardiomyocyte proliferation in culture demonstrated that FGF-stimulated myocyte proliferation was FAK-dependent and strongly suggests that the cardiac looping defects we observed in FAK-morphant embryos is due, at least in part, to a reduction in FGF-stimulated cardiomyocyte proliferation.

While this evidence is compelling, future studies will be required to fully demonstrate that FAK-dependent cardiomyocyte proliferation is, indeed, dependent on FGF-stimulated signaling pathways. To this end, valuable information could be gleaned from *in situ* hybrization analysis of known FGF-dependent genes in order to demonstrate whether FAK-depletion causes a specific disruption to these downstream effectors. Future studies will also

be directed toward a better understanding of the extent to which FAK is necessary for FGF-dependent cardiogenesis.

To this end, we will test the hypothesis that cardiac-restricted overexpression of active FAK can rescue the cardiac defects observed in the cardiac-restricted FGFR1-knockout mouse line. We have previously generated a line of mice which express SuperFAK (a highly activated mutant of FAK) under the direction of a cardiac-specific promoter. We will cross this line of mice to a second line of mice that have cardiac-restricted deletion of FGFR1. We will assess the gross morphology of the hearts of these double-transgenic mice at various stages of embryonic development and will perform immunohistochemical analysis of tissue sections to determine whether SuperFAK is sufficient to rescue the FGFR1-deficient phenotype. We will analyze cardiomyocyte proliferation by immunohistochemical analysis of BrdU incorporation in the developing heart. In addition, we have previously shown that inactivation of FAK leads to upregulation of p38 activity and regulates the expression of the p38-dependent cell cycle modifier, $p27^{kip}$ (DiMichele *et al.*, 2009) and we will assess these markers by Western blot analysis of heart tissue lysates.

While cardiomyocyte proliferation has been demonstrated to play a role in the cardiac looping process, other processes contribute to this complex morphogenetic event. Specifically, studies in zebrafish have demonstrated that regionalized cardiomyocyte migration is required during cardiac looping. Since FAK has been shown in many cell types to coordinate signaling events that lead to cell migration, it is possible that the cardiac looping defect caused by FAK-depletion could be due, in part, to defective migration of terminally differentiated cardiomyocytes. The analysis of directed cardiomyocyte migration in zebrafish was previously demonstrated utilizing 4D laser scanning confocal microscopy in

transgenic zebrafish expressing fluorescently-tagged cardiac specific markers. A similar approach in developing frog embryos could be used to determine whether FAK-depleted cardiomyocytes exhibit a defect in directed migration that contributes to defective cardiac looping. To this end, transgenic *Xenopus laevis* models expressing GFP under the direction of the myocyte-specific MHC promoter have previously been established and are available for experimental use.

The data presented in this dissertation are the first to demonstrate an *in vivo* role for Graf during development. We have established that Graf depletion in frog embryos leads to impaired myogenic differentiation and defective heart and somite formation. We further demonstrated that Graf depletion during embryogenesis led to a robust induction of Rho activity. The role of Rho in skeletal muscle differentiation has been contentious, in part, because Rho activity must be specifically and tightly regulated during this process. Our *in vivo* data strongly suggest that Graf is a critical regulator of Rho specifically during the intricate process of myogenic differentiation during embryogenesis. In order to further confirm the role of Graf in the skeletal muscle differentiation program, we have recently performed *in vitro* differentiation experiments utilizing the myoblast cell lines, C2C12 and L6, which are competent to spontaneously differentiate into mature myotubes under low-serum conditions. These studies have shown that Graf overexpression leads to precocious expression of the skeletal muscle differentiation markers, skeletal α-actin, α-actinin, tropomyosin, MHC, and troponin T, as assessed by RT-PCR, Western blot, and immunohistochemical analyses. Furthermore, Graf-depletion by transfection with Graf-specific siRNAs leads to a disruption of the differentiation program as assessed by myotube formation and by Western blot analysis of MHC. Additional Western blot analyses in Graf

siRNA-transfected myoblasts will be performed to confirm that expression of other markers of skeletal muscle terminal differentiation (e.g. tropomyosin, troponin T) is similarly decreased in the absence of Graf.

As noted previously, skeletal muscle terminal differentiation culminates in the fusion of myocytes into multi-nucleate myotubes. Notably, our expression analyses suggest that Graf is upregulated during the time of skeletal muscle differentiation and fusion, suggesting that Graf may play a role both in skeletal marker gene expression and in regulation of fusion. However, we were unable to assess a role for Graf during myocyte fusion in our present studies because *Xenopus* skeletal muscle does not undergo fusion until secondary myogenesis, a time after which Graf-depletion by Graf Mo-injection led to embryonic lethality. Therefore, future studies will examine whether Graf plays a role in myotube fusion using the C2C12 and L6 differentiation assays described above. Indeed, preliminary evidence strongly suggests that transfection of differentiating L6 cells with wild-type Graf leads to a robust increase in the number of multinucleated myotubes. Conversely, transfection with a GAP-dead mutant of Graf (in which GAP activity is ablated by a point mutation in the GAP domain) does not induce an increase in myotube fusion as assessed by multi-nucleation.

In order to establish a role for Graf in muscle fusion *in vivo*, we have begun to generate transgenic mouse lines which can be induced to over-express Graf (or GAP-dead Graf) by expression of CRE-recombinase. These mice will be crossed to established mouse lines expressing CRE under the direction of muscle-specific promoters and muscle fusion will be assessed by immunohistochemical analyses at various timepoints during embryogenesis and shortly after birth, a time of robust muscle fusion. We anticipate that Graf

(but not GAP-dead Graf) overexpression will lead to increased muscle fusion and overall muscle mass.

Since muscle fusion is a necessary step in muscle repair, we are interested in further determining whether Graf can lead to improved muscle repair after injury. In order to determine whether Graf expression is increased after injury, we will utilize previously established methods to injure the tibialis muscle and measure Graf expression by RT-PCR and Western blot analyses of tissue lysates from injured and uninjured muscle. Next, we will determine whether Graf overexpression in satellite cells leads to improved muscle repair. Pax7 is a transcription factor expressed by muscle satellite cells, a quiescent population of muscle precursor cells within adult muscle which maintain the capacity to proliferate and fuse with existing skeletal muscle during injury repair (Seale *et al.*, 2000). We will cross Pax7-Cre mice to our Graf-overexpressing mice to develop mice which overexpress Graf specifically in the satellite cells. We will then induce injury in the tibialis muscle as previously described in both wild-type and Pax7-Graf mice and assess the extent of repair at various time-points after surgery by immunohistochemical analyses of muscle biopsies.

Our *in vivo* data presented herein show that Graf-depletion leads to defects in intersomitic laminin deposition and mis-localization of β-dystroglycan and strongly suggest that Graf interacts with laminin and β-dystroglycan at the myoseptum. Our recent immunoprecipitation assays have confirmed that Graf interacts with β-dystroglycan (data not shown) further suggesting that Graf physically interacts with the DGC *in vivo*. These findings coupled with the previously established interaction between Graf and FAK, establishes the intriguing possibility that Graf may help to coordinate cytoskeletal interactions with the ECM through both the DGC and integrins. Notably, it has previously been shown that mice lacking

both dystrophin and α_7-integrin develop a more severe dystrophic phenotype than those lacking either dystrophin or the α_7-integrin alone (Rooney *et al.*, 2006). Furthermore, overexpression of $\alpha_7\beta_1$-integrin can partially rescue the dystrophic phenotype of mice lacking dystrophin and utrophin (Burkin *et al.*, 2001). Therefore, it appears that there is some functional redundancy and cross-talk between the integrin and the DGC in muscular dystrophy. Taken together, these findings suggest the exciting possibility that Graf may serve to coordinate integrin and DGC in normal muscle development and suggest that Graf could serve as a therapeutic target for muscle repair in these pathological conditions. Notably, the somite defects we observed in Graf-depleted embryos phenocopies the dystrophic phenotypes observed in a variety of model organisms including frog, zebrafish, and mice (Deniziak *et al.*, 2007; Hanel *et al.*, 2009; Kudo *et al.*, 2004; Postel *et al.*, 2008; Zoeller *et al.*, 2008). Future studies will assess the possibility that muscle-specific Graf overexpression can rescue the dystrophic phenotype in *mdx* mice (a dystrophin-mutant transgenic mouse line) and these studies are currently underway.

The data presented herein demonstrate that both FAK and Graf are required during embryogenesis and the phenotypes induced by depletion of either protein are similar yet distinctive. Given that these proteins physically interact, it is instructive to consider how these findings strengthen our understanding of the *in vivo* functions of FAK and Graf during development. For example, looping morphogenesis was disrupted by depletion of either FAK or Graf. However, the mechanisms underlying this phenotype appear distinct in these two models.

Our findings suggested that FAK depletion led to looping dysmorphogenesis due to diminished cardiomyocyte proliferation. By contrast, our analyses of Graf morphant embryos

suggested that looping morphogenesis (and cardia bifida, a phenotype not observed in FAK-depleted embryos) was due to impaired myogenic differentiation. A caveat to this interpretation is that our analyses of myogenic marker gene expression were determined in lysates from whole embryos. Thus, future analysis of isolated heart tissues would be required to determine whether cardiac differentiation was specifically impaired in the absence of Graf (since many of our antibodies cross-react with skeletal- and cardiac- specific isoforms). In addition, our studies did not specifically address whether Graf depletion also caused a reduction in cardiomyocyte proliferation; however we consider this possibility unlikely. First, we have performed a small pilot-study assessing cardiomyocyte proliferation comparing Con Mo- and Graf Mo-injected embryos and did not observe any statistical difference between groups (data not shown). Furthermore, given that Graf serves to downregulate Rho, a protein which is known to upregulate cardiomyocyte proliferation in a variety of model systems (see, for example, (Wei *et al.*, 2002; Zhao and Rivkees, 2003)), we would hypothesize that Graf depletion would increase, rather than decrease, cardiomyocyte proliferation. Thus, additional studies will need to be performed to confirm whether Graf has any effect (positive or negative) on cardiomyocyte proliferation. Nonetheless, our data suggest that FAK and Graf play distinct roles during cardiogenesis with FAK regulating cardiomyocyte proliferation and Graf regulating Rho-dependent myogenic differentiation.

The similarities and differences between the FAK- and Graf-morphant somite phenotypes are also noteworthy. Previous studies in *Xenopus* have demonstrated that FAK-inhibition (by FRNK-overexpression) in the presumptive somites leads to defects in somite rotation and formation (Kragtorp and Miller, 2006). Our analyses revealed no such defects; however, this was not unexpected since, in our model, FAK protein was not markedly

reduced during the early developmental stages during which somite rotation occurs. Another interpretation is that FAK is required for the initial specification of *Xenopus* somites and for the fibronectin binding known to regulate somite rotation but not for the further terminal differentiation of these tissues. Indeed, *in vitro* analyses in cultured myoblasts have previously shown that FAK is required for myoblast maintenance (specifically, proliferation of myoblasts prior to differentiation) and for late myotube fusion but appears not to regulate skeletal muscle marker gene expression (as described in Chapter I). Since FAK was not depleted in our frog model until after somite differentiation had begun and frog swimming muscle does not undergo multinucleation, we would not expect to observe a somite defect in FAK morphant embryos. By contrast, Graf-depletion led to a marked reduction in skeletal muscle differentiation and a striking somite defect. These differences suggest that Graf and FAK regulate different mechanisms of myogenic development with FAK responding to proliferative signaling and Graf regulating myogenic differentiation and sarcomerogenesis.

REFERENCES

Ahuja P, Sdek P, MacLellan WR. 2007. Cardiac myocyte cell cycle control in development, disease, and regeneration. Physiol Rev 87:521-544.

Alexander J, Rothenberg M, Henry GL, Stainier DY. 1999. casanova plays an early and essential role in endoderm formation in zebrafish. Dev Biol 215:343-357.

Baker LP, Daggett DF, Peng HB. 1994. Concentration of pp125 focal adhesion kinase (FAK) at the myotendinous junction. J Cell Sci 107 (Pt 6):1485-1497.

Beqaj S, Jakkaraju S, Mattingly RR, Pan D, Schuger L. 2002. High RhoA activity maintains the undifferentiated mesenchymal cell phenotype, whereas RhoA down-regulation by laminin-2 induces smooth muscle myogenesis. J Cell Biol 156:893-903.

Bojesen SE, Ammerpohl O, Weinhausl A, Haas OA, Mettal H, Bohle RM, Borkhardt A, Fuchs U. 2006. Characterisation of the GRAF gene promoter and its methylation in patients with acute myeloid leukaemia and myelodysplastic syndrome. Br J Cancer 94:323-332.

Borkhardt A, Bojesen S, Haas OA, Fuchs U, Bartelheimer D, Loncarevic IF, Bohle RM, Harbott J, Repp R, Jaeger U, Viehmann S, Henn T, Korth P, Scharr D, Lampert F. 2000. The human GRAF gene is fused to MLL in a unique t(5;11)(q31;q23) and both alleles are disrupted in three cases of myelodysplastic syndrome/acute myeloid leukemia with a deletion 5q. Proc Natl Acad Sci U S A 97:9168-9173.

Brade T, Gessert S, Kuhl M, Pandur P. 2007. The amphibian second heart field: Xenopus islet-1 is required for cardiovascular development. Dev Biol 311:297-310.

Brown DD, Martz SN, Binder O, Goetz SC, Price BM, Smith JC, Conlon FL. 2005. Tbx5 and Tbx20 act synergistically to control vertebrate heart morphogenesis. Development 132:553-563.

Burkin DJ, Wallace GQ, Nicol KJ, Kaufman DJ, Kaufman SJ. 2001. Enhanced expression of the alpha 7 beta 1 integrin reduces muscular dystrophy and restores viability in dystrophic mice. J Cell Biol 152:1207-1218.

Burridge K, Fath K, Kelly T, Nuckolls G, Turner C. 1988. Focal adhesions: transmembrane junctions between the extracellular matrix and the cytoskeleton. Annu Rev Cell Biol 4:487-525.

Carnac G, Primig M, Kitzmann M, Chafey P, Tuil D, Lamb N, Fernandez A. 1998. RhoA GTPase and Serum Response Factor Control Selectively the Expression of MyoD without Affecting Myf5 in Mouse Myoblasts. Mol. Biol. Cell 9:1891-1902.

Castellani L, Salvati E, Alema S, Falcone G. 2006. Fine regulation of RhoA and Rock is required for skeletal muscle differentiation. J Biol Chem 281:15249-15257.

Charrasse S, Comunale F, Grumbach Y, Poulat F, Blangy A, Gauthier-Rouviere C. 2006. RhoA GTPase regulates M-cadherin activity and myoblast fusion. Mol Biol Cell 17:749-759.

Charrasse S, Meriane M, Comunale F, Blangy A, Gauthier-Rouviere C. 2002. N-cadherin-dependent cell-cell contact regulates Rho GTPases and beta-catenin localization in mouse C2C12 myoblasts. J Cell Biol 158:953-965.

Chen H, Shi S, Acosta L, Li W, Lu J, Bao S, Chen Z, Yang Z, Schneider MD, Chien KR, Conway SJ, Yoder MC, Haneline LS, Franco D, Shou W. 2004. BMP10 is essential for maintaining cardiac growth during murine cardiogenesis. Development 131:2219-2231.

Choi M, Stottmann RW, Yang YP, Meyers EN, Klingensmith J. 2007. The bone morphogenetic protein antagonist noggin regulates mammalian cardiac morphogenesis. Circ Res 100:220-228.

Christine KS, Conlon FL. 2008. Vertebrate CASTOR is required for differentiation of cardiac precursor cells at the ventral midline. Dev Cell 14:616-623.

Clemente CF, Corat MA, Saad ST, Franchini KG. 2005. Differentiation of C2C12 myoblasts is critically regulated by FAK signaling. Am J Physiol Regul Integr Comp Physiol 289:R862-870.

David JP, Victoria LTB, Takashi M. 2003. Epicardium is required for the full rate of myocyte proliferation and levels of expression of myocyte mitogenic factors FGF2 and its receptor, FGFR-1, but not for transmural myocardial patterning in the embryonic chick heart. Developmental Dynamics 228:161-172.

de Pater E, Clijsters L, Marques SR, Lin Y-F, Garavito-Aguilar ZV, Yelon D, Bakkers J. 2009. Distinct phases of cardiomyocyte differentiation regulate growth of the zebrafish heart. Development 136:1633-1641.

Dehaan RL. 1963. Migration patterns of the precardiac mesoderm in the early chick embrvo. Exp Cell Res 29:544-560.

Deniziak M, Thisse C, Rederstorff M, Hindelang C, Thisse B, Lescure A. 2007. Loss of selenoprotein N function causes disruption of muscle architecture in the zebrafish embryo. Exp Cell Res 313:156-167.

Dickmeis T, Mourrain P, Saint-Etienne L, Fischer N, Aanstad P, Clark M, Strahle U, Rosa F. 2001. A crucial component of the endoderm formation pathway, CASANOVA, is encoded by a novel sox-related gene. Genes Dev 15:1487-1492.

DiMichele LA, Hakim ZS, Sayers RL, Rojas M, Schwartz RJ, Mack CP, Taylor JM. 2009. Transient Expression of FRNK Reveals Stage-Specific Requirement for Focal Adhesion Kinase Activity in Cardiac Growth. Circ Res 104:1201-1208.

Engel FB, Hsieh PC, Lee RT, Keating MT. 2006. FGF1/p38 MAP kinase inhibitor therapy induces cardiomyocyte mitosis, reduces scarring, and rescues function after myocardial infarction. Proc Natl Acad Sci U S A 103:15546-15551.

Engel FB, Schebesta M, Duong MT, Lu G, Ren S, Madwed JB, Jiang H, Wang Y, Keating MT. 2005. p38 MAP kinase inhibition enables proliferation of adult mammalian cardiomyocytes. Genes Dev 19:1175-1187.

Engelmann GL, Dionne CA, Jaye MC. 1991. Acidic fibroblast growth factor, heart development, and capillary angiogenesis. Ann N Y Acad Sci 638:463-466.

Engelmann GL, Dionne CA, Jaye MC. 1993. Acidic fibroblast growth factor and heart development. Role in myocyte proliferation and capillary angiogenesis. Circ Res 72:7-19.

Etienne-Manneville S, Hall A. 2002. Rho GTPases in cell biology. Nature 420:629-635.

Furuta Y, Ilic D, Kanazawa S, Takeda N, Yamamoto T, Aizawa S. 1995. Mesodermal defect in late phase of gastrulation by a targeted mutation of focal adhesion kinase, FAK. Oncogene 11:1989-1995.

George EL, Baldwin HS, Hynes RO. 1997. Fibronectins are essential for heart and blood vessel morphogenesis but are dispensable for initial specification of precursor cells. Blood 90:3073-3081.

George EL, Georges-Labouesse EN, Patel-King RS, Rayburn H, Hynes RO. 1993. Defects in mesoderm, neural tube and vascular development in mouse embryos lacking fibronectin. Development 119:1079-1091.

Georges-Labouesse EN, George EL, Rayburn H, Hynes RO. 1996. Mesodermal development in mouse embryos mutant for fibronectin. Dev Dyn 207:145-156.

Giancotti FG, Ruoslahti E. 1999. Integrin signaling. Science 285:1028-1032.

Goetz SC, Brown DD, Conlon FL. 2006. TBX5 is required for embryonic cardiac cell cycle progression. Development 133:2575-2584.

Goetz SC, Conlon FL. 2007. Cardiac progenitors and the embryonic cell cycle. Cell Cycle 6:1974-1981.

Grabbe C, Zervas CG, Hunter T, Brown NH, Palmer RH. 2004. Focal adhesion kinase is not required for integrin function or viability in Drosophila. Development 131:5795-5805.

Guan JL. 1997. Focal adhesion kinase in integrin signaling. Matrix Biol 16:195-200.

Guglieri M, Bushby K. Molecular treatments in Duchenne muscular dystrophy. Curr Opin Pharmacol.

Habas R, Kato Y, He X. 2001. Wnt/Frizzled activation of Rho regulates vertebrate gastrulation and requires a novel Formin homology protein Daam1. Cell 107:843-854.

Hagel M, George EL, Kim A, Tamimi R, Opitz SL, Turner CE, Imamoto A, Thomas SM. 2002. The adaptor protein paxillin is essential for normal development in the mouse and is a critical transducer of fibronectin signaling. Mol Cell Biol 22:901-915.

Hakim ZS, DiMichele LA, Doherty JT, Homeister JW, Beggs HE, Reichardt LF, Schwartz RJ, Brackhan J, Smithies O, Mack CP, Taylor JM. 2007. Conditional deletion of focal

adhesion kinase leads to defects in ventricular septation and outflow tract alignment. Mol Cell Biol 27:5352-5364.

Hamilton L. 1969. The formation of somites in Xenopus. J Embryol Exp Morphol 22:253-264.

Hanel ML, Wuebbles RD, Jones PL. 2009. Muscular dystrophy candidate gene FRG1 is critical for muscle development. Dev Dyn 238:1502-1512.

Harland RM. 1991. In situ hybridization: an improved whole-mount method for Xenopus embryos. Methods Cell Biol 36:685-695.

Harvey RP. 2002. Patterning the vertebrate heart. Nat Rev Genet 3:544-556.

Hasty P, Bradley A, Morris JH, Edmondson DG, Venuti JM, Olson EN, Klein WH. 1993. Muscle deficiency and neonatal death in mice with a targeted mutation in the myogenin gene. Nature 364:501-506.

Hayashi YK, Chou FL, Engvall E, Ogawa M, Matsuda C, Hirabayashi S, Yokochi K, Ziober BL, Kramer RH, Kaufman SJ, Ozawa E, Goto Y, Nonaka I, Tsukahara T, Wang JZ, Hoffman EP, Arahata K. 1998. Mutations in the integrin alpha7 gene cause congenital myopathy. Nat Genet 19:94-97.

Hens MD, DeSimone DW. 1995. Molecular analysis and developmental expression of the focal adhesion kinase pp125FAK in Xenopus laevis. Dev Biol 170:274-288.

Hildebrand JD, Schaller MD, Parsons JT. 1993. Identification of sequences required for the efficient localization of the focal adhesion kinase, pp125FAK, to cellular focal adhesions. J Cell Biol 123:993-1005.

Hildebrand JD, Taylor JM, Parsons JT. 1996. An SH3 domain-containing GTPase-activating protein for Rho and Cdc42 associates with focal adhesion kinase. Mol Cell Biol 16:3169-3178.

Hill CS, Wynne J, Treisman R. 1995. The Rho family GTPases RhoA, Rac1, and CDC42Hs regulate transcriptional activation by SRF. Cell 81:1159-1170.

Hoffman JI. 1995. Incidence of congenital heart disease: II. Prenatal incidence. Pediatr Cardiol 16:155-165.

Hoffman JI, Kaplan S. 2002. The incidence of congenital heart disease. J Am Coll Cardiol 39:1890-1900.

Honda H, Oda H, Nakamoto T, Honda Z, Sakai R, Suzuki T, Saito T, Nakamura K, Nakao K, Ishikawa T, Katsuki M, Yazaki Y, Hirai H. 1998. Cardiovascular anomaly, impaired actin bundling and resistance to Src-induced transformation in mice lacking p130Cas. Nat Genet 19:361-365.

Hsia DA, Mitra SK, Hauck CR, Streblow DN, Nelson JA, Ilic D, Huang S, Li E, Nemerow GR, Leng J, Spencer KS, Cheresh DA, Schlaepfer DD. 2003. Differential regulation of cell motility and invasion by FAK. J Cell Biol 160:753-767.

Ilic D, Furuta Y, Kanazawa S, Takeda N, Sobue K, Nakatsuji N, Nomura S, Fujimoto J, Okada M, Yamamoto T. 1995. Reduced cell motility and enhanced focal adhesion contact formation in cells from FAK-deficient mice. Nature 377:539-544.

Ilic D, Kovacic B, Johkura K, Schlaepfer DD, Tomasevic N, Han Q, Kim J-B, Howerton K, Baumbusch C, Ogiwara N, Streblow DN, Nelson JA, Dazin P, Shino Y, Sasaki K, Damsky CH. 2004. FAK promotes organization of fibronectin matrix and fibrillar adhesions. J Cell Sci 117:177-187.

Itoh N, Ornitz DM. 2004. Evolution of the Fgf and Fgfr gene families. Trends in Genetics 20:563-569.

Iwasaki K, Hayashi K, Fujioka T, Sobue K. 2008. Rho/Rho-associated kinase signal regulates myogenic differentiation via myocardin-related transcription factor-A/Smad-dependent transcription of the Id3 gene. J Biol Chem 283:21230-21241.

Kaarbo M, Crane DI, Murrell WG. 2003. RhoA is highly up-regulated in the process of early heart development of the chick and important for normal embryogenesis. Dev Dyn 227:35-47.

Kassar-Duchossoy L, Gayraud-Morel B, Gomes D, Rocancourt D, Buckingham M, Shinin V, Tajbakhsh S. 2004. Mrf4 determines skeletal muscle identity in Myf5:Myod double-mutant mice. Nature 431:466-471.

Keller R. 2000. The origin and morphogenesis of amphibian somites. Curr Top Dev Biol 47:183-246.

Kikuchi Y, Agathon A, Alexander J, Thisse C, Waldron S, Yelon D, Thisse B, Stainier DY. 2001. casanova encodes a novel Sox-related protein necessary and sufficient for early endoderm formation in zebrafish. Genes Dev 15:1493-1505.

Kikuchi Y, Trinh LA, Reiter JF, Alexander J, Yelon D, Stainier DY. 2000. The zebrafish bonnie and clyde gene encodes a Mix family homeodomain protein that regulates the generation of endodermal precursors. Genes Dev 14:1279-1289.

Kolker SJ, Tajchman U, Weeks DL. 2000. Confocal imaging of early heart development in Xenopus laevis. Dev Biol 218:64-73.

Kontaridis MI, Eminaga S, Fornaro M, Zito CI, Sordella R, Settleman J, Bennett AM. 2004. SHP-2 positively regulates myogenesis by coupling to the Rho GTPase signaling pathway. Mol Cell Biol 24:5340-5352.

Kozma R, Ahmed S, Best A, Lim L. 1996. The GTPase-activating protein n-chimaerin cooperates with Rac1 and Cdc42Hs to induce the formation of lamellipodia and filopodia. Mol Cell Biol 16:5069-5080.

Kragtorp KA, Miller JR. 2006. Regulation of somitogenesis by Ena/VASP proteins and FAK during Xenopus development. Development 133:685-695.

Kudo H, Amizuka N, Araki K, Inohaya K, Kudo A. 2004. Zebrafish periostin is required for the adhesion of muscle fiber bundles to the myoseptum and for the differentiation of muscle fibers. Dev Biol 267:473-487.

Langdon YG, Goetz SC, Berg AE, Swanik JT, Conlon FL. 2007. SHP-2 is required for the maintenance of cardiac progenitors. Development 134:4119-4130.

Lavine KJ, Ornitz DM. 2008. Fibroblast growth factors and Hedgehogs: at the heart of the epicardial signaling center. Trends Genet 24:33-40.

Lavine KJ, Schmid GJ, Smith CS, Ornitz DM. 2008. Novel tool to suppress cell proliferation in vivo demonstrates that myocardial and coronary vascular growth represent distinct developmental programs. Dev Dyn 237:713-724.

Lavine KJ, Yu K, White AC, Zhang X, Smith C, Partanen J, Ornitz DM. 2005. Endocardial and Epicardial Derived FGF Signals Regulate Myocardial Proliferation and Differentiation In Vivo. Developmental Cell 8:85-95.

Lea R, Papalopulu N, Amaya E, Dorey K. 2009. Temporal and spatial expression of FGF ligands and receptors during Xenopus development. Dev Dyn 238:1467-1479.

Lisi MT, Cohn RD. 2007. Congenital muscular dystrophies: new aspects of an expanding group of disorders. Biochim Biophys Acta 1772:159-172.

Longenecker KL, Zhang B, Derewenda U, Sheffield PJ, Dauter Z, Parsons JT, Zheng Y, Derewenda ZS. 2000. Structure of the BH domain from graf and its implications for Rho GTPase recognition. J Biol Chem 275:38605-38610.

MacMullin A, Jacobs JR. 2006. Slit coordinates cardiac morphogenesis in Drosophila. Dev Biol 293:154-164.

Marsden M, DeSimone DW. 2001. Regulation of cell polarity, radial intercalation and epiboly in Xenopus: novel roles for integrin and fibronectin. Development 128:3635-3647.

Martinsen BJ, Frasier AJ, Baker CVH, Lohr JL. 2004. Cardiac neural crest ablation alters Id2 gene expression in the developing heart. Developmental Biology 272:176-190.

Mayer U. 2003. Integrins: redundant or important players in skeletal muscle? J Biol Chem 278:14587-14590.

Mayer U, Saher G, Fassler R, Bornemann A, Echtermeyer F, von der Mark H, Miosge N, Poschl E, von der Mark K. 1997. Absence of integrin alpha 7 causes a novel form of muscular dystrophy. Nat Genet 17:318-323.

McCormick F. 1989. ras GTPase activating protein: signal transmitter and signal terminator. Cell 56:5-8.

Meadows SM, Warkman AS, Salanga MC, Small EM, Krieg PA. 2008. The myocardin-related transcription factor, MASTR, cooperates with MyoD to activate skeletal muscle gene expression. Proceedings of the National Academy of Sciences 105:1545-1550.

Meriane M, Roux P, Primig M, Fort P, Gauthier-Rouviere C. 2000. Critical activities of Rac1 and Cdc42Hs in skeletal myogenesis: antagonistic effects of JNK and p38 pathways. Mol Biol Cell 11:2513-2528.

Mohammadi M, McMahon G, Sun L, Tang C, Hirth P, Yeh BK, Hubbard SR, Schlessinger J. 1997. Structures of the tyrosine kinase domain of fibroblast growth factor receptor in complex with inhibitors. Science 276:955-960.

Mohun T, Orford R, Shang C. 2003. The Origins of Cardiac Tissue in the Amphibian, Xenopus laevis. Trends in Cardiovascular Medicine 13:244-248.

Mohun T WR, Gionti E, Logan M. . 1994. Myogenesis in Xenopus laevis. Trends in Cardiovascular Medicine 4:146-151.

Mohun TJ, Leong LM, Weninger WJ, Sparrow DB. 2000. The morphology of heart development in Xenopus laevis. Dev Biol 218:74-88.

Moorman AF, Christoffels VM. 2003. Cardiac chamber formation: development, genes, and evolution. Physiol Rev 83:1223-1267.

Nabeshima Y, Hanaoka K, Hayasaka M, Esumi E, Li S, Nonaka I, Nabeshima Y. 1993. Myogenin gene disruption results in perinatal lethality because of severe muscle defect. Nature 364:532-535.

Nieuwkoop PD, Faber J. 1994. Normal table of Xenopus laevis (Daudin) : a systematical and chronological survey of the development from the fertilized egg till the end of metamorphosis. New York: Garland Pub. 252 p., 210 leaves of plates p.

Nishiyama T, Kii I, Kudo A. 2004. Inactivation of Rho/ROCK signaling is crucial for the nuclear accumulation of FKHR and myoblast fusion. J Biol Chem 279:47311-47319.

O'Brien SP, Seipel K, Medley QG, Bronson R, Segal R, Streuli M. 2000. Skeletal muscle deformity and neuronal disorder in Trio exchange factor-deficient mouse embryos. Proc Natl Acad Sci U S A 97:12074-12078.

Olson EN. 2006. Gene regulatory networks in the evolution and development of the heart. Science 313:1922-1927.

Panagopoulos I, Kitagawa A, Isaksson M, Morse H, Mitelman F, Johansson B. 2004. MLL/GRAF fusion in an infant acute monocytic leukemia (AML M5b) with a cytogenetically cryptic ins(5;11)(q31;q23q23). Genes Chromosomes Cancer 41:400-404.

Parsons JT. 2003. Focal adhesion kinase: the first ten years. J Cell Sci 116:1409-1416.

Pasumarthi KBS, Kardami E, Cattini PA. 1996. High and Low Molecular Weight Fibroblast Growth Factor-2 Increase Proliferation of Neonatal Rat Cardiac Myocytes but Have Differential Effects on Binucleation and Nuclear Morphology : Evidence for Both Paracrine and Intracrine Actions of Fibroblast GrowthFactor-2. Circ Res 78:126-136.

Paulssen RH, Woodson J, Liu Z, Ross EM. 1996. Carboxyl-terminal fragments of phospholipase C-beta1 with intrinsic Gq GTPase-activating protein (GAP) activity. J Biol Chem 271:26622-26629.

Peng X, Wu X, Druso JE, Wei H, Park AY, Kraus MS, Alcaraz A, Chen J, Chien S, Cerione RA, Guan JL. 2008. Cardiac developmental defects and eccentric right ventricular hypertrophy in cardiomyocyte focal adhesion kinase (FAK) conditional knockout mice. Proc Natl Acad Sci U S A 105:6638-6643.

Postel R, Vakeel P, Topczewski J, Knoll R, Bakkers J. 2008. Zebrafish integrin-linked kinase is required in skeletal muscles for strengthening the integrin-ECM adhesion complex. Dev Biol 318:92-101.

Pourquie O. 2001. Vertebrate somitogenesis. Annu Rev Cell Dev Biol 17:311-350.

Quach NL, Biressi S, Reichardt LF, Keller C, Rando TA. 2009. Focal adhesion kinase signaling regulates the expression of caveolin 3 and beta1 integrin, genes essential for normal myoblast fusion. Mol Biol Cell 20:3422-3435.

Ramakers GJ. 2002. Rho proteins, mental retardation and the cellular basis of cognition. Trends Neurosci 25:191-199.

Reiter JF, Alexander J, Rodaway A, Yelon D, Patient R, Holder N, Stainier DY. 1999. Gata5 is required for the development of the heart and endoderm in zebrafish. Genes Dev 13:2983-2995.

Ribeiro I, Kawakami Y, Buscher D, Raya A, Rodriguez-Leon J, Morita M, Rodriguez Esteban C, Izpisua Belmonte JC. 2007. Tbx2 and Tbx3 Regulate the Dynamics of Cell Proliferation during Heart Remodeling. PLoS ONE 2:e398.

Richardson A, Parsons T. 1996. A mechanism for regulation of the adhesion-associated proteintyrosine kinase pp125FAK. Nature 380:538-540.

Ridley AJ. 1996. Rho: theme and variations. Curr Biol 6:1256-1264.

Ridley AJ, Hall A. 1992. The small GTP-binding protein rho regulates the assembly of focal adhesions and actin stress fibers in response to growth factors. Cell 70:389-399.

Rooney JE, Welser JV, Dechert MA, Flintoff-Dye NL, Kaufman SJ, Burkin DJ. 2006. Severe muscular dystrophy in mice that lack dystrophin and alpha7 integrin. J Cell Sci 119:2185-2195.

Rosamond W, Flegal K, Furie K, Go A, Greenlund K, Haase N, Hailpern SM, Ho M, Howard V, Kissela B, Kittner S, Lloyd-Jones D, McDermott M, Meigs J, Moy C, Nichol G, O'Donnell C, Roger V, Sorlie P, Steinberger J, Thom T, Wilson M, Hong Y. 2008. Heart disease and stroke statistics--2008 update: a report from the American Heart Association Statistics Committee and Stroke Statistics Subcommittee. Circulation 117:e25-146.

Ross RS, Borg TK. 2001. Integrins and the myocardium. Circ Res 88:1112-1119.

Rudnicki MA, Schnegelsberg PN, Stead RH, Braun T, Arnold HH, Jaenisch R. 1993. MyoD or Myf-5 is required for the formation of skeletal muscle. Cell 75:1351-1359.

Sadaghiani B, Thiébaud CH. 1987. Neural crest development in the Xenopus laevis embryo, studied by interspecific transplantation and scanning electron microscopy. Developmental Biology 124:91-110.

Schier AF, Neuhauss SC, Helde KA, Talbot WS, Driever W. 1997. The one-eyed pinhead gene functions in mesoderm and endoderm formation in zebrafish and interacts with no tail. Development 124:327-342.

Seale P, Sabourin LA, Girgis-Gabardo A, Mansouri A, Gruss P, Rudnicki MA. 2000. Pax7 is required for the specification of myogenic satellite cells. Cell 102:777-786.

Sieg DJ, Hauck CR, Schlaepfer DD. 1999. Required role of focal adhesion kinase (FAK) for integrin-stimulated cell migration. J Cell Sci 112 (Pt 16):2677-2691.

Small EM, Warkman AS, Wang D-Z, Sutherland LB, Olson EN, Krieg PA. 2005. Myocardin is sufficient and necessary for cardiac gene expression in Xenopus. Development 132:987-997.

Sordella R, Jiang W, Chen G-C, Curto M, Settleman J. 2003. Modulation of Rho GTPase Signaling Regulates a Switch between Adipogenesis and Myogenesis. Cell 113:147-158.

Srivastava D, Olson EN. 2000. A genetic blueprint for cardiac development. Nature 407:221-226.

Stenson PD, Ball EV, Mort M, Phillips AD, Shiel JA, Thomas NS, Abeysinghe S, Krawczak M, Cooper DN. 2003. Human Gene Mutation Database (HGMD): 2003 update. Hum Mutat 21:577-581.

Szeto DP, Griffin KJ, Kimelman D. 2002. HrT is required for cardiovascular development in zebrafish. Development 129:5093-5101.

Takano H, Komuro I, Oka T, Shiojima I, Hiroi Y, Mizuno T, Yazaki Y. 1998. The Rho family G proteins play a critical role in muscle differentiation. Mol Cell Biol 18:1580-1589.

Taylor JM, Hildebrand JD, Mack CP, Cox ME, Parsons JT. 1998. Characterization of graf, the GTPase-activating protein for rho associated with focal adhesion kinase. Phosphorylation and possible regulation by mitogen-activated protein kinase. J Biol Chem 273:8063-8070.

Taylor JM, Macklem MM, Parsons JT. 1999. Cytoskeletal changes induced by GRAF, the GTPase regulator associated with focal adhesion kinase, are mediated by Rho. J Cell Sci 112 (Pt 2):231-242.

Taylor JM, Rovin JD, Parsons JT. 2000. A role for focal adhesion kinase in phenylephrine-induced hypertrophy of rat ventricular cardiomyocytes. J Biol Chem 275:19250-19257.

Tcherkezian J, Lamarche-Vane N. 2007. Current knowledge of the large RhoGAP family of proteins. Biol Cell 99:67-86.

Timpl R, Brown JC. 1996. Supramolecular assembly of basement membranes. Bioessays 18:123-132.

Travaglione S, Messina G, Fabbri A, Falzano L, Giammarioli AM, Grossi M, Rufini S, Fiorentini C. 2005. Cytotoxic necrotizing factor 1 hinders skeletal muscle differentiation in vitro by perturbing the activation/deactivation balance of Rho GTPases. Cell Death Differ 12:78-86.

Trinh LA, Stainier DY. 2004a. Cardiac development. Methods Cell Biol 76:455-473.

Trinh LA, Stainier DY. 2004b. Fibronectin regulates epithelial organization during myocardial migration in zebrafish. Dev Cell 6:371-382.

van der Flier A, Sonnenberg A. 2001. Function and interactions of integrins. Cell Tissue Res 305:285-298.

Wang SM, Tsai YJ, Jiang MJ, Tseng YZ. 1997. Studies on the function of rho A protein in cardiac myofibrillogenesis. J Cell Biochem 66:43-53.

Wei L, Imanaka-Yoshida K, Wang L, Zhan S, Schneider MD, DeMayo FJ, Schwartz RJ. 2002. Inhibition of Rho family GTPases by Rho GDP dissociation inhibitor disrupts cardiac morphogenesis and inhibits cardiomyocyte proliferation. Development 129:1705-1714.

Wei L, Zhou W, Croissant JD, Johansen F-E, Prywes R, Balasubramanyam A, Schwartz RJ. 1998. RhoA Signaling via Serum Response Factor Plays an Obligatory Role in Myogenic Differentiation. Journal of Biological Chemistry 273:30287-30294.

Wilson PA, Hemmati-Brivanlou A. 1995. Induction of epidermis and inhibition of neural fate by Bmp-4. Nature 376:331-333.

Wunnenberg-Stapleton K, Blitz IL, Hashimoto C, Cho KW. 1999. Involvement of the small GTPases XRhoA and XRnd1 in cell adhesion and head formation in early Xenopus development. Development 126:5339-5351.

Xu W, Baribault H, Adamson ED. 1998. Vinculin knockout results in heart and brain defects during embryonic development. Development 125:327-337.

Yelon D, Ticho B, Halpern ME, Ruvinsky I, Ho RK, Silver LM, Stainier DY. 2000. The bHLH transcription factor hand2 plays parallel roles in zebrafish heart and pectoral fin development. Development 127:2573-2582.

Yue Q, Wagstaff L, Yang X, Weijer C, Munsterberg A. 2008. Wnt3a-mediated chemorepulsion controls movement patterns of cardiac progenitors and requires RhoA function. Development 135:1029-1037.

Zaffran S, Frasch M. 2002. Early signals in cardiac development. Circ Res 91:457-469.

Zhang X, Wright CV, Hanks SK. 1995. Cloning of a Xenopus laevis cDNA encoding focal adhesion kinase (FAK) and expression during early development. Gene 160:219-222.

Zhao Z, Rivkees SA. 2003. Rho-associated kinases play an essential role in cardiac morphogenesis and cardiomyocyte proliferation. Dev Dyn 226:24-32.

Zhidkova NI, Belkin AM, Mayne R. 1995. Novel isoform of beta 1 integrin expressed in skeletal and cardiac muscle. Biochem Biophys Res Commun 214:279-285.

Zoeller JJ, McQuillan A, Whitelock J, Ho SY, Iozzo RV. 2008. A central function for perlecan in skeletal muscle and cardiovascular development. J Cell Biol 181:381-394.